







The Annelid Community of a Natural Deep-sea Whale Fall off Eastern Australia

MAGDALENA N. GEORGIEVA^{1,2} , HELENA WIKLUND^{1,4,5} , DINO A. RAMOS^{1,6} ,
LENKA NEAL¹ , CHRISTOPHER J. GLASBY^{3,7,8} , AND LAETITIA M. GUNTON³ 

¹ Life Sciences Department, Natural History Museum, London, United Kingdom

² Univ. Brest, CNRS, Ifremer, UMR6197 Biologie et Ecologie des Ecosystèmes marins Profonds, Plouzané, France

³ Australian Museum Research Institute, Australian Museum, Sydney, Australia

⁴ Department of Marine Sciences, University of Gothenburg, Gothenburg, Sweden

⁵ Gothenburg Global Biodiversity Centre, Gothenburg, Sweden

⁶ University of Grenada, Grenada, Spain

⁷ Natural Sciences, Museum and Art Gallery of the Northern Territory, Darwin, Australia

⁸ Research Institute for the Environment and Livelihoods, Charles Darwin University, Darwin, Australia

ABSTRACT. In the deep ocean, whale falls (deceased whales that sink to the seafloor) act as a boost of productivity in this otherwise generally food-limited setting, nourishing organisms from sharks to microbes during the various stages of their decomposition. Annelid worms are habitual colonizers of whale falls, with new species regularly reported from these settings and their systematics helping to resolve biogeographic patterns among deep-sea organic fall environments. During a 2017 expedition of the Australian research vessel *RV Investigator* to sample bathyal to abyssal communities off Australia's east coast, a natural whale fall was opportunistically trawled at ~1000 m depth. In this study, we provide detailed taxonomic descriptions of the annelids associated with this whale-fall community, using both morphological and molecular techniques. From this material we describe nine new species from five families (Dorvilleidae: *Ophryotrocha dahlgreni* sp. nov., *Ophryotrocha hanneloreae* sp. nov., *Ophryotrocha ravarae* sp. nov.; Hesionidae: *Vrijenhoekia timoharai* sp. nov.; Nereididae: *Neanthes adriangloveri* sp. nov., *Neanthes visicete* sp. nov.; Orbiniidae: *Orbiniella jamesi* sp. nov.), including two belonging to the bone-eating genus *Osedax* (Siboglinidae: *Osedax waadjum* sp. nov., *Osedax byronbayensis* sp. nov.) that are the first to be described from Australian waters. We further provide systematic accounts for 10 taxa within the Ampharetidae, Amphinomidae, Microphthalmidae, Nereididae, Orbiniidae, Phyllodocidae, Protodrilidae, Sphaerodoridae and Phascolosomatidae. Our investigations uncover unique occurrences and for the first time enable the evaluation of biogeographic links between Australian whale falls and others in the western Pacific as well as worldwide.

Keywords: polychaete, chemosynthesis, organic fall, bathyal, Bathymodiolinae, Pacific Ocean

ZooBank registration: urn:lsid:zoobank.org:pub:32014E75-6253-41C0-BEDC-7A461321A0A1

ORCID iD: Magdalena N. Georgieva 0000-0002-1129-0571; Helena Wiklund 0000-0002-8252-3504; Dino A. Ramos 0000-0002-4069-5383; Lenka Neal 0000-0002-3857-8428; Christopher J. Glasby 0000-0002-9464-1938; Laetitia M. Gunton 0000-0003-4758-4974

Corresponding author: Magdalena N. Georgieva m.georgieva@nhm.ac.uk

Submitted: 2 February 2022 **Accepted:** 4 April 2023 **Published:** 17 May 2023 (in print and online simultaneously)

Publisher: The Australian Museum, Sydney, Australia (a statutory authority of, and principally funded by, the NSW State Government)

Citation: Georgieva, Magdalena N., Helena Wiklund, Dino A. Ramos, Lenka Neal, Christopher J. Glasby, and Laetitia M. Gunton. 2023. The annelid community of a natural deep-sea whale fall off eastern Australia. In *RV Investigator—Abyssal Annelida*, ed. E. K. Kupriyanova and L. M. Gunton. *Records of the Australian Museum* 75(3): 167–213. <https://doi.org/10.3853/j.2201-4349.75.2023.1800>

Copyright: © 2023 Georgieva, Wiklund, Ramos, Neal, Glasby, Gunton. This is an open access article licensed under a Creative Commons Attribution 4.0 International License (CC BY 4.0), which permits unrestricted use, distribution, and reproduction in any medium, provided the original authors and source are credited.



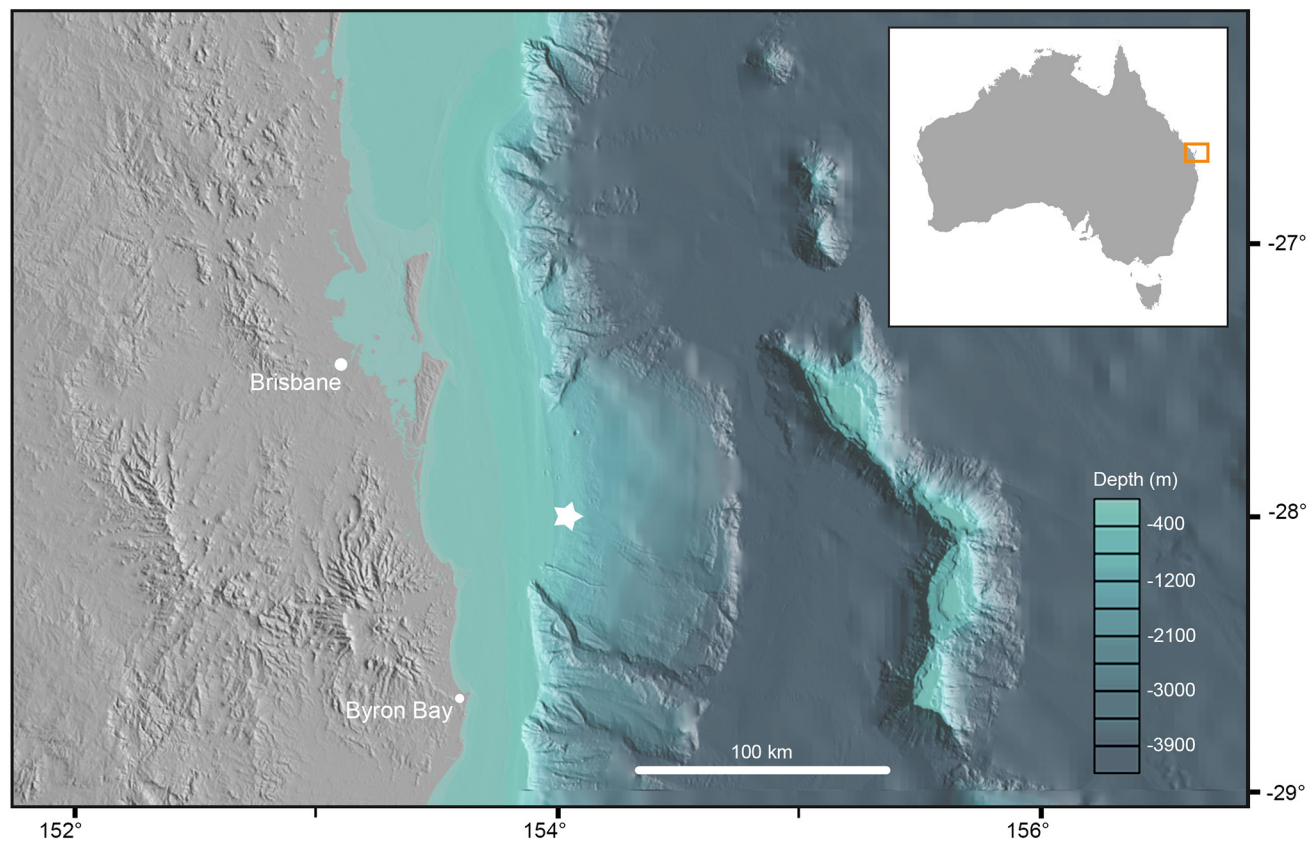


Figure 1. Location of the whale fall (white star) trawled off Byron Bay, Australia, during the IN2017_V03 expedition.

Introduction

Whales that sink and settle on the seafloor upon their death, known as whale falls, represent an important food source in the generally food-limited deep sea, as well as having a crucial role as dispersal and evolutionary stepping stones for deep-sea fauna (Smith & Baco, 2003; Smith *et al.*, 2015, 1989). As a carcass decomposes it eventually becomes a chemosynthetic habitat, and during its decomposition is colonized by different successional stages of organisms, some of which are highly specialized for life on decaying vertebrate remains. Perhaps the most notable whale-fall specialists are annelids of the genus *Osedax* (Siboglinidae), also known as “zombie” worms, which embed “root” tissue into decaying vertebrate bones and feed by using bacterial endosymbionts to extract organic compounds from the bones. Annelid taxa are the most abundant and diverse component of whale-fall communities in general (Smith *et al.*, 2015), with families such as Ampharetidae, Dorvilleidae and Hesionidae (Shimabukuro *et al.*, 2019) being commonly encountered within these habitats.

Since the first observations in a manned submersible of an intact whale skeleton off southern California in 1987 (Smith *et al.*, 1989), several natural whale falls have been opportunistically encountered during remotely operated vehicle (ROV), submersible and trawl deployments, while further understanding of whale-fall communities has been greatly aided by the experimental sinking of cetacean remains (e.g., Smith *et al.*, 2015; Fujiwara *et al.*, 2007; Dahlgren *et al.*, 2006). Both types of whale fall are poorly represented in the

western Pacific, and especially around South-East Asia and in Australian waters. From near Australian waters, a whale skull was recovered at 880 m northeast off Chatham Island with new species of gastropod (Marshall, 1987), Sipuncula (Gibbs, 1987), and a bivalve (Dell, 1987, 1995). Whale bones with associated molluscs were collected from various other locations off New Zealand including the Chatham Rise at depths of 372–379 m, 587 m, 900 m and 937–955 m, Chatham Islands at 1242 m depth, Banks Peninsula at 844 m and Challenger Plateau at 908–912 m and 1116–1120 m (Marshall, 1994; Dell, 1995). More recently, two new species of *Osedax* have been reported from a whale skull at 390 m depth on the Pukaki Rise (Berman, 2022), which are the first records of this genus from New Zealand. Further north off the coast of Japan, whale-fall communities are known from a natural whale fall at 4000 m at the Torishima Seamount (Wada *et al.*, 1994) as well as a number of whale carcasses sunk off southern Japan at 219–254 m (Fujiwara *et al.*, 2007). The above studies reported Amphioxiformes, a number of rare species, as well as the unusual presence of protodrilid polychaetes in association with the whale bones.

During a voyage of the RV *Investigator* (IN2017_V03) to sample bathyal and abyssal zones off the eastern coast of Australia, a natural whale fall was collected during beam trawl sampling in the Byron Bay area (Fig. 1; Gunton *et al.*, 2021; O’Hara *et al.*, 2020). This study documents in detail the annelid fauna colonizing the first whale fall reported from Australian waters and compares this community with other known whale falls from the Pacific Ocean, as well as whale falls from the Atlantic and Southern Oceans.

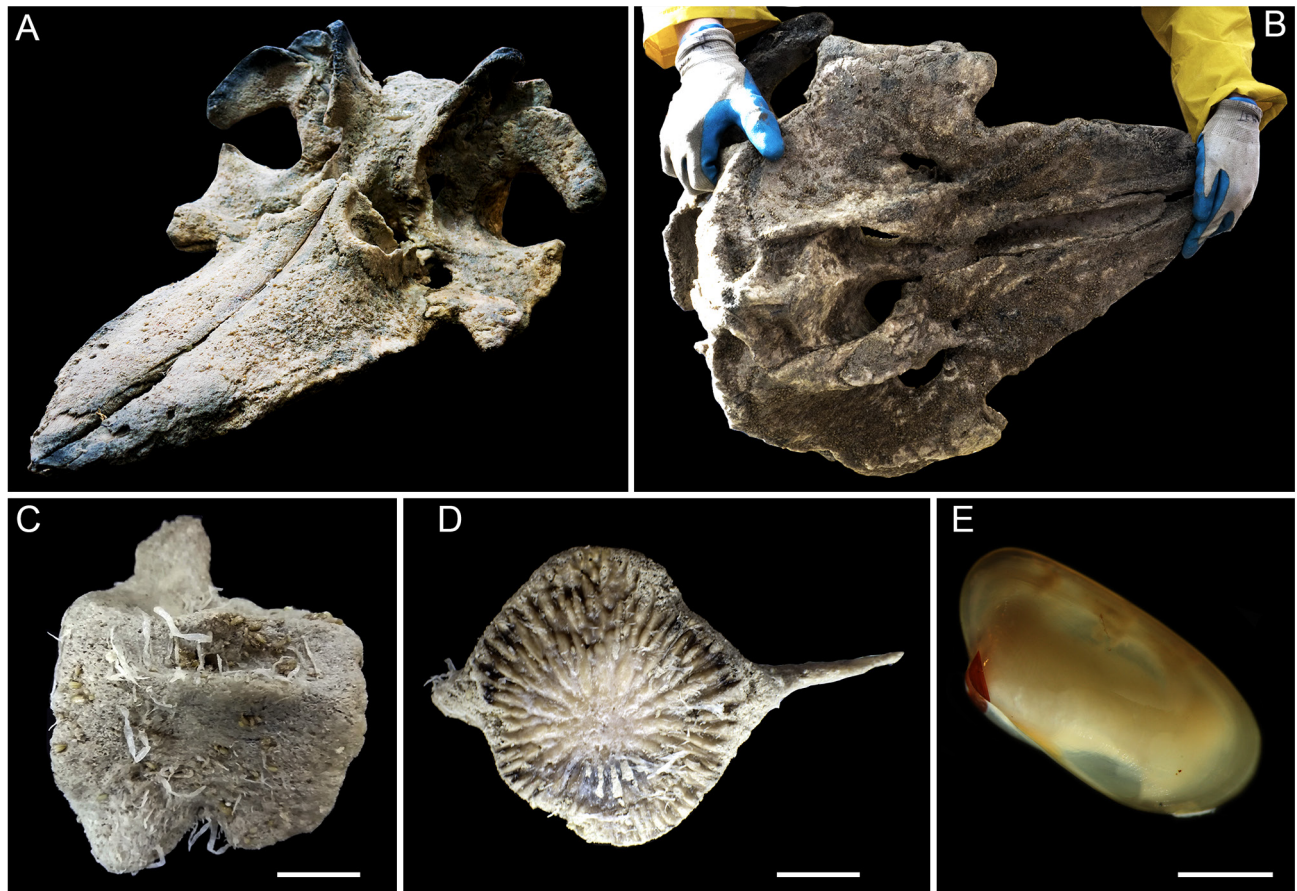


Figure 2. Detail of the whale bones trawled during the IN2017_V03 expedition, and the dominant bivalve taxon associated with these; (A) top of whale skull; (B) underside of whale skull, covered in numerous small bivalves, hands for scale; (C) side of whale vertebra with *Osedax* tubes and small bivalves visible, scale bar is 30 mm; (D) cross-section view of whale vertebra with *Osedax* tubes, scale bar is 30 mm; (E) detail of the small bivalve associated with the whale bones, scale bar is 10 mm.

Materials and methods

Sample collection

The natural whale fall was recovered as part of a 4-metre beam trawl deployment during RV *Investigator* voyage IN2017_V03 “Sampling the Abyss”. The trawl (operation 100) was conducted on 9 June 2017 in the Byron Bay area (start 28.05°S 154.08°E; end 28.10°S 154.08°E), at 999–1013 m depth (Fig. 1). The whale fall consisted of a complete skull and several vertebrae of a pilot whale (*Globicephala macrorhynchus*), with no remaining soft tissue (Fig. 2A–D). Upon recovery, the whale bones were temporarily placed in chilled seawater and inspected for associated invertebrates. A subset of the associated annelids was photographed alive, then subsequently preserved in 80% or 95% ethanol. Seawater in which the bones were kept prior to preservation was also sieved using 300 µm mesh, and retained macrofauna were preserved in 80% ethanol. The majority of whale bones were subsequently frozen at -20°C, with the exception of three vertebrae preserved in 95% ethanol.

Annelid specimens were shipped to the Australian Museum, Sydney, Australia (AM) and the Natural History Museum, London, United Kingdom (NHM) for identification. The whale bones were deposited at Museums Victoria, Melbourne, Australia (MV). Material deposited

at the AM is registered with the prefix “AM W.”, while specimens registered at MV have the prefix “NMV”, and those at the NHM bear the prefix “NHMUK”. Specimens for which all tissue was used up for the molecular analysis were given the prefix WF_. Registration numbers were assigned to individual specimens. We use “undes.” for undescribed.

Morphological and molecular taxonomy

Samples from the whale fall were sorted to genus level and examined using stereo and compound microscopes equipped with camera attachments to identify key morphological features of specimens, which were subsequently photographed. Small fragments of tissue were cut from specimens from non-taxonomically informative body regions and used to extract DNA for molecular taxonomy. Unfortunately, many specimens were in a poor condition, thus morphological data is limited.

DNA extractions were performed using a DNeasy Blood and Tissue Kit (Qiagen) following instructions provided by the manufacturer. Approximately 650 bp of cytochrome c oxidase subunit I (COI), 450 bp of 16S rRNA (16S), and 1800 bp of 18S rRNA (18S) were amplified using primers outlined in Table S1. PCR reactions contained 0.5 µl of each primer (10 µM), 1 µl template DNA and 10.5 µl of Red Taq DNA Polymerase 1.1X MasterMix (VWR) in a mixture of total 12.5 µl. The PCR reaction protocol was as follows:

94°C/5 min, (94°C/45 s, 55°C/45 s, 72°C/2 min) × 35 cycles, 72°C/10 min. PCR products were visualized using 1% agarose gel, purified and subsequently sequenced using either an ABI 3730XL DNA Analyser (Applied Biosystems) at the NHM Sequencing Facility, UK, or for samples deposited at the AM, sent to Macrogen South Korea where they were purified and standard Sanger sequencing was performed.

The newly-generated sequences were aligned with existing annelid sequences available on NCBI GenBank (Tables S2–12) using Geneious v.10.2.5 (Kearse *et al.*, 2012). The most appropriate substitution model for each locus was determined according to the Akaike Information Criterion in JModelTest v.2.1.10 (Guindon & Gascuel, 2003; Darriba *et al.*, 2012). Phylogenetic analyses were performed using MrBayes v.3.2.6 (Ronquist *et al.*, 2012) on combined datasets of COI, 16S, and 18S (depending on the availability of data for each taxonomic group), with each analysis run for 10,000,000 generations using the above models. Uncorrected pairwise distances for COI sequence data were calculated using PAUP* v.4.0a (build 166; Swofford, 2002) or calculated in Geneious (Tables S13–S19).

Results

Fauna associated with the whale fall

The most visually dominant colonizer of the whale bones was found to be a small or juvenile mytilid (Fig. 2E), which was observed in high densities on the top and underside of the skull (Fig. 2A–B), as well as in small clusters on vertebrae (Fig. 2C). COI and 16S sequences for one of the mytilid specimens (NHM_230B) showed 99–100% similarity to sequences available on NCBI GenBank for the species *Terua arcuatilis* (COI: FJ937036, 16S: HF545067), described from deep waters off New Zealand. In addition to mytilids, actinarians, sponges, nemerteans, gastropods and a holothurian were observed on the whalebones. The tubes of *Osedax* annelids were also clearly visible on bone surfaces, being abundant on the upper skull surface as well on vertebrae (Fig. 2A, C–D), while errant annelids found in high numbers in crevices and surfaces of whale bones as well as in the bone washings included phyllodocids, orbiniids, dorvilleids, hesionids and protodrilids. A taxonomic account of two of the observed whale-fall polychaete species, *Boudemos* sp. (Chrysopetalidae) and *Pleijelius* sp. (Hesionidae), will be provided in a separate publication (C. Watson, personal communication).

Taxonomy

Ampharetidae Malmgren, 1866

Paramytha Kongsrud, Eilertsen, Alvestad, Kongshavn, & Rapp, 2017

Paramytha cf. *ossicola* Queirós, Ravara, Eilertsen, Kongsrud, & Hilário, 2017

Fig. 3

Ampharetidae gen. spp. Gunton *et al.*, 2021: 19–20.

Material examined. AM W.51926, AM W.52208, IN2017_V03_100; 9 June 2017; off Byron Bay, NSW, Australia, beam trawl, start: 28.05°S 154.08°E, 999 m, end: 28.10°S 154.08°E, 1013 m. DNA vouchers: AM W.51926 (16S, 18S), AM W.52208 (16S), WF_AMH_3 (16S).

Description. Based on AM W.52208. Anterior section only (~1 mm length, ~0.5 mm width) for 14 chaetigers, posterior used for molecular analysis. Body cylindrical (Fig. 3A). Prostomium and peristomium fused, not divided into lobes (Fig. 3B). Prostomium without glandular ridges; nuchal organs and eyespots not observed. Buccal tentacles not observed. Paleae absent. Four pairs of branchiae, arrangement 2+2 (Fig. 3A), branchiae somewhat flattened, with longitudinal median furrow. Branchiophores distinct lobes attached to body wall.

Notopodia as rounded lobes, with capillary chaetae starting from segment 3 (Fig. 3D). Uncini from segment 5, thoracic uncini arranged in single row of approximately 13 in number (Fig. 3C). Thoracic uncini with teeth arranged in 3 horizontal rows above main rostral tooth and basal prow (Fig. 3E). The rest of body not observed.

Methyl green staining, prostomium speckled on ventral side and ventral bands encompassing whole ventral surface. Notopodia and neuropodia not darkly stained.

Distribution. IN2017_V03, Station 100. Pilot whale carcass, off Byron Bay, New South Wales, Australia in 999–1013 m.

Remarks. Morphologically this material very closely resembles *Paramytha ossicola* Queirós, Ravara, Eilertsen, Kongsrud, & Hilário, 2017, described from cow carcasses submerged in the Setúbal Canyon (NE Atlantic), 1000 m depth (Queirós *et al.*, 2017). It resembles *P. ossicola* in all observable morphological characters except for arrangement of branchiae where it differs, 2+2 in this species and 2+1+1 in *P. ossicola*. The close evolutionary relationship between our species (*Paramytha* cf. *ossicola*) and *Paramytha ossicola* is also supported by our molecular analysis (Fig. 4). The three *Paramytha* species (*Paramytha schanderi* Kongsrud, Eilertsen, Alvestad, Kongshavn, & Rapp, 2017—described from the Arctic Loki Castle hydrothermal vent field at 2350 m, *Paramytha ossicola* and *Paramytha* cf. *ossicola*) were recovered in a strongly supported clade (posterior probability, pp 1.0; Fig. 4), while *Paramytha ossicola* and *Paramytha* cf. *ossicola* were recovered as sister groups (pp 1.0; Fig. 4). Uncorrected intraspecific divergence between 16S sequences of *Paramytha* cf. *ossicola* was 0% (Table S13), this is less than the intraspecific divergence recorded in *Paramytha schanderi* 0.4–1.1% and *Paramytha* sp. 0–0.4% (Kongsrud *et al.*, 2017). The 16S interspecific genetic distance between *Paramytha* cf. *ossicola* and the closely

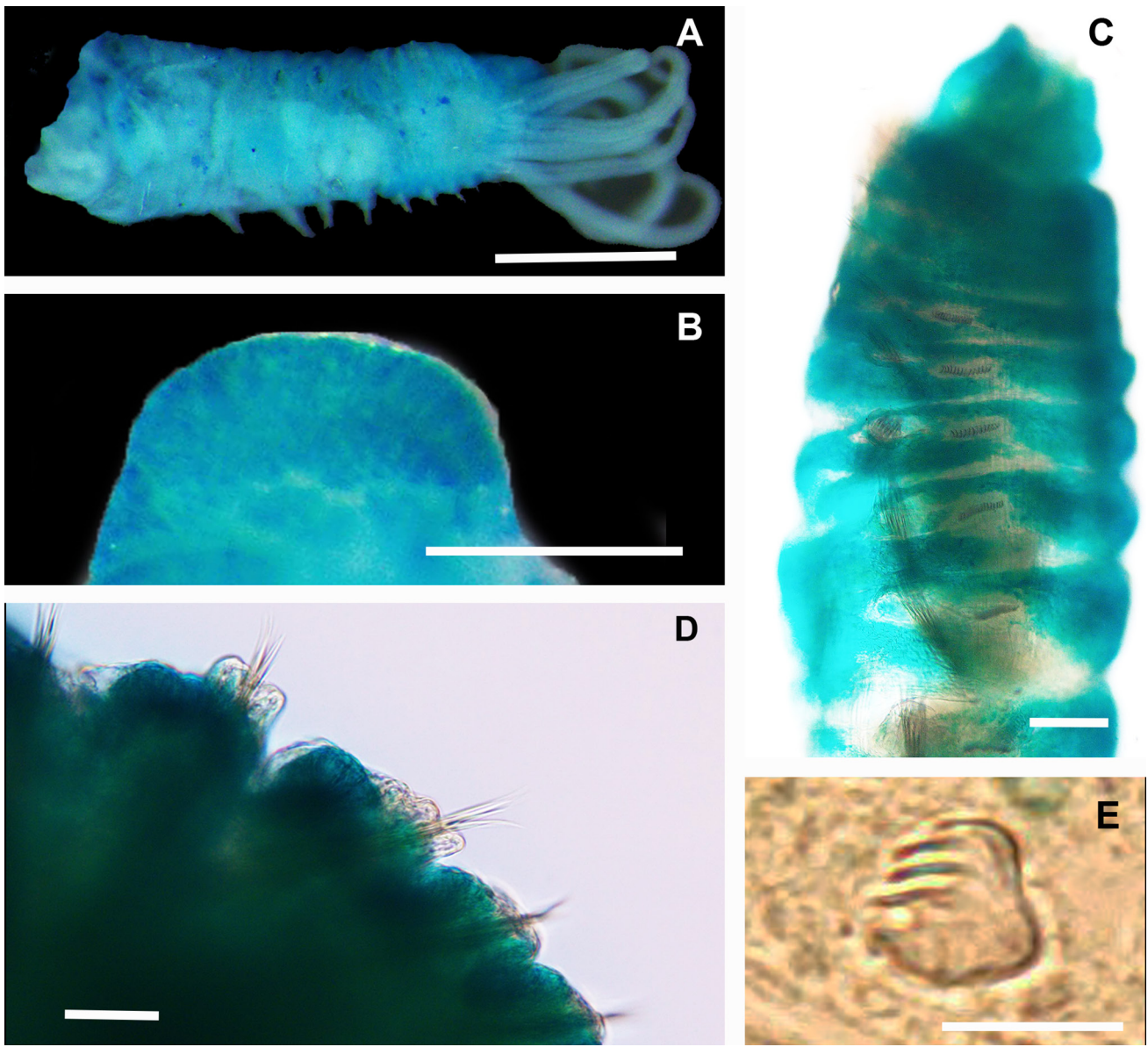


Figure 3. *Paramytha* cf. *ossicola*, specimen AM W.52208 stained with methyl blue; (A) dorsal view anterior section, scale bar is 0.5 mm; (B) prostomium, scale bar is 0.25 mm; (C) notochaetae, scale bar is 50 μ m; (D) lateral view of anterior, scale bar is 50 μ m; (E) thoracic uncinus, scale bar is 50 μ m.

related *Paramytha ossicola* averaged 3.9%; this is less than the distance recorded between *Paramytha schanderi* and *Paramytha* sp. which ranged from 17.6–19.4% (Kongsrud *et al.*, 2017). It is difficult to definitively designate these specimens to *Paramytha ossicola* or to a separate species, as all specimens are in poor morphological condition. We therefore identify these specimens as *Paramytha* cf. *ossicola*.

Amphinomidae Lamarck, 1818

Paramphinome M. Sars in G. Sars, 1872

Paramphinome cf. *australis* Monro, 1930

Fig. 5

Paramphinome cf. *australis* Gunton *et al.*, 2021: 21–22, fig. 5C,D

Material examined. NHMUK ANEA 2022.435, AM W.52195, AM W.52197, IN2017_V03_100; 9 June 2017; off Byron Bay, NSW, Australia, beam trawl, start: 28.05°S

154.08°E, 999 m, end: 28.10°S 154.08°E, 1013 m. DNA vouchers: NHMUK ANEA 2022.435 (COI, 16S, 18S), AM W.52195 (16S), WF_AMP_2 (COI, 16S), AM W.52197 (16S).

Description. Descriptions based on AM W.52197. Body shape elongate (Fig. 5A), specimen complete, around 4 mm length. Eyes absent. Prostomium rounded. One median unpaired antenna (Fig. 5B), pair of lateral antennae. One or two pairs of strongly curved hooks on chaetiger 1 (Fig. 5C) depending on body size (smaller individuals one, larger individuals two). Arborescent branchiae beginning on chaetiger 4 to chaetiger 7 (Fig. 5D). Parapodia biramous. Notochaetae: capillary chaetae with step-like serrations and smooth unadorned spines. Notoacicula two per fascicle. Neurochaetae long thin capillaries with basal spurs, long thin capillaries no basal spurs, subdistally inflated bifurcate chaetae serrated prongs. Neuroacicula two per fascicle (Fig. 5E). Pygidium unadorned.

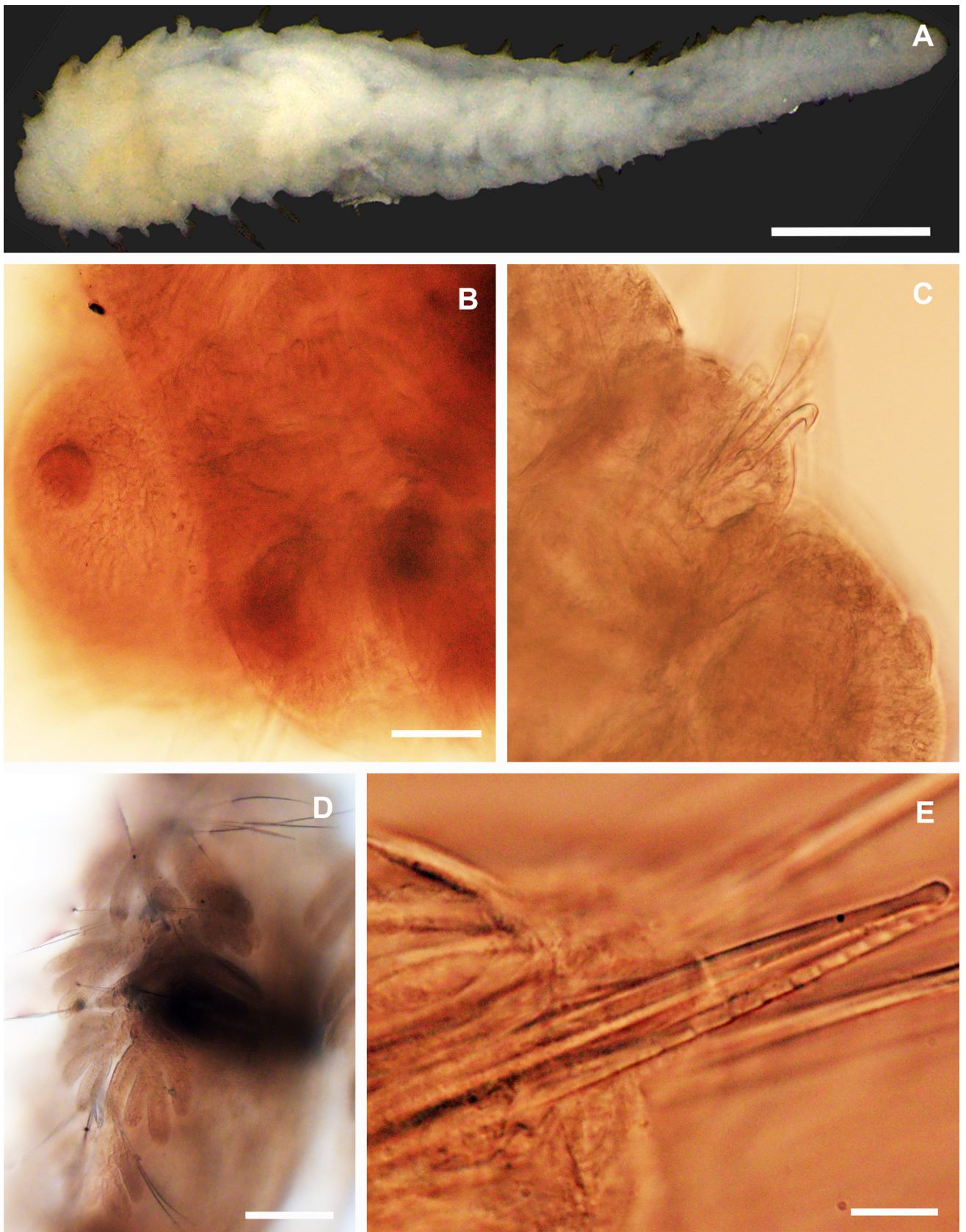


Figure 5. *Paramphinome cf. australis* AM W.52197. (A) Whole body of specimen dorsal view scale bar 1 mm; (B) prostomium with one median antenna, scale bar is 50 μm ; (C) strongly curved hooks on chaetiger 1, scale bar is 20 μm ; (D) arborescent branchiae, scale bar is 20 μm ; (E) neuroaricula, scale bar is 20 μm .

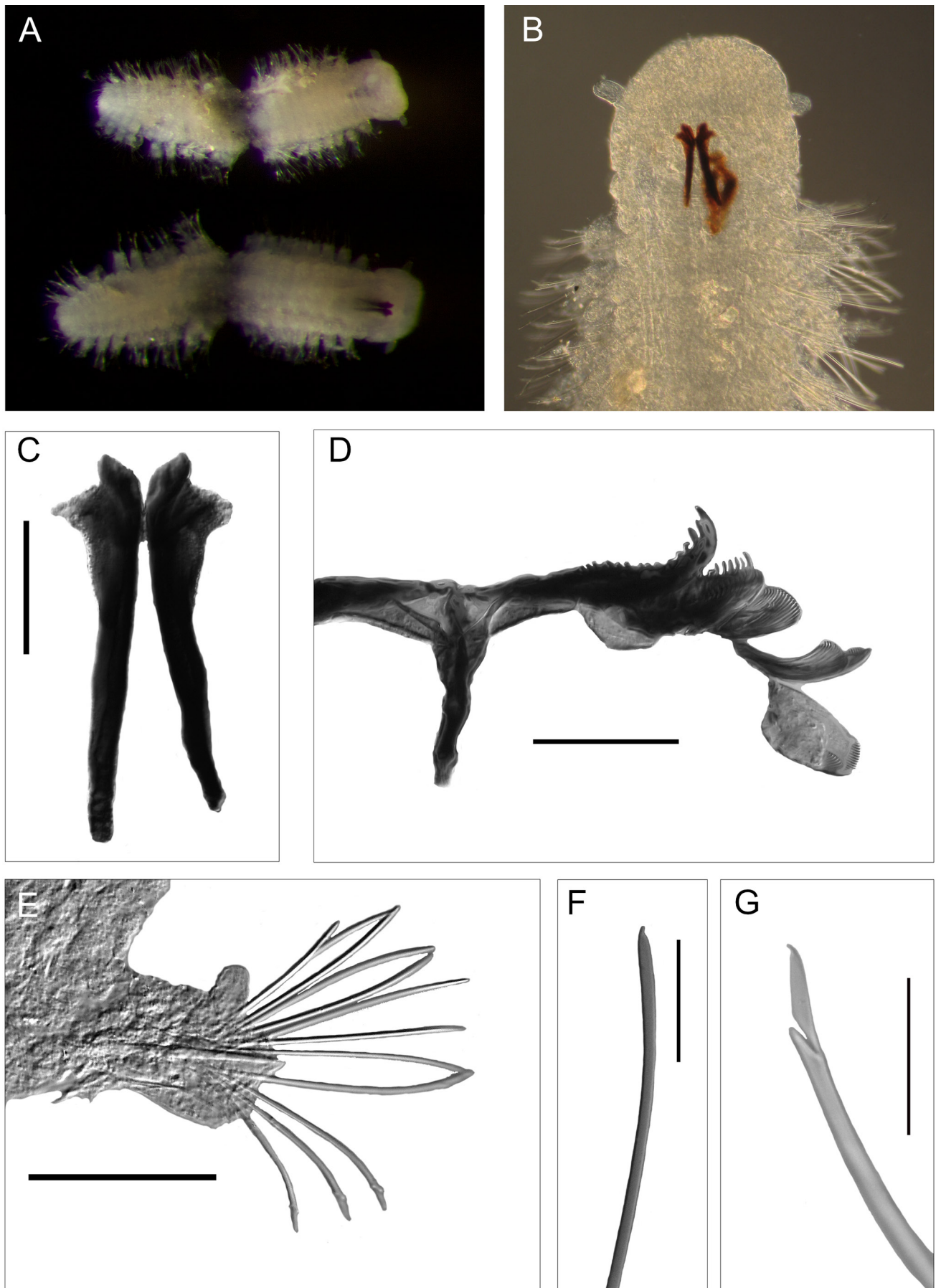


Figure 7. *Ophryotrocha dahlgreni* sp. nov. (A) Photo of holotype, dorsal and ventral side, holotype 1 mm long; (B) anterior end; (C) mandibles, scale bar is 50 μ m; (D) everted maxillae on one side, scale bar is 50 μ m; (E) parapodium, scale bar is 100 μ m; (F) supra-acicular simple chaeta, scale bar is 25 μ m; (G) sub-acicular compound falcigerous chaeta, scale bar is 25 μ m.

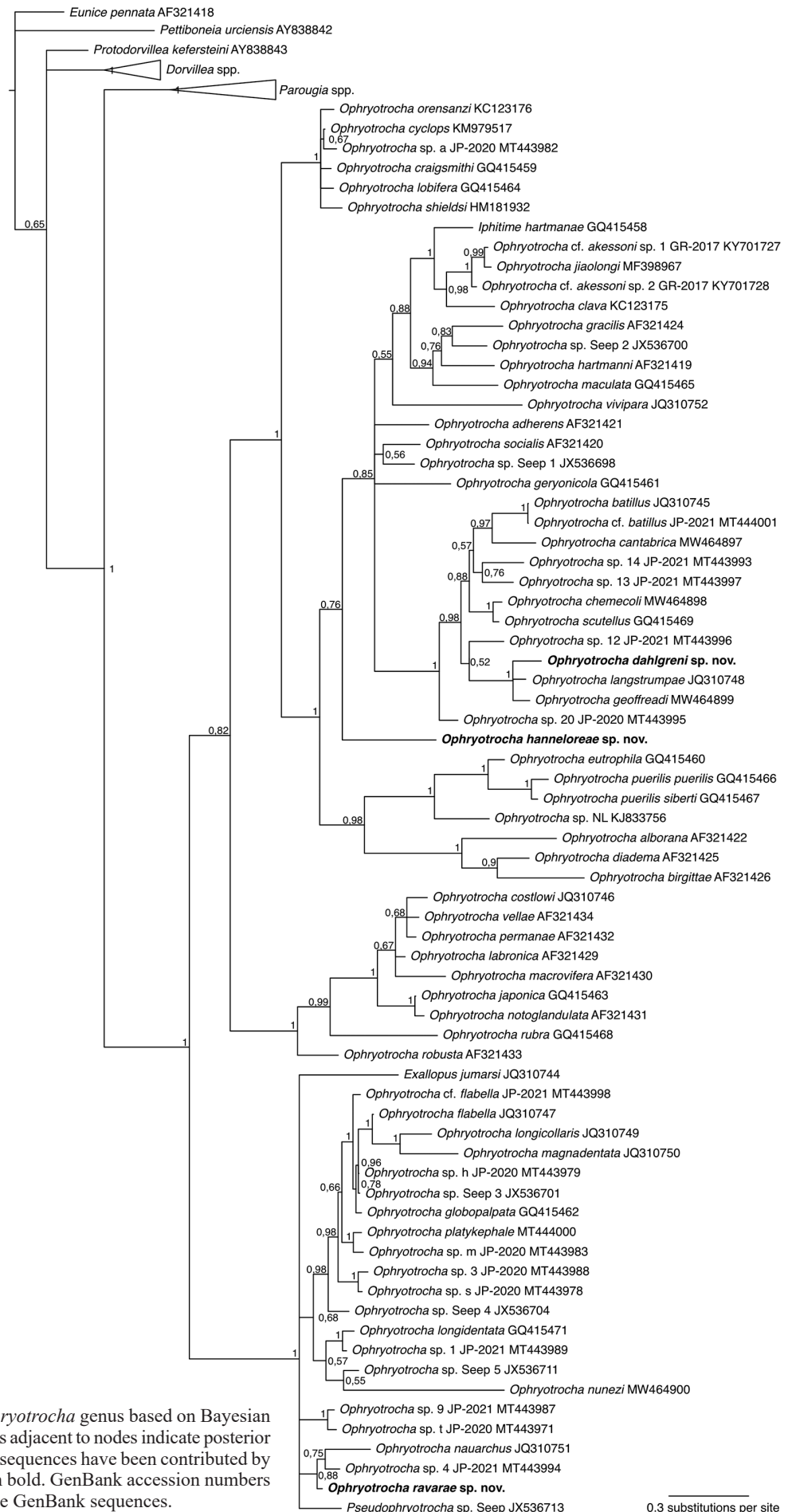


Figure 8. Phylogeny of the *Ophryotrocha* genus based on Bayesian analysis of the 16S gene. Numbers adjacent to nodes indicate posterior probabilities, and taxa for which sequences have been contributed by the present study are indicated in bold. GenBank accession numbers are given after taxa names for the GenBank sequences.

described from whale fall in eastern Pacific Ocean, and *O. geoffreadi* Ravara, Wiklund, and Cunha, 2021 described from experimentally deployed wood substrate in Gulf of Cadiz. The new species differs from *O. langstrumpae* in the shape of the parapodia and chaetae, where the new species lacks ventral cirri and has short blades on the compound sub-acicular chaetae. *Ophryotrocha geoffreadi* has large, triangular-shaped apophyses, but its rod-like mandibles have straight, serrated cutting edges, while in the new species the tips are gently curving outwards and lack serration.

Ophryotrocha hanneloreae sp. nov.

urn:lsid:zoobank.org:act:875C94C2-FCFD-432B-96FB-6C9A053ADE04

Fig. 9

Holotype: AM W.53697 (body length 1.3 mm for 20 chaetigerous segments), IN2017_V03_100; 9 June 2017; off Byron Bay, NSW, Australia, beam trawl, start: 28.05°S 154.08°E, 999 m, end: 28.10°S 154.08°E, 1013 m. **Paratypes:** NMV F296819–296821, NHMUK ANEA 2022.775–777, same locality as holotype. DNA vouchers: AM W.53695–53696, same locality as holotype.

Description. Body length up to 3 mm for examined, complete specimens. Body compressed dorsoventrally, anterior body with similar width from head to mid-body, then tapering towards pygidium (Fig. 9A). Head rounded with simple antennae, approximately equal length to palpostyles. Biarticulated palps, palpophores large, equal length to palpostyles (Fig. 9A). Mandibles forked without dentition, inner peak larger than outer peak (Fig. 9B). Maxillae P-type with a pair of forceps and seven pairs of free denticles (D1–7). Forceps with coarse teeth increasing in size from base to tip, D1–3 with progressively slightly finer teeth, D3 with a larger distal fang. Denticles 4–7 with fine evenly sized teeth (Fig. 9B, 9C). Two peristomial achaetous segments, the first twice as long as the second (Fig. 9A). Parapodia uniramous with short distal dorsal cirri, without ventral cirri (Fig. 9D).

Supra-acicular chaetae simple (Fig. 9E), sub-acicular chaetae compound with short blades (Fig. 9F), sub-acicular lobe with simple chaeta.

Pygidium with terminal anus, two lateral cirri and a mid-ventral stylus.

Distribution. IN2017_V03, Station 100. Pilot whale carcass, off Byron Bay, New South Wales, Australia in 999–1013 m.

Etymology. This species is named in honour of Dr Hannelore Paxton at Macquarie University, Australia, for her comprehensive work with *Ophryotrocha* worms, and for sharing her expertise especially regarding the jaw morphology of eunicids.

Remarks. The new species is morphologically most similar to *Ophryotrocha longicollaris* Wiklund *et al.*, 2012. The two species differ in shape of parapodia where the new species has larger dorsal cirri, shorter anal cirri, and P-type maxillae while *O. longicollaris* has only been reported having K-type maxillae. In the phylogenetic tree (Fig. 8), this species does not occur near *O. longicollaris*, but instead is recovered in an unresolved position in a large clade containing the type species of the genus. The single gene 16S may not be enough to resolve the position.

Ophryotrocha ravarae sp. nov.

urn:lsid:zoobank.org:act:73278737-0C9F-452F-9DC3-590D0078106A

Fig. 10

Holotype: AM W.53701 (length 1.6 mm for 19 chaetigerous segments), IN2017_V03_100; 9 June 2017; off Byron Bay, NSW, Australia, beam trawl, start: 28.05°S 154.08°E, 999 m, end: 28.10°S 154.08°E, 1013 m. **Paratypes:** NMV F296822–296824, and NHMUK ANEA 2022.772–774, same locality as holotype. DNA vouchers: AM W.53698–53700, same locality as holotype.

Description. Body length up to 1.6 mm for type material. Body compressed dorsoventrally, width tapering towards pygidium. Rounded head, anterior half flattened with high transverse ridge at level of antennae and palps. Long antennae, simple palps equally long but thinner (Fig. 10A, 10D). Mandibles and maxillae weakly sclerotized, mandibles rod-like with dentate inner ridge, maxillae K-type with blunt forceps tips and seven free denticles (Fig. 10B).

Parapodia uniramous with long dorsal cirri inserted mid-dorsal on parapodia, without ventral cirri (Fig. 10C). Supra-acicular chaetae simple (Fig. 10F), sub-acicular chaetae compound falcigers with short blades (Fig. 10E), sub-acicular lobe with one compound chaeta. Pygidium with terminal anus, pygidial cirri not observed (Fig. 10E).

Distribution. IN2017_V03, Station 100. Pilot whale carcass, off Byron Bay, New South Wales, Australia in 999–1013 m.

Etymology. This species is named in honour of Dr Ascensão Ravara, University of Aveiro, Portugal, for her extensive knowledge of and love for *Ophryotrocha*.

Remarks. In the phylogenetic tree (Fig. 8), this species falls in a clade with *Ophryotrocha nauarchus* Wiklund *et al.*, 2012 described from a whale-fall habitat and an undescribed species from a seep, both off the California coast in the eastern Pacific Ocean. However, the support for this clade is low. The head shape of the new species is similar to *O. nauarchus*, but the new species has longer palps and differs in the shape of the parapodia with the dorsal cirri being placed further distally on the parapodium, and the compound chaetae having short blades. The head shape of the new species is similar to *Ophryotrocha scutellus* Wiklund, Glover, & Dahlgren, 2009, but the shape of the parapodia is different between the species, with *O. scutellus* having long ventral cirri on parapodia.

Microphthalmidae Hartmann-Schröder, 1971

Microphthalmus Meczniow, 1865

Microphthalmus sp.

Fig. 11

Material examined. NHMUK ANEA 2022.434, NHMUK ANEA 2022.412–420, NHMUK ANEA 2022.437–438, IN2017_V03_100; 9 June 2017; off Byron Bay, NSW, Australia, beam trawl, start: 28.05°S 154.08°E, 999 m, end: 28.10°S 154.08°E, 1013 m. DNA vouchers: NHMUK ANEA 2022.434 (COI, 16S, 18S), WF_SYL_2 (COI, 16S), same locality.

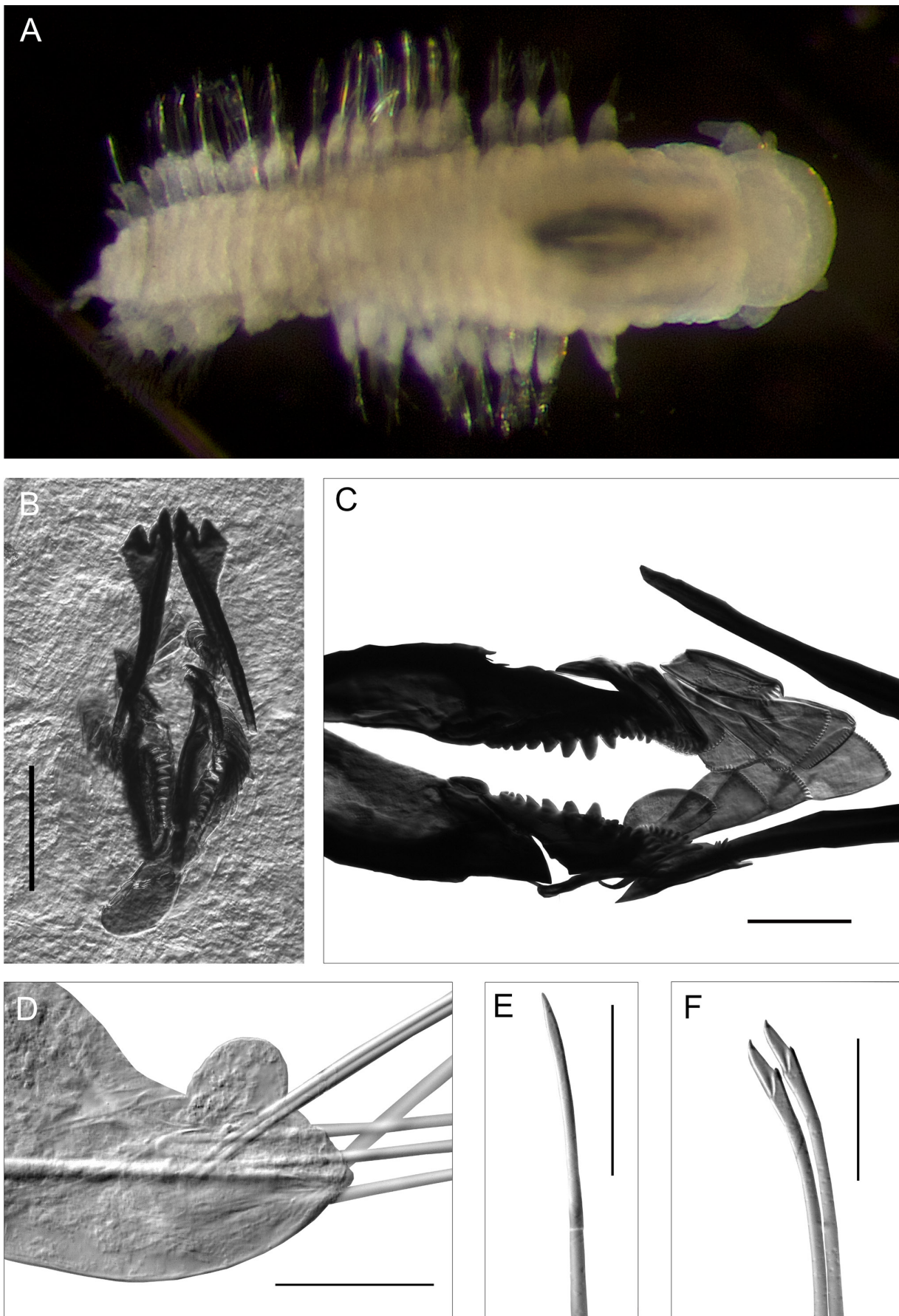


Figure 9. *Ophryotrocha hanneloreae* sp. nov. (A) Photo of holotype, dorsal side, holotype 1.3 mm long; (B) anterior end with jaws, scale bar is 25 µm; (C) details of maxillae elements with mandible shafts, scale bar is 50 µm; (D) parapodium, scale bar is 50 µm; (E) supra-acicular simple chaeta, scale bar is 50 µm; (F) sub-acicular compound falcigerous chaeta, scale bar is 50 µm.

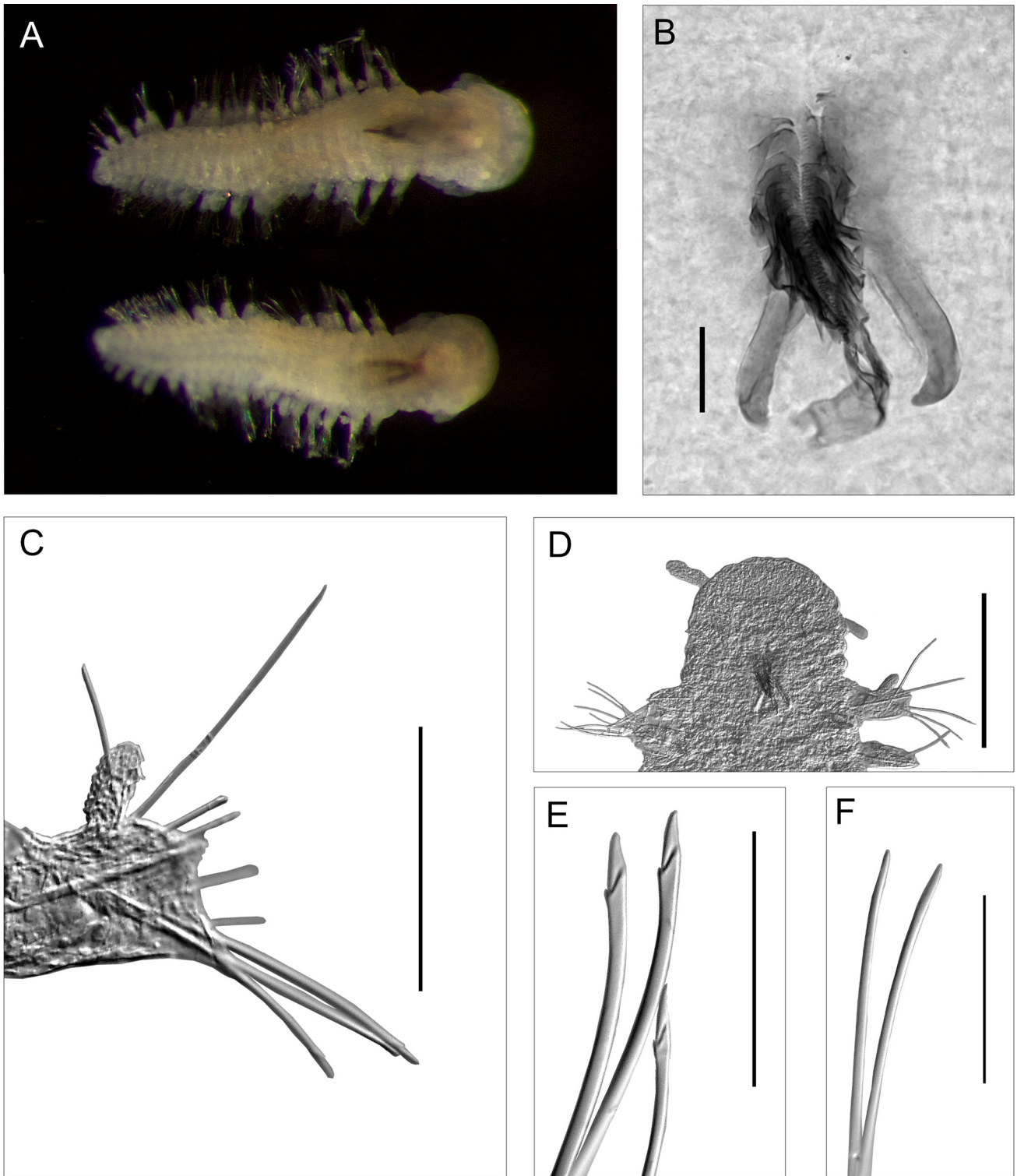


Figure 10. *Ophryotrocha ravarae* sp. nov. (A) Photo of holotype, dorsal and ventral side, holotype 1.6 mm long; (B) weakly sclerotized jaws, scale bar is 25 μ m; (C) parapodium, scale bar is 100 μ m; (D) overview of anterior end, scale bar is 250 μ m; (E) supra-acicular simple chaeta, scale bar is 50 μ m; (F) sub-acicular compound falcigerous chaeta, scale bar is 50 μ m.

Description. Complete specimens 1.1–1.8 mm long with 18–42 segments, appearing biannulate (Fig. 11A). Body width is similar throughout, with its mid-body chaetigers 0.14–0.24 mm wide, not including the parapodia, only slightly tapering on both ends. Ethanol-preserved specimens appearing white to light brown.

Prostomium semicircular, anteriorly slightly cleft, broader

than long (Fig. 11B). Prostomial appendages are all cirriform. One pair of dorsal antennae and one pair of shorter palps terminally located. Median antenna inserted near posterior end of prostomium. Eyes absent.

First three segments shorter than others and lack chaetae, bearing six pairs of cirriform tentacular cirri (Fig 11B). Dorsal and ventral cirri present from segment 4. Dorsal

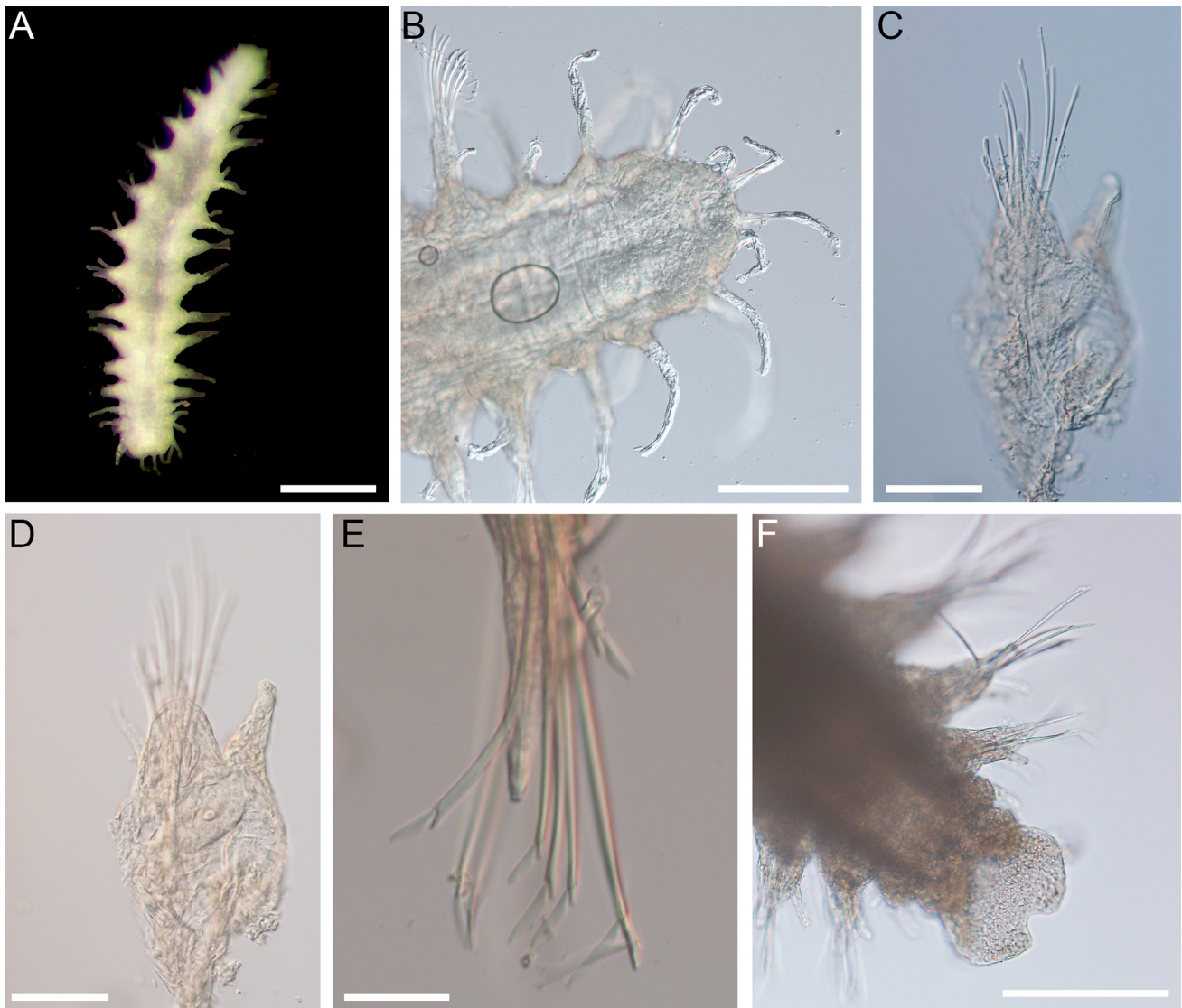


Figure 11. *Microphthalmus* sp. (A) Photo of an ethanol-preserved specimen (NHMUK ANEA 2022.412–420), scale bar is 0.25 mm; (B) light micrograph of prostomium and three anterior achaetous segments (NHMUK ANEA 2022.434), scale bar is 100 µm; (C, D) light micrographs of parapodium with the prechaetal (C) and postchaetal (D) lobes in focus (NHMUK ANEA 2022.434), scale bars are 50 µm; (E) light micrograph of heterogomph falcigers with different lengths (NHMUK ANEA 2022.434), scale bar is 20 µm; (F) light micrograph of ventral aspect of the posterior end showing anal lamellae (NHMUK ANEA 2022.412–420), scale bar is 100 µm.

cirri shorter on segment 4 than those on segment 5 onwards. Ventral cirri triangular, shorter, and thicker than cirriform dorsal cirri. Body width similar along most of the length (0.14–0.24 mm).

Parapodia uniramous. Neuropodia with a pointed prechaetal lobe (Fig. 11C) and blunt postchaetal lobe (Fig. 11D). Length of prechaetal lobe equal to or exceeds that of dorsal cirri. Neurochaetae all heterogomph falcigers with blades of different lengths having serrated edges (Fig. 11E).

Pygidium short, with two short anal cirri with swollen bases. Ventral anal lamellae bilobed, with smooth margins and lacking papillae (Fig. 11F).

Distribution. IN2017_V03, Station 100. Pilot whale carcass, off Byron Bay, New South Wales, Australia in 999–1013 m.

Remarks. The genus *Microphthalmus* has been identified in previous studies of whale-fall annelids in the Atlantic (Sumida *et al.*, 2016) and the Pacific (Dahlgren *et al.*, 2004) but no descriptions or molecular data for these have been published to date. This genus is also difficult to place phylogenetically (Fig. 12). Sumida *et al.* (2016) indicated that the *Microphthalmus* collected from the Atlantic whale fall was a new species, however whether our specimens represent the same species cannot be determined at present due to the lack of information from previous studies. Male copulatory organs were not examined, which have been suggested to be the most suitable morpho-anatomical character for differentiating between species (Westheide, 2013).

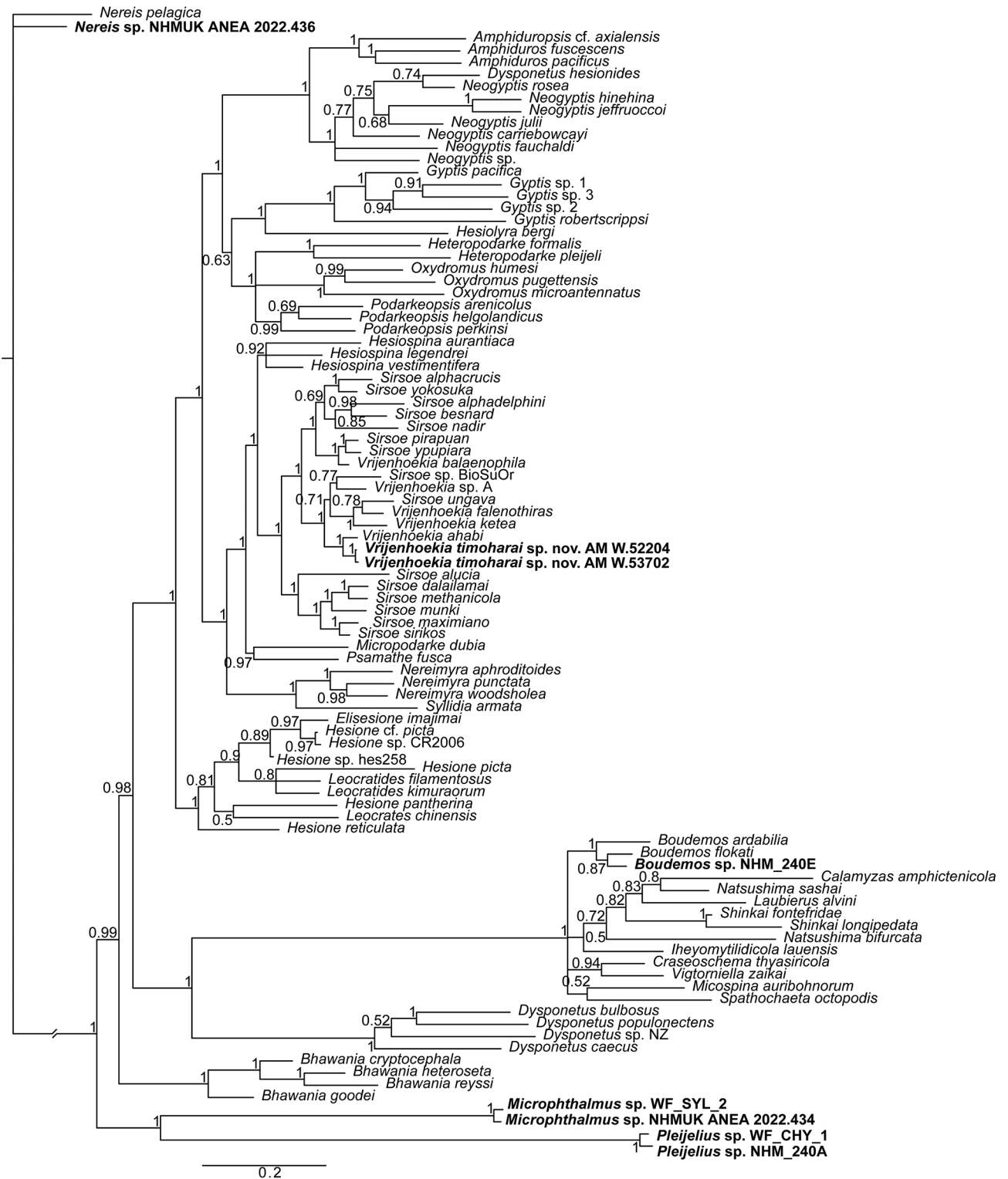


Figure 12. Phylogeny for the Hesionidae, Microphthalimidae and Chrysopetalidae families based on Bayesian analysis of a combined dataset of the genes COI, 16S and 18S. Numbers adjacent to nodes indicate posterior probabilities, and taxa for which sequences have been contributed by the present study are indicated in bold.

Hesionidae Grube, 1850

Vrijenhoekia

Pleijel, Rouse, Ruta, Wiklund, & Nygren, 2008

Vrijenhoekia timoharai sp. nov.

urn:lsid:zoobank.org:act:58CD4F18-8DE3-429B-A15E-07F803358649

Fig. 13

Vrijenhoekia ketea species complex Gunton *et al.*, 2021: 51–52, fig. 12F

Holotype: AM W.53702, IN2017_V03_100; 9 June 2017; off Byron Bay, NSW, Australia, beam trawl, start: 28.05°S 154.08°E, 999 m, end: 28.10°S 154.08°E, 1013 m. **Paratype:** AM W.52204, same locality as holotype. DNA vouchers: AM W.53702 (COI, 16S, 18S), AM W.52204 (COI, 16S).

Description. Body of AM W.53702 complete, approximately 2.3 mm wide (including parapodia but not chaetae) and 7.5 mm long, with 32 segments (Fig. 13A). Body stout with tapered pygidium. Ethanol-preserved specimen pale yellow.

Prostomium (Fig. 13B) rectangular, considerably wider than long, with no posterior incision discernible. Palps biarticulated with palpophores thicker than palpostyles, but a similar length to palpostyles. Paired antennae similar in length to palps, tapered, with antennophores not discernible. Eyes absent, median tubercle very small relative to others observed for genus, facial tubercle with bulbous end and approximately half length of antennae. Nuchal organs small and not dorsally extended. Everted proboscis (Fig. 13C) lacking papillae.

Parapodia triangular and stout (Fig. 13D), with long, tapering and terminally rounded dorsal cirri slightly longer than width of body, longest in segments 1 to 5. Cirrophores distinct and small. Ventral cirri similar throughout length of body, distinctly tapered, same length as parapodia, inserted subterminally, with cirrophores indistinct. Notochaetae absent, neurochaetae begin on segment 1, with at least two aciculae per neuropodium. Neurochaetae numerous (at least 50), compound, with blades finely serrated on one side (Fig. 13E). Median and dorsal blades appearing longer than ventral blades. Pygidial cirri and papillae either absent or not observed (Fig. 13F).

Distribution. IN2017_V03, Station 100. Pilot whale carcass, off Byron Bay, New South Wales, Australia in 999–1013 m.

Etymology. The species is named in honour of Dr Tim O'Hara of Museums Victoria, Australia, the Chief Scientist of the "Sampling the Abyss" voyage, for enabling the deep-sea discoveries herein.

Remarks. Our phylogenetic analysis (Fig. 12) resolves IN2017_V03 *Vrijenhoekia timoharai* sp. nov. as being a new *Vrijenhoekia* species, most closely related to *Vrijenhoekia ahabi* Summers, Pleijel, & Rouse, 2015 (pp 1.0), described from a whale fall in Monterey Canyon off California at 2893 m depth, from which it demonstrates an uncorrected COI genetic distance of 6% (Table S15). In general, for the genus, *V. timoharai* sp. nov. shows 6–19% distance to all other *Vrijenhoekia* species while a genetic distance of 0.8% was observed between the two individuals sequenced. *Vrijenhoekia timoharai* sp. nov. has the shallowest distribution in this genus

to date (all others were collected at ~2890 m depth), being closest to that of an undescribed *Vrijenhoekia* species from the Guaymas Basin reported from 1562 m (Summers *et al.*, 2015). According to the species authors, it is not possible to distinguish the three *Vrijenhoekia* species *V. ahabi*, *V. ketea* Summers, Pleijel, & Rouse, 2015 and *V. falenothiras* Summers, Pleijel, & Rouse, 2015 morphologically, despite significant genetic differences between them. IN2017_V03 *V. timoharai* sp. nov. is larger than *V. ahabi*, being closer in size to *V. ketea* but not as large as *Vrijenhoekia balaenophila* Pleijel, Rouse, Ruta, Wiklund, & Nygren, 2008. In comparison to *V. ahabi*, *V. ketea*, and *V. falenothiras*, *V. timoharai* sp. nov. has a distinctly bulbous facial tubercle that distinguishes it from the former species, as well as less elongated parapodia and slightly longer dorsal cirri.

Nereididae Blainville, 1818

Neanthes Kinberg, 1865

Neanthes adriangloveri sp. nov.

urn:lsid:zoobank.org:act:15430CA5-8D8A-4C21-8EBD-0F1547AAE835

Fig. 14

Neanthes sp. 2. Gunton *et al.*, 2021: 70–71, fig. 15E, F

Holotype: AM W.53703, IN2017_V03_100; 9 June 2017; off Byron Bay, NSW, Australia, beam trawl, start: 28.05°S 154.08°E, 999 m, end: 28.10°S 154.08°E, 1013 m.

Description. Holotype posteriorly incomplete, 41 mm long for 54 chaetigers and with maximum width of 2.6 mm. Body shape cylindrical, tapering towards pygidium. Live specimen with reddish iridescent colouration (Fig. 14A), with a distinct bright red dorsal blood vessel in the anterior half of the specimen. Ethanol-preserved specimen pale yellow.

Prostomium (Fig. 14B) trapezoidal, as wide as long, with dorsal depression that extends from anterior tip to almost posterior margin of prostomium. One pair of cirriform, distally tapering antennae, of similar length to palps. One pair of palps, with robust cylindrical palpophores and smaller broadly conical palpostyles. One pair of eyes faintly visible on living specimen (Fig. 14A), but not discernible after preservation (Fig. 14B); eyes very small, reddish, located near the posterior margin of prostomium. Tentacular belt (first adult annulus) almost twice as long as the first chaetiger (somewhat distorted by the slightly everted pharynx), with four pairs of tentacular cirri. Tentacular cirri with short, cylindrical cirrophores and cirriform, distally tapering styles; the postero-dorsal pair longest extending to the third or fourth chaetiger (Fig. 14B); the ventral pair short with styles reaching the length of palps.

Pharynx with smooth brown jaws with 9 teeth on cutting edge. Paragnaths all conical, arranged as follows: Area I—3 paragnaths longitudinally aligned; II—16–17 paragnaths in a patch of 3 rows; III—cluster of >60 paragnaths in rectangular patch 4–5 rows deep; IV—cluster of >30 paragnaths in each triangular patch; V—none; VI—circular cluster of 7–9 paragnaths; VII–VIII—>120 paragnaths in two bands, with slightly smaller paragnaths distally; bands joined by a series of paragnaths in the pharyngeal grooves (absent on the ridges).



Figure 13. *Vrijenhoekia timoharai* sp. nov. holotype AM W.53702. (A) Ethanol-preserved entire specimen (prostomium features have been outlined in grey for clarity), scale bar is 1 mm; (B) dorsal view of prostomium stained with Shirlastain, scale bar is 500 μ m; (C) ventral view of partially everted pharynx stained with Shirlastain, scale bar is 1 mm; (D) parapodium, scale bar is 200 μ m; (E) neurochaetae, scale bar is 30 μ m; (F) dorsal view of pygidium, scale bar is 500 μ m. Abbreviations: *a*, antennae; *ft*, facial tubercle; *ma*, median antennae; *no*, nuchal organ; *pp*, palpophore; *ps*, palpostyle; *dc*, dorsal cirri; *dcp*, dorsal cirriphore; *nra*, neuroacicula; *vc*, ventral cirri; *chb*, chaetal blade; *chs*, chaetal shaft.

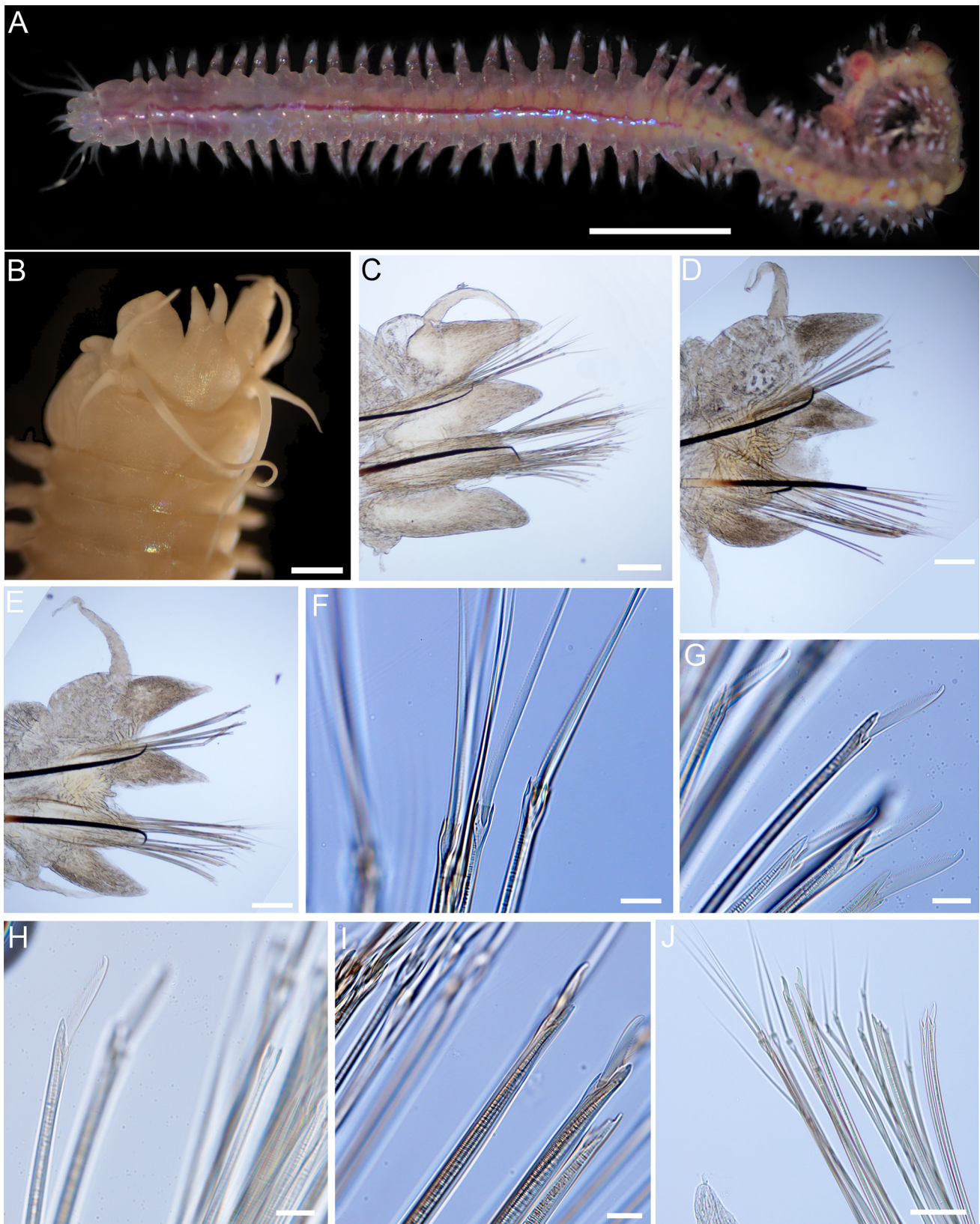


Figure 14. *Neanthes adriangloveri* sp. nov., holotype AM W.53703. (A) Live specimen, scale bar is 5 mm; (B) detail of prostomium, scale bar is 500 μm ; (C) anterior parapodium (number 5), scale bar is 200 μm ; (D) mid-body parapodium (number 35), scale bar is 200 μm ; (E) parapodium from near end of incomplete holotype specimen (number 48), scale bar is 200 μm ; (F) notospinigers (parapodium number 5), scale bar is 20 μm ; (G) subneurofalcigers (parapodium number 5), scale bar is 20 μm ; (H) supraneurofalcigers (parapodium number 5), scale bar is 20 μm ; (I) supraneurofalcigers (parapodium number 35), scale bar is 20 μm ; (J) neuropodium of parapodium number 48, scale bar is 100 μm .

First two chaetigers sub-biramous (notoaciculæ absent), following biramous (with two acicula) (Fig. 14C–E). Dorsal cirri on sub-biramous chaetigers slightly longer and inserted at base of dorsal notopodial ligules. Dorsal notopodial ligule and ventral notopodial ligules similar conical shape and size, slightly longer than neuropodial ligules. Ventral cirri of a similar length to ventral neuropodial ligules.

Parapodia of biramous chaetigers (Fig. 14C–E) with notopodial dorsal cirri inserted at the base of, and up to 1.5 times length of dorsal notopodial ligules, longest in anterior third of specimen; those of mid and posterior body area heavily vascularized (Fig. 14D–E). Biramous parapodia progressively changing throughout the body in form and size (Fig. 14C–E), becoming smaller posteriorly. Anterior notopodia (Fig. 14C) with long smooth dorsal cirrus, approximately 1.5× the length of corresponding dorsal notopodial ligule; dorsal notopodial ligule large and broadly conical, prechaetal lobe reduced, ventral notopodial ligule large and conical, slightly smaller than dorsal ligule. Anterior neuropodia (Fig. 14C) with prechaetal ligule short, conical, postchaetal ligule broad and low; ventral ligule broadly conical, extending just short of postchaetal ligule; ventral cirrus slender, cirriform distally tapering, approaching the length of ventral ligule. Mid-body notopodia (Fig. 14D) with smooth dorsal cirrus shorter than in anterior parapodia, but slightly exceeding the length of the corresponding dorsal ligule to which it is medially attached; dorsal ligule as for anterior ones, prechaetal lobe and ventral notopodial ligules as for anterior ones. Mid-body neuropodia (Fig. 14D) with prechaetal and postchaetal ligules as for anterior ones; ventral ligule broadly conical extending to level of corresponding postchaetal ligule; ventral cirrus slender, cirriform and distinctly shorter than corresponding ligule. Posterior notopodia (Fig. 14E) with smooth dorsal cirrus approximately 1.5× length of corresponding dorsal ligule to which it is medially attached; dorsal notopodial ligule as for anterior ones, except somewhat constricted at the attachment of dorsal cirrus as basal portion appearing highly vascularized (possible early epitokal modification); prechaetal and ventral notopodial ligules as for anterior ones. Posterior neuropodia (Fig. 14E) with prechaetal and postchaetal ligules as for anterior ones (Fig. 14C); ventral ligule as for mid-body ones (Fig. 14D); ventral cirrus slender, cirriform and extending just short of corresponding ligule (Fig. 14E).

Chaetae of three main types: homogomph and heterogomph spinigers and heterogomph falcigers (Fig. 14F–J). Blades of spinigers finely serrated (Fig. 14F), blades of falcigers unidentate (with a tendon), finely serrated along their entire length, 20–30 teeth (Fig. 14G–I). Their presence/absence and number changing throughout the body. Each ramus with dark internal acicula (Fig. 14C–E); notoaciculæ slightly curved distally; neuroaciculæ curved almost 90° distally. In anterior parapodia (represented by chaetiger 5) the chaetae as follows: notochaetae all supra-acicular, 11 per fascicle all homogomph spinigers; supra-acicular

neurochaetae consisting of 12 homogomph spinigers and 7 heterogomph falcigers; sub-acicular neurochaetae composed of 3 heterogomph spinigers and 17 heterogomph falcigers. In mid-body parapodia (represented by chaetiger 35) the chaetae are as follow: notochaetae all supra-acicular, 7 per fascicle all homogomph spinigers; supra-acicular neurochaetae consisting of 12 homogomph spinigers and 3 heterogomph falcigers; sub-acicular neurochaetae composed of 6 heterogomph spinigers and ~3 heterogomph falcigers. In posterior parapodia (represented by chaetiger 48) the chaetae as follows: all notochaetae homogomph spinigers, 5 per fascicle; supra-acicular neurochaetae composed of 10 homogomph spinigers and 2 heterogomph falcigers, sub-acicular neurochaetae composed of 5 heterogomph spinigers and 4 heterogomph falcigers (Fig. 14J).

Pygidium not observed (missing) on holotype AM W.53703.

Distribution. IN2017_V03, Station 100. Pilot whale carcass, off Byron Bay, New South Wales, Australia in 999–1013 m.

Etymology. This species is named in honour of Dr Adrian Glover of the Natural History Museum, United Kingdom, deep-sea biologist and polychaetologist, for his work with whale-fall fauna.

Remarks. We were unable to obtain molecular data for this species. The presence of visible eyes (albeit only one pair rather than the typical two pairs) in living specimens distinguishes *N. adriangloveri* sp. nov. from the deep-sea *Neanthes* species *Neanthes shinkai* Shimabukuro, Santos, Alfaro-Lucas, Fujiwara, & Sumida, 2017, *Neanthes abyssorum* Hartman, 1967, *Neanthes kermadeca* (Kirkegaard, 1995), and *Neanthes typhla* (Monro, 1930). The eyes of *N. adriangloveri* sp. nov. are also different from those of the deep-sea *Neanthes* species with large or four clearly visible eyes, such as *Neanthes goodayi* Drennan, Wiklund, Rabone, Georgieva, Dahlgren, & Glover, 2021 and *Neanthes suluensis* Kirkegaard, 1995. In comparison to the geographically close deep-sea *Neanthes* species *Neanthes articulata* Knox, 1960 (type locality: Chatham Islands), *Neanthes kerguelensis* (McIntosh, 1885) (Kerguelen Islands), *Neanthes papillosa* (Day, 1963) (off Cape Town) and *Neanthes donggungensis* Hsueh, 2019 (off Taiwan), *N. adriangloveri* sp. nov. has a greater number of paragnaths in most pharyngeal regions compared to *N. articulata*. *Neanthes kerguelensis* has much longer tentacular cirri compared to *N. adriangloveri* sp. nov., *N. papillosa* has neuropodial falcigers that are all heterogomph with long blades and slender tips, and *N. donggungensis* has a larger and thicker body. Finally, the most notable features of this species, which in combination potentially distinguish it from all other *Neanthes*—the presence of a single pair of eyes and distally curved aciculæ (especially pronounced in the neuropodia)—both require further assessment based on more specimens: small eyes that are only visible in live specimens may easily be overlooked and bent aciculæ may be attributable to muscle contraction during preservation.

Neanthes visicete sp. nov.

urn:lsid:zoobank.org:act:18CD5A8D-DFB6-4E46-9694-FA3EC5D5E51E

Fig. 15

Neanthes sp. 1. Gunton *et al.*, 2021: 70–71, fig. 15C, D

Holotype: AM W.53704, IN2017_V03_100; 9 June 2017; off Byron Bay, NSW, Australia, beam trawl, start: 28.05°S 154.08°E, 999 m, end: 28.10°S 154.08°E, 1013 m. **Paratype:** AM W.52209, same locality as holotype. DNA vouchers: AM W.53704 (COI, 16S, 18S), AM W.52209 (16S).

Description. Holotype complete, pinkish-purple when alive, with whitish notopodial ligules and noticeable iridescence (Fig. 15A); 85 chaetigers, up to 50 mm long and a maximum of 2.6 mm wide (without parapodia), tapering towards posterior.

Prostomium (Fig. 15B) trapezoidal, longer than wide, with a dorsal depression that extends from anterior tip to just below eyes. One pair of short antennae approximately one-quarter length of prostomium and one pair of elongated palps with cylindrical palpophore and oval-shaped palpostyle, extending just beyond antennae. Two pairs of eyes, anterior pair roughly oval-shaped, posterior pair slightly larger, kidney-shaped, and slightly closer together.

Tentacular belt (first adult annulus) slightly longer than first chaetiger, with four pairs of tentacular cirri each with distinct cirrophores; posterodorsal pair longest, extending back to fifth chaetiger. Pharynx with smooth brown jaws and 7 or 8 teeth on cutting edge, paragnaths all conical. Paragnath arrangement as follows: Areas I—13 paragnaths; II—rectangular cluster of ≥ 30 paragnaths; III—widely spaced rectangular cluster of *c.* 45 paragnaths; IV—dense triangular cluster of *c.* 50 paragnaths; V—none; VI—small circular cluster of 6–8 paragnaths; VII–VIII—strip of *c.* 50 paragnaths arranged in 2 or 3 rows.

Chaetigers 1–2 sub-biramous (notoacaculae absent), followed by biramous chaetigers. Sub-biramous chaetigers with dorsal cirri slightly shorter than dorsal notopodial ligule; dorsal cirri inserted at base of ligule. Dorsal notopodial ligule of similar shape and length as ventral notopodial ligule; conical and slightly shorter than neuroacicular ligule. Ventral cirri slightly shorter than ventral neuropodial ligule (two-thirds of length).

Parapodia of biramous chaetigers (Fig. 15C, E–G) with notopodia larger than neuropodia, notopodial dorsal cirri inserted at base of, and slightly shorter than (around two-thirds length) or same length as dorsal notopodia ligules. Notopodium consisting of three similar-sized ligules/lobes: dorsal notopodial ligule conical and prominent, largest structure of parapodia; prechaetal notopodial lobe slightly smaller than dorsal notopodial ligule anteriorly, $\frac{2}{3}$ its length in mid-body and $\frac{1}{2}$ its length posteriorly; ventral notopodial ligule conical, slightly smaller than dorsal notopodial ligule throughout. Neuropodia with three distinct lobes/ligules:

prechaetal neuropodial lobe conical, approximately $\frac{2}{3}$ length of postchaetal lobe anteriorly and posteriorly, pre- and postchaetal lobes approximately equal in size in mid-body; ventral ligule conical, extending just short of pre- and postchaetal lobes in anterior and mid-body, equal to those lobes in posterior body.

Notochaetae (Fig. 15H) all homogomph spinigers arising from supra-acicular fascicle. Neurochaetae (Fig. 15I–L) arranged in sub- and supra-acicular fascicles, both with homogomph spinigers; homogomph (and sesquigomph) falcigers present in both fascicles anteriorly, falcigers only present in ventral fascicle in mid-body and by posterior body absent altogether. Blades of spinigers and falcigers finely serrated (Fig. 15K–L); spiniger blade length decreasing from dorsal to ventral side; falciger blades elongate, unidentate, and very finely serrated along entire length. Dark noto- and neuroacaculae present in each ramus of the biramous parapodia (Fig. 15E–G); notoacaculae slightly curved upward distally; neuroacaculae more or less straight.

In anterior parapodia (represented by chaetiger 13 and 14): notochaetae comprising 12–14 homogomph spinigers per fascicle; supra-acicular neurochaetae comprising 8–10 homogomph spinigers and 3–4 homogomph/sesquigomph falcigers; sub-acicular neurochaetae comprising 7–13 homogomph spinigers and 6–8 homogomph/sesquigomph falcigers. In mid-body parapodia (represented by chaetiger 28): notochaetae comprising 21 homogomph spinigers per fascicle; supra-acicular neurochaetae comprising 12 homogomph spinigers (homogomph/sesquigomph falcigers have disappeared); sub-acicular neurochaetae comprising 16 homogomph spinigers and 3 homogomph/sesquigomph falcigers. In posterior parapodia (represented by chaetiger 67): notochaetae comprising 14 homogomph spinigers per fascicle; supra-acicular neurochaetae comprising 7 homogomph spinigers (homogomph/sesquigomph falcigers not present); sub-acicular neurochaetae comprising 10 homogomph spinigers (homogomph/sesquigomph falcigers not present).

Pygidium (Fig. 15D) with distinct ventral lobe, pygidial cirri probably absent (no obvious cirri scars on the pygidial rim or ventral lobe) or lost.

Distribution. IN2017_V03, Station 100. Pilot whale carcass, off Byron Bay, New South Wales, Australia in 999–1013 m.

Etymology. Named derived from the Latin root “visitar” for a visitor, and “cete”, a whale, referring to the new species’ occurrence on a whale fall. Noun in apposition.

Remarks. Our Nereididae molecular phylogeny (Fig. 16) resolves *Neanthes visicete* sp. nov. in a clade with *Neanthes acuminata* Ehlers, 1868, however, with poor support. While a Nereididae phylogenetic analysis by Villalobos-Guerrero *et al.* (2022) recovered *Alitta* and *Nectoneanthes* in a clade with *Neanthes acuminata*, *Alitta*, and *Nectoneanthes* occurred in a separate clade in our phylogenetic analysis,

Figure 15 (facing page). *Neanthes visicete* sp. nov., holotype specimen AM W.53704. (A) Living complete individual, scale bar is 5 mm; (B) detail of prostomium, scale bar is 1 mm; (C) detail of parapodia from middle of body, scale bar is 500 μ m; (D) detail of ventral side of pygidium, scale bar is 500 μ m; (E) anterior parapodium (number 13), scale bar is 250 μ m; (F) mid-body parapodium (number 28), scale bar is 100 μ m; (G) parapodium from near posterior (number 67), scale bar is 200 μ m; (H) notopodial homogomph spinigers, scale bar is 50 μ m; (I) neuropodial homogomph spinigers and homogomph falcigers, dorsal fascicle, scale bar is 50 μ m; (J) neuropodial homogomph spinigers and homogomph falcigers, ventral fascicle, scale bar is 50 μ m; (K) neuropodial supra-acicular homogomph spinigers, scale bar is 20 μ m; (L) neuropodial sub-acicular long and short-bladed spinigers, scale bar is 20 μ m. Abbreviations: hos, homogomph spiniger; hof, homogomph falciger.

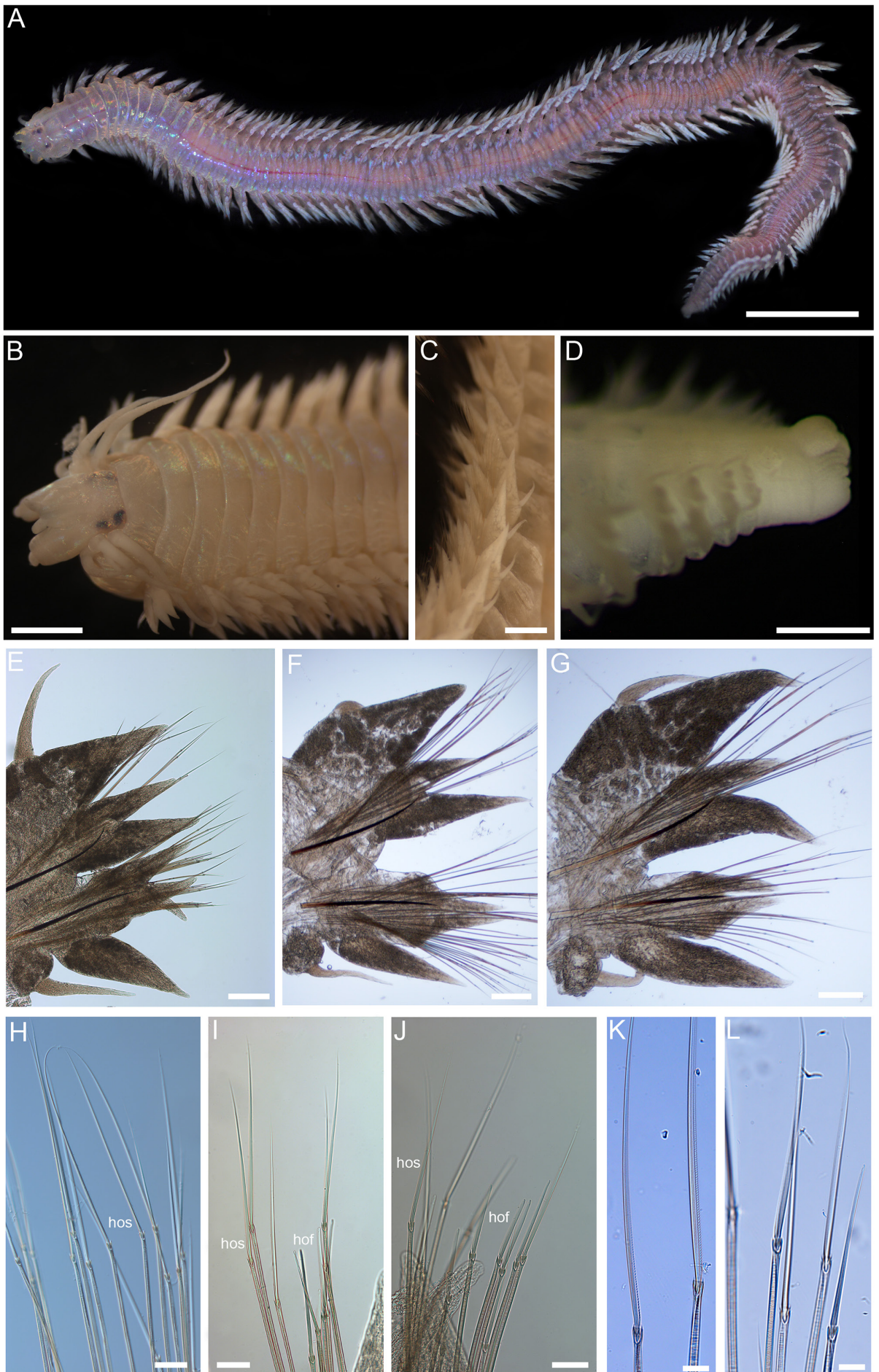


Figure 15. See caption on facing page.

2021), but these specimens have very large eyes and are thus again clearly distinguishable from *N. visicete* sp. nov.

Neanthes visicete sp. nov. and *Neanthes adriangloveri* sp. nov. are only the second and third formally described *Neanthes* to be found associated with a whale fall. The first, *N. shinkai*, was described from abyssal depths of the south-west Atlantic. This species is quite different from the two new *Neanthes* species described here in lacking prechaetal notopodial lobes, postchaetal neuropodial lobes and eyes; in these features and in our molecular phylogeny *N. shinkai* more closely resembles our *Nereis* sp. (see following account). Shimabukuro *et al.* (2017) analysed the carbon and nitrogen isotopes of *N. shinkai* and concluded that it was an omnivore that was feeding mainly on the organic matter from the whale.

Comparative morphology. Although *Neanthes* is one of the most species-rich genera of Nereididae with about 80 valid species, only 25 species share with *N. visicete* sp. nov. some important parapodial features including dorsal notopodial ligule that is similar sized along the body (as opposed to enlarged posteriorly), presence of prechaetal notopodial lobes and presence of a postchaetal neuropodial lobe (Villalobos-Guerrero & Idris, 2021, table 2). This group of 25 can be narrowed down to nine by including an unusual feature of the new species, the presence of homogomph spinigers in the sub-acicular fascicle of the neuropodia: *N. acuminata*, *N. arenaceodentata*, *N. articulata*, *Neanthes chingrighattensis* (Fauvel, 1932), *N. cricognatha*, *N. kerguelensis*, *N. picteti* (Malaquin & Dehorne, 1907), *N. pleijeli* de León-González & Salazar-Vallejo, 2003 and *N. suluensis*. Considering the paragnath numbers of these nine species, the new species is—as also found using molecular data—closest to *Neanthes acuminata*, *N. arenaceodentata* and *N. cricognatha*, but differs in having a greater number of paragnaths in Area III (c. 45 vs 23–28 in *acuminata*; 20–34 in *N. cricognatha*), and fewer in this area than *arenaceodentata* (82) and having paragnaths absent in Area V, vs present and merging with a broad band of paragnaths in Areas VII–VIII in *N. acuminata*, *N. arenaceodentata* and *N. cricognatha*. *Neanthes visicete* sp. nov. has a high number of paragnaths in Area I (13) which distinguishes it from *N. articulata* (1), *N. chingrighattensis* (2–6; *chingrighattensis* also has the unusual presence of a neuropodial superior lobe which is absent in the new species), *N. kerguelensis* (0–4), *N. picteti* (2) and *N. pleijeli* (2). The new species can be distinguished from the poorly known *N. suluensis* by having 2 or 3 rows of paragnaths in Areas VII–VIII (only 1 in *suluensis*). Finally, the new species can be distinguished from all known *Neanthes* species by lacking heterogomph falcigers, by its distinct ventral pygidial lobe (although pygidial features are poorly known in Nereididae), and its distinctive living colouration (pinkish-purple with whitish dorsal notopodial ligules and noticeable iridescence).

The presence of a large prechaetal notopodial lobes throughout the body in the new species (and the *N. acuminata* species complex), such that the notopodia appear to have three similar-sized lobes/ligules, also occurs in *Alitta*, *Nectoneanthes* and *Leonnates* (Bakken, 2006; Bakken *et al.*, 2022). One might therefore question the placement of the new species in *Neanthes* considering its lack of heterogomph falcigers; however, the new species is here treated as a *Neanthes* because it lacks the presence of an expanded dorsal

notopodial ligule of *Alitta*, it lacks the ovoid lobe above the dorsal cirrus of *Nectoneanthes*, and the oral ring papillae of *Leonnates*.

Although closest to *Neanthes* in overall morphology (because the concept of *Neanthes* is currently so broad), the species does not fit the current definition of *Neanthes* (Bakken *et al.*, 2022; Villalobos-Guerrero *et al.*, 2022), because of its lack of neuropodial heterogomph falcigers. It has homogomph and sesquigomph falcigers, and they are restricted to anterior and mid-body chaetigers. This emendation is best made in a future revision of the genus.

Nereis Linnaeus, 1758

Nereis sp.

Fig. 17

Material examined. NHMUK ANEA 2022.436, AM W.52210, IN2017_V03_100; 9 June 2017; off Byron Bay, NSW, Australia, beam trawl, start: 28.05°S 154.08°E, 999 m, end: 28.10°S 154.08°E, 1013 m. DNA vouchers: NHMUK ANEA 2022.436 (COI, 16S, 18S), AM W.52210 (16S).

Description. The best-preserved specimen NHMUK.2022.436 complete (Fig. 17A), 14.2 mm long and a maximum of 1.3 mm wide (excluding parapodia) for 55 chaetigers. Pharynx partially extended, body tapering towards the posterior. Specimen not observed alive, colour in ethanol pale yellow (Fig. 17A).

Specimen AM W.52210 posteriorly incomplete, 8.2 mm long and a maximum width of 0.9 mm (excluding parapodia) for 33 chaetigers; in moderately poor condition probably due to fixation in ethanol resulting in paragnath shedding and most cirri and some ligules/lobes in process of falling off.

Prostomium trapezoid (Fig. 17B), approximately as wide as long. One pair of cirriform, distally tapering antennae, approximately the same length as palps. One pair of robust palps, with cylindrical palpophores and smaller oval palpstyles. Eyes not observed. Tentacular belt (first adult annulus) approximately 1.5× length of the subsequent segments, with four pairs of tentacular cirri. Tentacular cirri with cylindrical tentaculophores, only two shorter pairs with styles attached, styles smooth not extending beyond prostomium (Fig. 17B).

Pharynx partially everted (Fig. 17C), with brown jaws with 9 teeth on cutting edge. Paragnaths all small (of similar size), conical, dark brown in colour and arranged as follows: Area I—2 paragnaths; II—cluster of 14–16 paragnaths; III—0–3 paragnaths (unclear, possibly damaged during dissection); IV—9 paragnaths; V—none; VI—6 paragnaths; VII–VIII—30–40 small paragnaths arranged in two irregular rows.

First two chaetigers uniramous, the following biramous. Dorsal cirri on uniramous chaetigers slightly longer and inserted at the base of dorsal notopodial ligules. Dorsal and ventral ligules a similar conical shape and size, slightly longer than ligules adjacent to chaetae. Ventral cirri of a similar length to ventral ligules.

Biramous parapodia progressively change throughout the body in form and size, becoming smaller posteriorly (Fig. 17D–17F). Anterior notopodia (Fig. 17D) with long smooth dorsal cirrus, approximately twice the length of

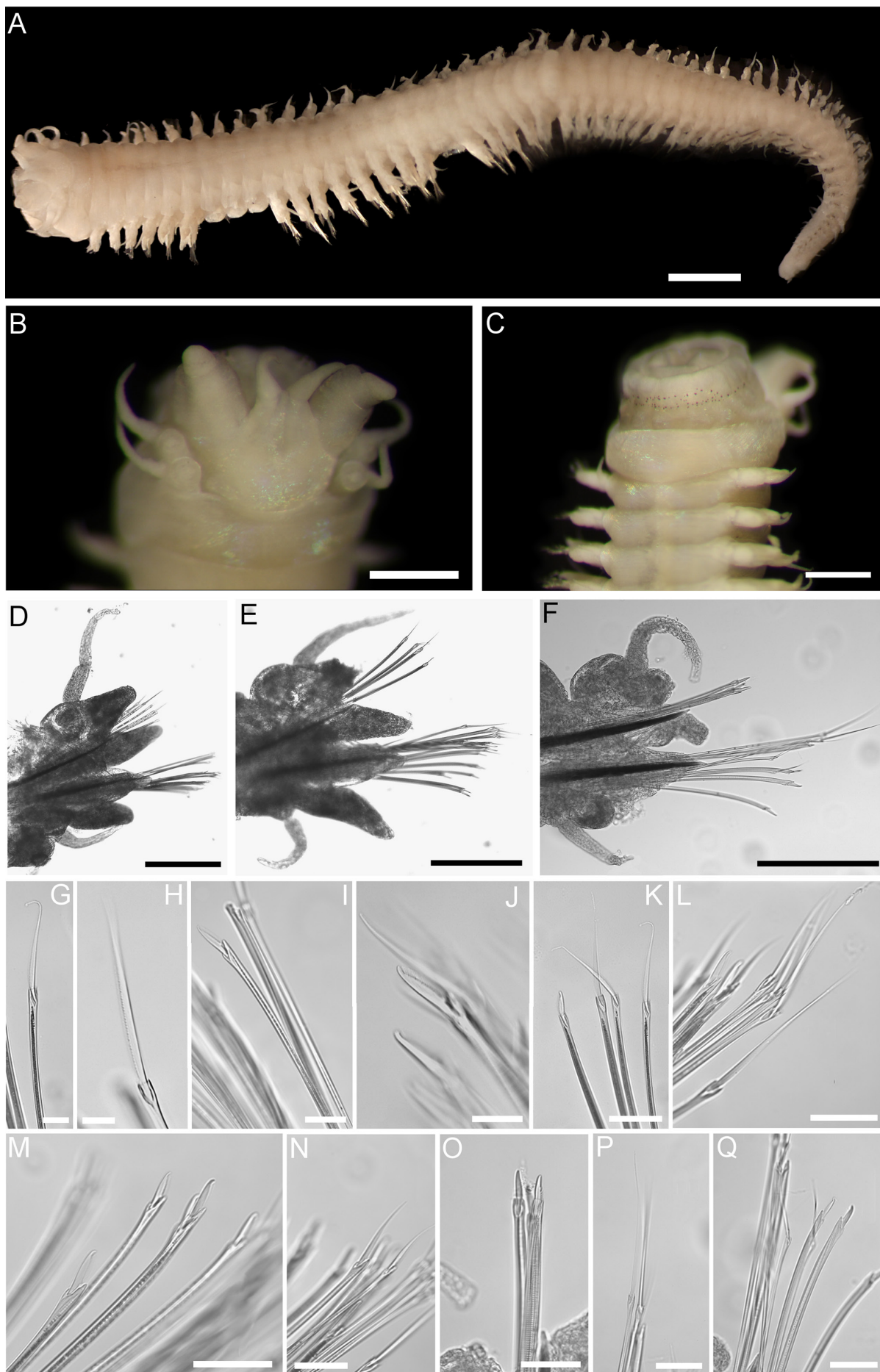


Figure 17. See caption on facing page.

corresponding dorsal ligule (Fig. 17D); dorsal ligule large and broadly conical, prechaetal ligule reduced, postchaetal ligule large and conical, similar to dorsal ligule (Fig. 17D). Anterior neuropodia (Fig. 17D) with prechaetal ligule short, broadly conical (Fig. 17D), postchaetal ligule elongated and conical (Fig. 17D); ventral ligule broadly conical, just shorter than postchaetal ligule; ventral cirrus slender, cirriform distally tapering, approaching the length of ventral ligule. Mid-body notopodia (Fig. 17E) with smooth dorsal cirrus shorter than in anterior parapodia, but greatly exceeding the length of the corresponding dorsal ligule to which it is medially attached; dorsal ligule short and very broad (Fig. 17E), prechaetal ligule short and broadly conical (Fig. 17E), postchaetal ligule very elongated, conical (Fig. 17E). Mid-body neuropodia (Fig. 17E) with reduced prechaetal ligule (Fig. 17E), postchaetal ligule very elongated, conical (Fig. 17E); ventral ligule elongated, relatively narrow and conical (Fig. 17E), approximately same length as corresponding postchaetal ligule; ventral cirrus slender, cirriform and distinctly shorter than corresponding ligule. Posterior notopodia (Fig. 17F) with smooth dorsal cirrus shorter than in preceding notopodia but exceeding the length of corresponding dorsal ligule to which it is medially attached (Fig. 17F); dorsal ligule very short and broad somewhat constricted at the attachment of dorsal cirrus; prechaetal ligule short and broad, tapering into sharp tip (Fig. 17F), postchaetal ligule elongated, distally rounded (Fig. 17F). Posterior neuropodia (Fig. 17F) with prechaetal ligule reduced (Fig. 17F), postchaetal ligule elongated, conical with sharp tip (Fig. 17F); ventral ligule short and rounded; ventral cirrus slender, cirriform and distinctly longer than corresponding ligule (Fig. 17F).

Chaetae of two main types as spinigers and falcigers, both can be homogomph or heterogomph. All blades of spinigers finely serrated, all blades of falcigers unidentate, serrated. Presence/absence of chaetae and their number changes throughout the body. Each ramus with a straight, dark internal acicula (Fig. 17D–F). In anterior parapodia (represented by chaetigers 6, 7) the chaetae as follows (Fig. 17G–J): notochaetae all supra-acicular, 4–7 per fascicle all homogomph spinigers; supra-acicular neurochaetae consisting of 1–3 homogomph spinigers and 1–2 heterogomph falcigers; sub-acicular neurochaetae composed of 8–10 heterogomph falcigers. In mid-body parapodia (represented by chaetigers 20, 22) the chaetae as follows (Fig. 17K–N): notochaetae all supra-acicular, 4

per fascicle consisting of 1–3 homogomph spinigers and 1–2 homogomph falcigers; supra-acicular neurochaetae consisting of 4–5 homogomph spinigers with particularly long blades and 1–2 heterogomph falcigers; sub-acicular neurochaetae composed of 0–2 heterogomph spinigers and 3–7 heterogomph falcigers. In posterior parapodia (represented by chaetiger 36) the chaetae as follows (Fig. 17O–Q): all notochaetae homogomph falcigers, 3 per fascicle; supra-acicular neurochaetae composed of 2 homogomph spinigers and 2 heterogomph falcigers; sub-acicular neurochaetae composed of 3 heterogomph spinigers and 3 heterogomph falcigers.

Pygidium rounded; cirri not observed.

Distribution. IN2017_V03, Station 100. Pilot whale carcass, off Byron Bay, New South Wales, Australia in 999–1013 m.

Remarks. Two specimens collected as part of this study likely belong to genus *Nereis*, as they possess homogomph falcigers in the posterior notopodia. The description above builds upon that of Gunton *et al.* (2021; referred to as *Nereis* sp. 1) which was based on one of the two specimens examined here; despite the additional morphological information from the second specimen and the support from sequence data, we are reluctant to formally name the new species for the reasons below.

Nereis is currently the most species-rich genus within Nereididae, with many deep-water species, a problematic taxonomic history, morphological characters affected by the reproductive status of the specimen as well as exhibiting a high level of homoplasy (e.g., Bakken & Wilson, 2005; Santos *et al.*, 2006). Further, molecular information obtained from the specimens included in this study suggests that specimens identified here as *Nereis* sp. are genetically similar to *Neanthes shinkai* (Fig. 16; COI genetic *p*-distance between *Nereis* sp. and *Neanthes shinkai* was 12.6%; Table S16); *N. shinkai* is also described from a whale fall, but one located at 4200 m depth on the São Paulo Ridge in the Southwest Atlantic (Shimabukuro *et al.*, 2017). A number of other *Nereis* species are also included in the well-supported clade containing *Nereis* sp. and *Neanthes shinkai* (Fig. 16). We are also aware of colleagues who are in the process of describing a new eyeless species of *Nereis* from the southwest Atlantic, and there is a chance that it could be the same as our IN2017_V03 specimens. Solving taxonomic problems is beyond the remit of this study and as a result we assign the specimens to genus only.

Figure 17 (facing page). *Nereis* sp., specimen NHMUK ANEA 2022.436. (A) Complete preserved specimen, dorsal view, scale bar is 1 mm; (B) detail of prostomium in dorsal view, scale bar is 500 µm; (C) partially everted pharynx, scale bar is 500 µm; (D) anterior parapodium (number 6), scale bar is 250 µm; (E) mid-body parapodium (number 20), scale bar is 250 µm; (F) parapodium from near posterior (number 36), scale bar is 250 µm. G–Q, chaetal types; A–D from 6th parapodium, E–H from 20th parapodium, I–K from 36th parapodium; (G) notopodial homogomph spiniger, scale bar is 25 µm; (H) neuropodial supra-acicular homogomph spiniger, scale bar is 25 µm; (I) neuropodial supra-acicular heterogomph falciger, scale bar is 50 µm; (J) neuropodial sub-acicular heterogomph falciger, scale bar is 25 µm; (K) notochaetal bundle, scale bar is 50 µm; (L) neurochaetal supra-acicular bundle, scale bar is 50 µm; (M) neuropodial sub-acicular heterogomph falcigers, scale bar is 50 µm; (N) neuropodial sub-acicular heterogomph spinigers, scale bar is 50 µm; (O) notopodial homogomph falcigers, scale bar is 50 µm; (P) neuropodial supra-acicular homogomph spinigers, scale bar is 50 µm; (Q) neuropodial sub-acicular heterogomph spinigers and falcigers, scale bar is 50 µm.

Orbiniidae Hartman, 1942***Orbiniella* Day, 1954*****Orbiniella jamesi* sp. nov.**

urn:lsid:zoobank.org:act:BECCFCE3-8F48-4E0A-B9D4-A1547389E69E

Fig. 18

Holotype: AM W.53705, IN2017_V03_100; 9 June 2017; off Byron Bay, NSW, Australia, beam trawl, start: 28.05°S 154.08°E, 999 m, end: 28.10°S 154.08°E, 1013 m. **Paratype:** AM W.52199, same locality as holotype. Other specimens examined: NHMUK ANEA 2023.1201–1202, same locality as holotype. DNA vouchers: AM W.53705 (COI), AM W.52199 (16S).

Description. Holotype AM W.53705 complete, ~8 mm long and 0.4 mm wide (widest, excluding chaetae) for ~84 chaetigers. Specimen NHMUK ANEA 2023.1201 complete, ~7 mm long and 0.4 mm wide for ~80 chaetigers. Specimen NHMUK ANEA 2023.1202 complete, ~7 mm long and 0.4 mm wide for ~80 chaetigers. Specimen AM W.52199 anterior fragment with 21 chaetigers. Body somewhat dorsoventrally flattened throughout, not divided into distinct regions; longest chaetigers in mid-body, shortest in posterior body; posterior parapodia not dorsally elevated. Live specimen (holotype AM W.53705) reddish in colour (Fig. 18A), ethanol-preserved specimen off-white (Fig. 18B).

Prostomium bluntly conical (Fig. 18C), without appendages, eyes absent. Nuchal organs only detected as lateral pits on prostomium. Peristomium approximately twice as long as prostomium, weakly annulated dorsally, but distinct annulation observed ventrally, with two achaetous rings of similar size.

Notopodia low mounds from which chaetae emerge (Fig. 18D); neuropodial postchaetal lobes from chaetiger 4 (5 in specimen AM W.52199), extending posteriorly to approximately start of branchiate region, whereafter they appear to be absent (or minute); best developed about mid-body where they slender, subconical-shaped, approximately 0.25× length of chaetae (Fig. 18E). Branchiae present; absent in anterior-most segments; becoming apparent after segment 55. Branchiae initially small and ovoid (Fig. 18F), increasing in length towards posterior to a maximum size of approximately $\frac{2}{3}$ length of chaetae, strap-like (Fig. 18G); reducing slightly in size over the last few chaetigers.

Chaetae include both crenulated capillaries (Fig. 18H) and short acicular spines (Fig. 18H) in both rami; furcate setae absent; no evidence of imbedded aciculae. Notochaetae bundles of crenulated capillaries of various lengths throughout; straight slightly serrated spines present from chaetiger 1 (up to 3 per ramus observed). Neurochaetae generally slenderer than notochaetae composed of crenulated capillaries and up to 3 spines; neuropodial spines slenderer and longer than those in notopodia, distally slightly curved into slender tip. Pygidium with two broad lobes, anal cirri not observed.

Distribution. IN2017_V03, Station 100. Pilot whale carcass, off Byron Bay, New South Wales, Australia in 999–1013 m.

Etymology. Named for James Hayhurst, for his support to one of the authors (M. Georgieva) during a multitude of scientific endeavours.

Remarks. *Orbiniella jamesi* sp. nov. specimens with neuropodial postchaetal lobes exhibit identical COI sequences to *Orbiniella* sp. without such lobes (Figs 19, 20). Support values in our phylogenetic analysis are generally low, with our specimens being resolved as most closely related to a *Scoloplos acutissimus* specimen whereas the only *Orbiniella* specimen for which genetic data was available falls outside of this group.

Specimens collected in this study belong to Orbiniidae that lack a distinct body division into thorax and abdomen regions due to a dorsal shift of chaetae. Such forms are currently included in genera *Methanoaricia*, *Orbiniella* (Parapar, Moreira, & Helgason, 2015), *Proscoplos*, *Protoariciella*, and *Uncorbinia* (Beesley *et al.*, 2000; Solis-Weiss & Fauchald, 1989; Blake, 2000; Parapar *et al.*, 2015). *Methanoaricia* however differs from orbiniid specimens presented here in having a long and narrow prostomium, while *Proscoplos* are generally small and along with *Protoariciella* and *Uncorbinia* have hooked chaetae. *Uncorbinia* has only a single described species from northwestern Australia and is considered to be a probable synonym of *Califa* (Blake, 2000).

Assignment of the IN2017_V03 orbiniid specimens to the existing genus *Orbiniella* also reflects our molecular phylogenetic results for the family Orbiniidae (Fig. 19), which largely do not demonstrate clear genetic definitions. We therefore reserve the establishment of a new genus until current genetic relationships are better known, but we proceed with the formalization of new species *Orbiniella jamesi* sp. nov. We tentatively assign the new species to genus *Orbiniella* due to possession of a broadly conical prostomium, bi-annulate peristomium, poorly developed parapodia, lack of furcate chaetae, no obvious division of body into thorax and abdomen, and no dorsal shift of parapodia.

To date, only one other orbiniid species is known from a chemosynthetic environment, *Methanoaricia dendrobranchiata* Blake, 2000. This species has large branched branchiae which may be advantageous in the generally lower oxygen conditions prevalent in these environments. It is therefore possible that branchiae might be a character common to orbiniids that occur within chemosynthetic environments, however further discoveries are necessary to verify this.

***Orbiniella* sp.**

Fig. 20

Material examined. NHMUK ANEA 2022.431, NHMUK ANEA 2022.421–430 (juveniles), AM W.52198, AM W.52200, IN2017_V03_100; 9 June 2017; off Byron Bay, NSW, Australia, beam trawl, start: 28.05°S 154.08°E, 999 m, end: 28.10°S 154.08°E, 1013 m. DNA vouchers: NHMUK

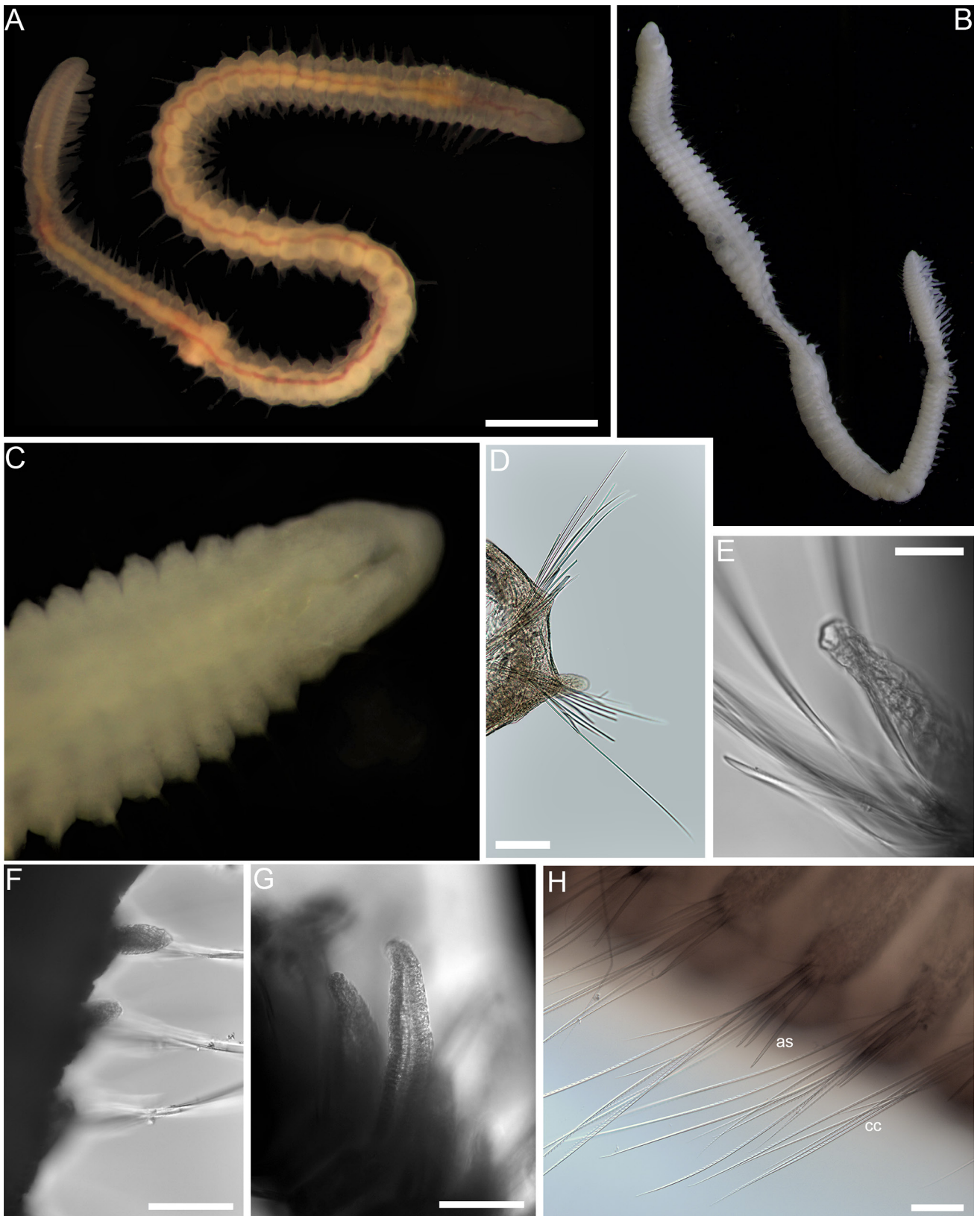


Figure 18. *Orbinella jamesi* sp. nov. (A) Live specimen (holotype AM W.53705), scale is 1 mm; (B) preserved specimen (holotype AM W.53705) in ventro-lateral view; (C) prostomium in dorsal view, NHMUK ANEA 2023.1201; (D) anterior parapodium with postchaetal lobe (holotype AM W.53705), scale bar is 100 µm; (E) mid-body neuropodial postchaetal lobe, specimen NHMUK ANEA 2023.1201, scale bar is 25 µm; (F) small ovoid branchiae, specimen NHMUK ANEA 2023.1201, scale bar is 100 µm; (G) elongated strap-like branchiae, specimen NHMUK ANEA 2023.1201, scale bar is 100 µm; (H) chaetal types (crenulated capillaries and short acicular spines) of anterior parapodia, scale is 50 µm. Abbreviations: as, acicular spines; cc, crenulated capillaries.

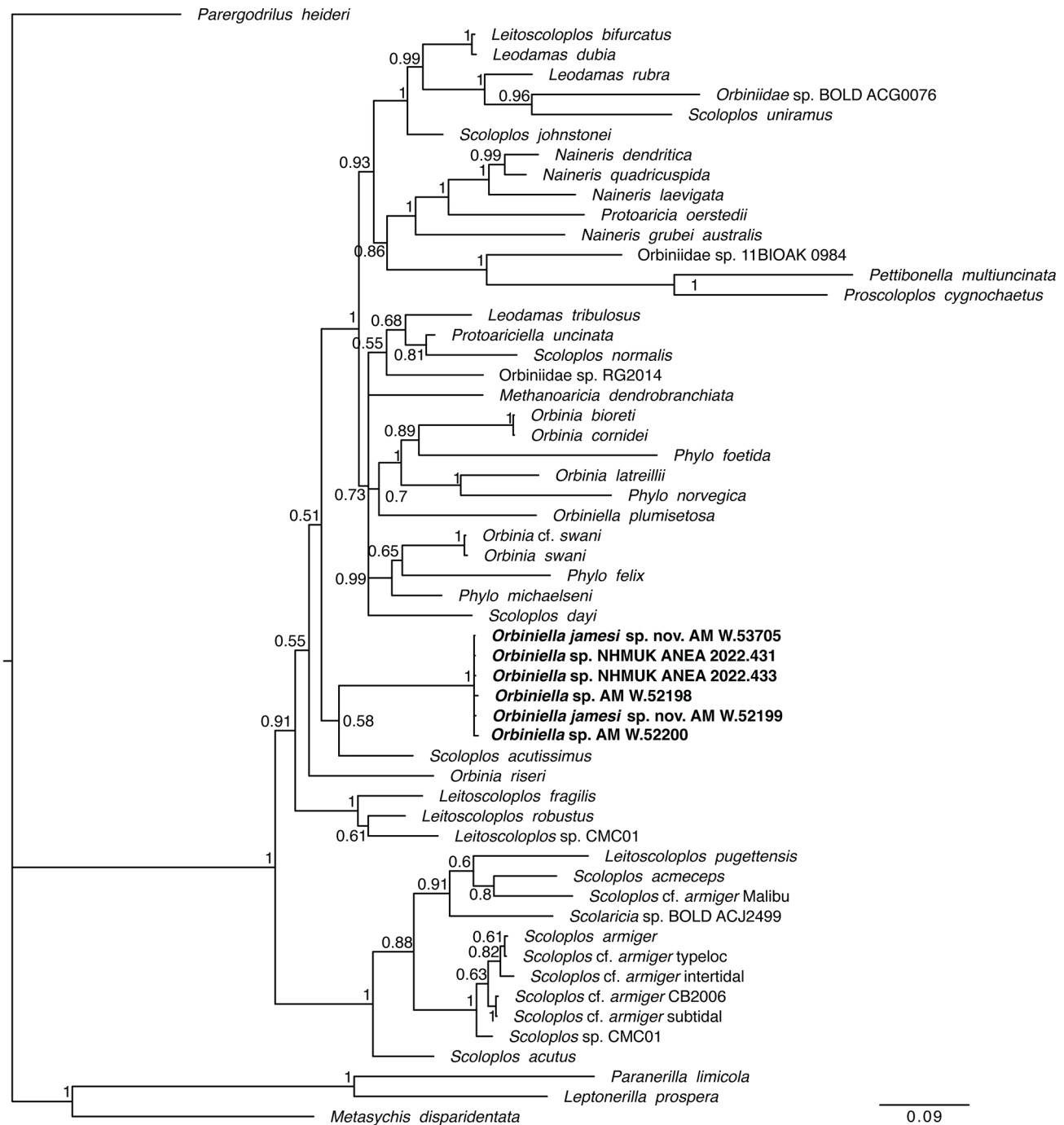


Figure 19. Phylogeny of the Orbinidae family based on Bayesian analysis of a combined dataset of the genes COI, 16S and 18S. Numbers adjacent to nodes indicate posterior probabilities, and taxa for which sequences have been contributed by the present study are indicated in bold.

ANEA 2022.431 (COI, 16S), NHMUK ANEA 2022.433 (COI, 16S), AM W.52198 (16S), AM W.52200 (16S).

Description. Best preserved specimen NHMUK ANEA 2022.431 complete, ~9 mm long and 0.7 mm wide for ~95 chaetigers. Specimen AM W.52198 anterior fragment with 15 chaetigers. Specimen AM W.52200 anterior end, with ~40 discernible chaetigers. Body somewhat dorsoventrally flattened throughout, not divided into distinct regions; individual chaetigers narrow, similar throughout; posterior parapodia not dorsally elevated (Fig. 20A). Live specimens

not observed, ethanol-preserved specimens tanned (Fig 20A).

Prostomium bluntly conical (Fig. 20B), without appendages, eyes absent. Nuchal organs only detected as lateral pits on prostomium. Peristomium approximately twice as long as prostomium, weakly annulated, but two achaetous rings likely present.

Parapodia reduced to low mounds from which chaetae emerge; no neuropodial postchaetal lobes. Branchiae present; absent in anterior-most segments and becoming apparent after approximately 30 segments in adult specimens (Fig. 20A). Branchiae initially small and conical, increasing

greatly in length towards posterior where they become strap-like, slender and elongated (Fig. 20C); greatly reduced in size again in the few posteriormost chaetigers.

Chaetae include both crenulated capillaries (Fig. 20D) and short acicular spines (Fig. 20E) in both rami; furcate setae absent; no evidence of imbedded aciculae. Notochaetae as bundles of crenulated capillaries of various lengths throughout; straight slightly serrated spines present from chaetiger 1 (up to 3 per ramus observed). Neurochaetae generally slenderer than notochaetae composed of crenulated capillaries and up to 3 spines; neuropodial spines slenderer than in notopodial one, distally slightly curved into slender tip. Pygidium with two broad lobes, anal cirri not observed.

Variation. Juveniles (Fig. 20F) small specimens with length of 1.2–4 mm and width of 0.1–0.2 mm, for 20 to ~50 chaetigers, branchiae always present, appearing ~chaetiger

10 regardless of size, parapodial lobes never developed.

Distribution. IN2017_V03, Station 100. Pilot whale carcass, off Byron Bay, New South Wales, Australia in 999–1013 m.

Remarks. Specimens assigned here to *Orbiniella* sp. are morphologically similar to *Orbiniella jamesi* sp. nov., but differ in the following characters: neuropodial postchaetal lobes are absent, body is more robust, posterior branchiae are shorter and thicker than in *O. jamesi* sp. nov. The development and number of neuropodial postchaetal lobes have been suggested to differ among developmental stages in Orbiniidae, but here the differences were observed in specimens of similar length (7–9 mm) and possessing similar number of chaetigers (90–95). A number of very small juveniles (Fig. 20F) were also found in the samples. However, the molecular results indicate that specimens assigned here to *Orbiniella* sp. and *Orbiniella jamesi* sp. nov., as well as

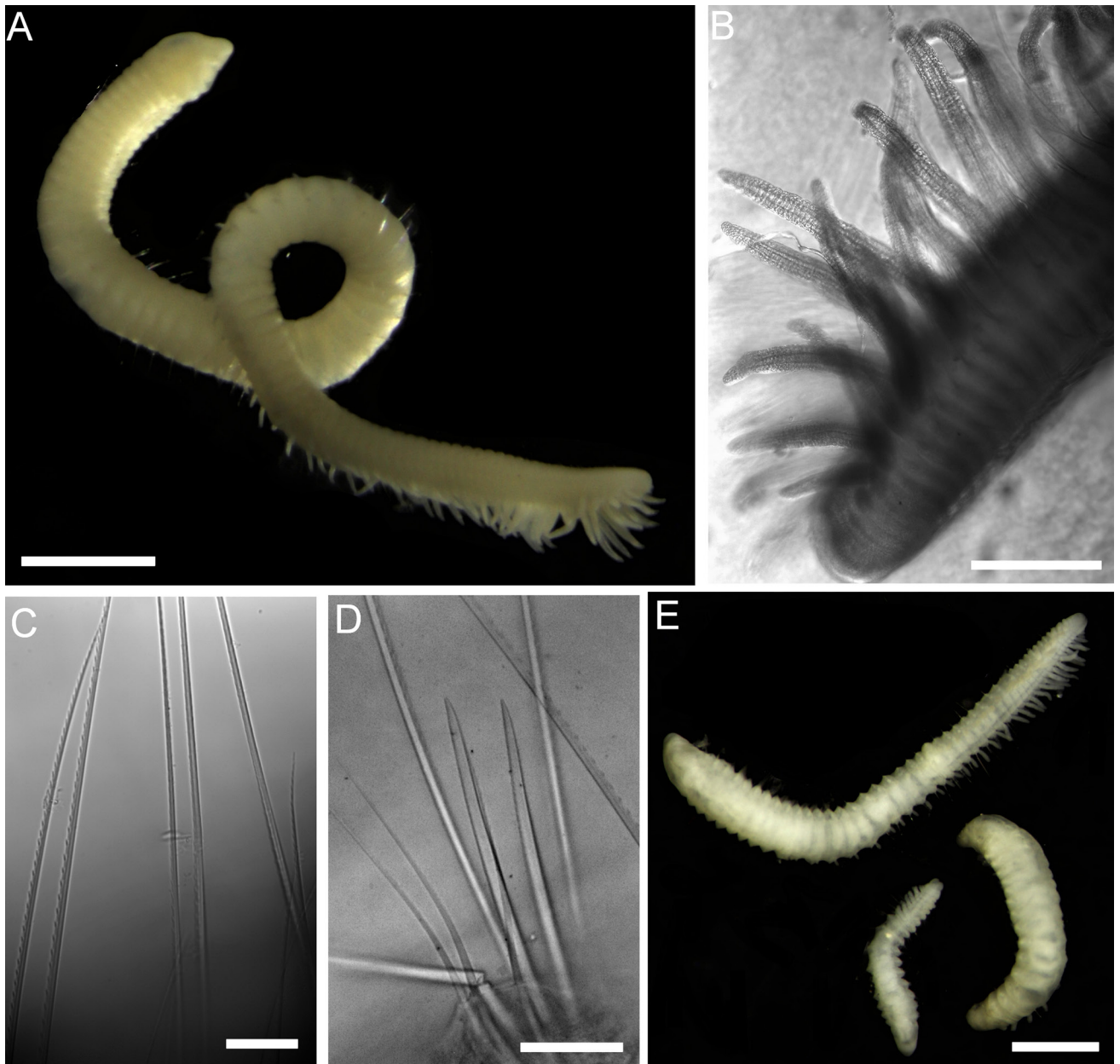


Figure 20. *Orbiniella* sp. specimen NHMUK.2022.431. (A) Preserved specimen in lateral view, scale bar is 1 mm; (B) branchiae from posterior segments, scale bar is 250 μ m; (C) example of crenulated capillaries, scale bar is 25 μ m; (D) example of spines, scale bar is 25 μ m; (E) juveniles (NHMUK ANEA 2022.421–430), scale bar is 500 μ m.

juvenile specimens represent the same species (Fig. 19). Currently, the understanding of developmental stages in Orbiniidae is limited despite some recent advances (see Blake, 2021) and we thus tentatively ascribe the specimens without neuropodial postchaetal lobes to *Orbiniella* sp., rather than *Orbiniella* sp. nov. that has well-developed lobes. Gunton *et al.* (2021, fig. 18F) assigned a specimen fitting *Orbiniella jamesi* sp. as described here to an unknown genus of Protoariciinae, but this placement is at odds with the molecular phylogeny of this study which shows protoariciines in a more crown position compared to *Orbiniella* (Fig. 19).

Phyllodocidae Örsted, 1843

Eumida Malmgren, 1865

Eumida cf. *longicirrata* Hartmann-Schröder, 1975

Fig. 21

Material examined. NHMUK ANEA 2022.406, NHMUK ANEA 2022.407–408, NHMUK ANEA 2022.439, IN2017_V03_100; 9 June 2017; off Byron Bay, NSW, Australia, beam trawl, start: 28.05°S 154.08°E, 999 m, end: 28.10°S 154.08°E, 1013 m. DNA vouchers: NHMUK ANEA 2022.404 (COI, 16S, 18S), AM W.52192 (COI, 16S), AM W.52193 (COI, 16S), AM W.52194 (COI, 16S), same locality.

Description. Complete specimens measuring 2.8–7.6 mm long with 20–42 segments, appearing biannulate (Fig. 21A). Segments widest anteriorly (0.53–0.67 mm) and tapering posteriorly.

Prostomium pentagonal with rounded corners, wider than long (Fig. 21B). Anterior end of prostomium with pair of antennae slightly longer than prostomium dorsally and similar pair of palps ventrally. A median antenna, shorter and thinner than frontal antennae, inserted near middle of prostomium. Eyes absent.

Proboscis fully everted in one specimen (NHMUK ANEA 2022.404), funnel-shaped, with ~40 terminal cirri and low papilla in concentric rows on the column (Fig. 21C). Partially-everted proboscis appears columnar in other specimens (NHMUK ANEA 2022.439).

First and second segments appear fused, with the first pair of tentacular cirri inserted ventral to the prostomium. Four tentacular cirri on segments 1–3 cylindrical, tapering distally ($1 + C\frac{1}{4} + C\frac{1}{8}$). In preserved specimens, the cirrus on segment 1 reaches segments 5–6, the dorsal cirrus on segment 2 reaches segments 6–7, the ventral cirrus on segment 2 reaches segments 5–7, and the cirrus on segment 3 reaches segments 7–8.

Dorsal cirri present from segment 4, ventral cirrus from the segment 3. Dorsal cirrus lanceolate, 1.5–2× longer than parapodial lobe, around 2.5–3× longer than wide (Fig. 21D). Ventral cirrus lanceolate, slightly longer than parapodial lobe,

around 2.5–3× longer than wide.

Parapodia uniramous with a single acicula and numerous heterogomph spinigers (Fig. 21E). Shaft of chaetae with apical teeth and blade with fine serration.

Pygidium broad and blunt, with two terminal tear-shaped cirri easily detached (Fig. 21F).

Distribution. IN2017_V03, Station 100. Pilot whale carcass, off Byron Bay, New South Wales, Australia in 999–1013 m.

Remarks. Recognized *Eumida* species lacking eyes include *Eumida alvini* Eibye-Jacobsen, 1991, *Eumida angolensis* Böggemann, 2009, *Eumida (Eumida) longicirrata* Hartmann-Schröder, 1975, and *Eumida nuchala* (Uschakov, 1972). Among these, the IN2017_V03 *Eumida* specimens most closely resembled *E. longicirrata*, which has the median antenna inserted slightly anterior to the middle of the prostomium unlike the other species where it is inserted closer to the posterior end. The other species are also distinct from the IN2017_V03 specimens in the following ways: *E. alvini* have the median antenna longer than the frontal pair as well as very long tentacular and dorsal cirri; *E. angolensis* have oval prostomium and “bottle-shaped” tentacular cirri (Böggemann, 2009); *E. nuchala* have enlarged nuchal organs and ventral cirri much longer than the parapodial lobe.

Raised semicircular structures on the posterior end of the prostomium, described for *E. longicirrata*, were difficult to observe in the IN2017_V03 specimens. This was also the case for other specimens identified as *E. longicirrata* (Ravara *et al.*, 2017). The micropapillae observed in the proboscis of the IN2017_V03 specimens is contrary to the smooth proboscis described for *E. longicirrata*. The presence of >40 oral papillae (NHMUK ANEA 2022.404) is unusual since most *Eumida* species often have 17, except for *E. alvini*, which can range from 22–50 (Eibye-Jacobsen, 1991). Estimates of tentacular cirri lengths, measured by the extent of reach along body segments, are similar to *E. longicirrata*. It should be noted that live specimens were observed to have more contracted segments compared to preserved specimens (Fig. 21), so this measurement differs between the two. Based on the illustrations of the holotype of *E. longicirrata*, estimates of cirri length were measured from live specimens while the IN2017_V03 specimens were measured from preserved specimens.

Incorporating the COI sequences of IN2017_V03 specimens and all available sequences of the closely allied genus *Sige* in GenBank with those used by Teixeira *et al.* (2020) places these samples within a clade of *Sige* spp. and sister group to *Sige fusigera* Malmgren, 1865 (Fig. 22). The Australian specimens, however, lack the characteristic pointed superior parapodial lobe of other *Sige* species (Eklöf *et al.*, 2007). San Martín *et al.* (2021) found *Sige*, *Eumida* and other closely related genera to be paraphyletic and polyphyletic in their analyses. Further investigation is warranted to explore the relationship among these genera. This is the first report of eyeless *Eumida* species occurring at 1000 m. Previous records were collected at depths >3000 m.

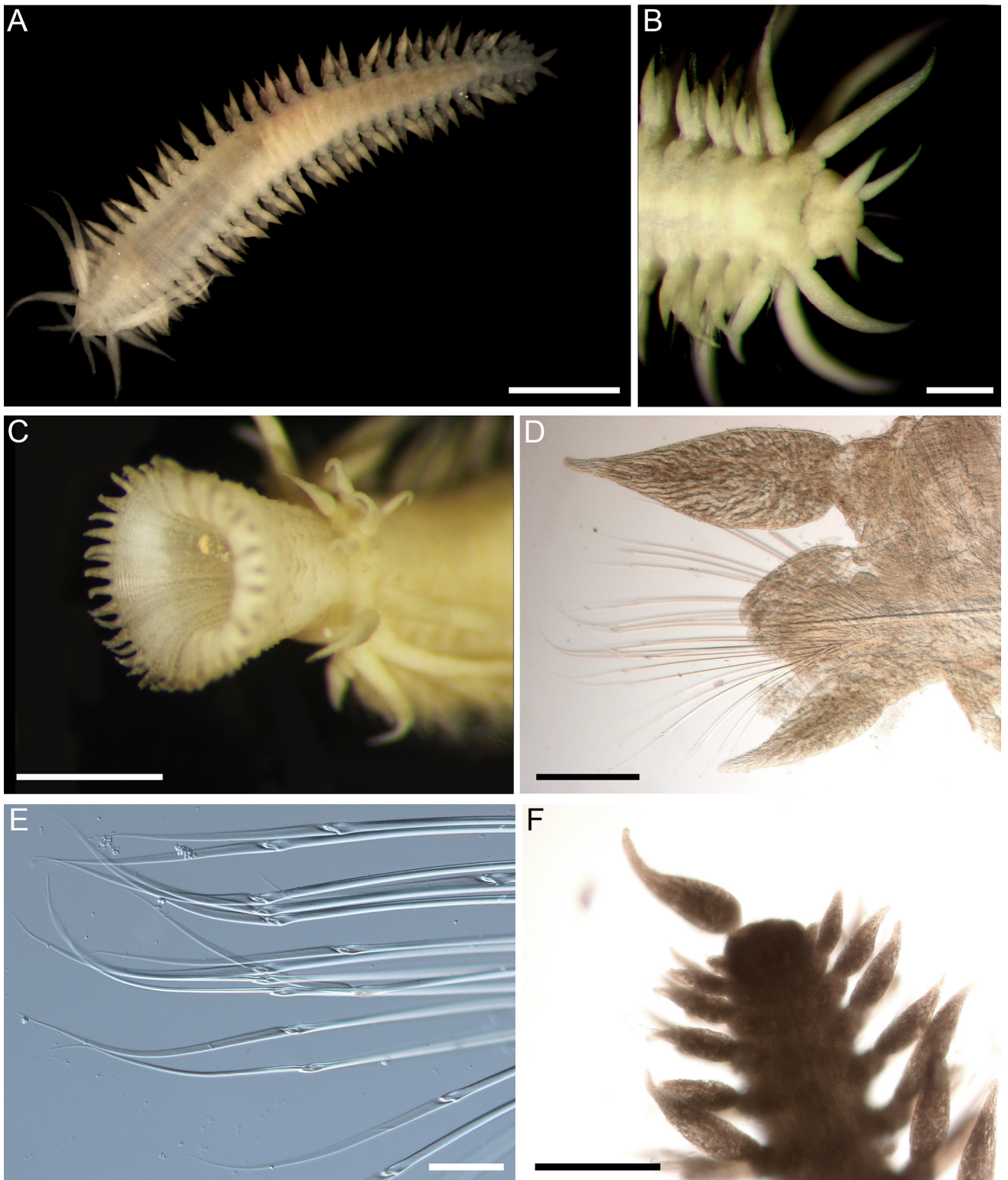


Figure 21. *Eumida cf. longicirrata*. (A) Photo of a live specimen (NHMUK ANEA 2022.406), scale bar is 1 mm; (B) ventral aspect of the anterior end showing the prostomium and tentacular cirri (NHMUK ANEA 2022.407–408), scale bar is 250 µm; (C) fully everted proboscis (NHMUK ANEA 2022.404), scale bar is 750 µm; (D) light micrograph of mid-body parapodium (NHMUK ANEA 2022.404), scale bar is 200 µm; (E) light micrograph of heterogomph spinigers (NHMUK ANEA 2022.404), scale bar is 50 µm; (F) light micrograph of pygidium missing one anal cirrus (NHMUK ANEA 2022.406), scale bar is 250 µm.

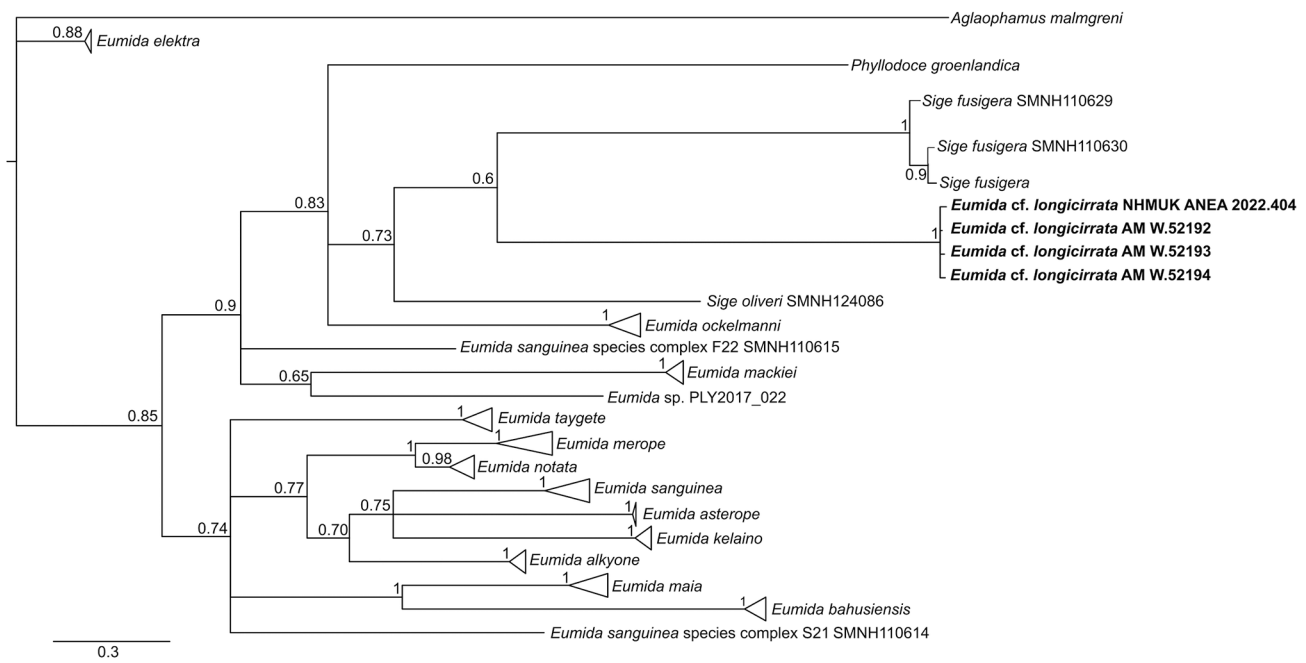


Figure 22. Phylogeny of the genus *Eumida* (Phyllocodidae) based on Bayesian analysis of the COI gene only. Numbers adjacent to nodes indicate posterior probabilities, and taxa for which sequences have been contributed by the present study are indicated in bold.

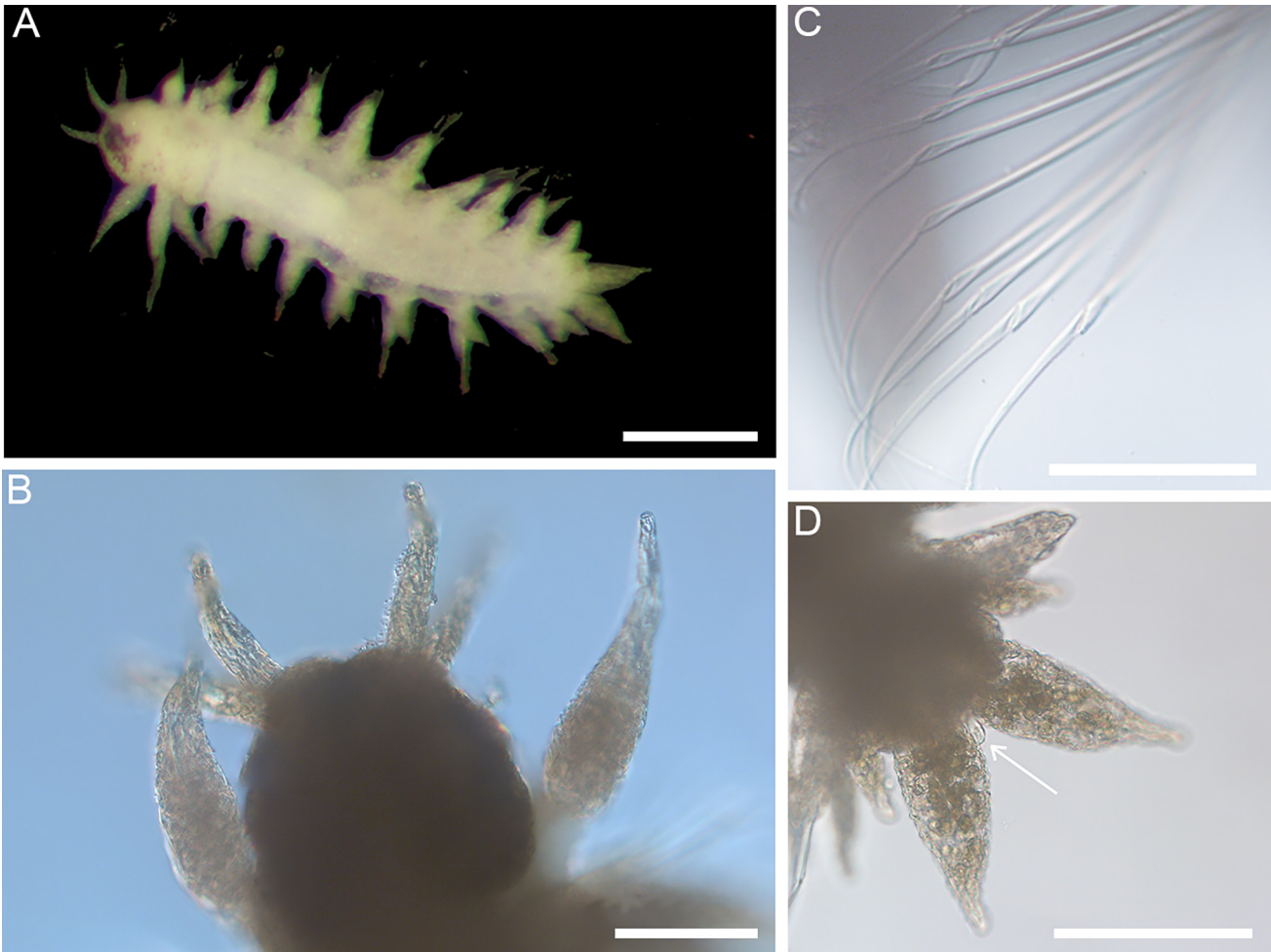


Figure 23. *Pseudomystides* sp., specimen NHMUK ANEA 2022.409–411. (A) Photo of an ethanol-preserved specimen, scale bar is 200 μ m; (B) light micrograph of prostomium and tentacular cirri of the first segment, scale bar is 75 μ m; (C) light micrograph of compound spinigers, scale bar is 25 μ m; (D) light micrograph of pygidium with anal cirri and papilla (arrow), scale bar is 100 μ m.

Pseudomystides* Bergström, 1914*?*Pseudomystides* sp.**

Fig. 23

Material examined. NHMUK ANEA 2022.409–411, NHMUK ANEA 2022.441, IN2017_V03_100; 9 June 2017; off Byron Bay, NSW, Australia, beam trawl, start: 28.05°S 154.08°E, 999 m, end: 28.10°S 154.08°E, 1013 m.

Description. Complete specimens 0.75–1.67 mm long with 11–14 segments (Fig. 23A). Segments of equal widths (0.13–0.27 mm) along length of body.

Prostomium wider than long and terminally cleft (Fig. 23B). Prostomium sometimes more darkly pigmented than rest of body. Terminal protuberance present where paired antennae and palps inserted. Frontal antennae and palps digitiform, both approximately same length as prostomium. Median antenna smaller and thinner than paired antenna and inserted near center of prostomium. Eyes absent. Proboscis retracted in all specimens.

First and second segments appearing fused, with first pair of tentacular cirri inserted ventral to prostomium. Three tentacular cirri with broad bases tapering to a pointed tip ($1 + C\frac{1}{2} + C\frac{3}{4}$). Cirri on segment 1 reaching segments 2–3, dorsal cirri on segment 2 reaching segments 4–5, ventral cirri on segment 2 reaching segment 4. No dorsal cirri present on segment 3.

Dorsal cirri present from segment 4, ventral cirrus from segment 3. Dorsal cirrus lanceolate, around 2× longer than wide, typically directed posterolaterally. Ventral cirrus lanceolate to digitiform, around 4× longer than wide. Both structures similar in size to parapodial lobe. Uniramous parapodia with compound spinigers having blades slightly shorter than shaft (Fig. 23C).

Pygidium broad and blunt with two tear-drop-shaped anal cirri (Fig. 23D). Median pygidial papilla present.

Distribution. IN2017_V03, Station 100. Pilot whale carcass, off Byron Bay, New South Wales, Australia in 999–1013 m.

Remarks. Phyllodocid genera that have three tentacular cirri in the first two segments and the third segment lacking a dorsal cirrus include *Hesionura* Hartmann-Schröder, 1958, *Mystides* Théel, 1879, and *Pseudomystides* Bergström, 1914 (Eklöf *et al.*, 2007). *Hesionura* and *Mystides* both have a pair of antennae and palps, fewer than the IN2017_V03 specimens. We assign these specimens to *Pseudomystides* since an additional median antenna is described in three of the five described species. Within the genus *Pseudomystides*, these differ from the other species in having far fewer segments, a broad prostomium, unlike *Pseudomystides limbata* (Saint-Joseph, 1888) and *Pseudomystides varica* (Uschakov, 1958), and digitiform to lanceolate dorsal and ventral cirri, unlike *Pseudomystides bathysiphonicola* (Hartmann-Schröder, 1983), *Pseudomystides brevicirra* Böggemann, 2009, and *Pseudomystides spinachia* Petersen & Pleijel in Pleijel, 1993. The median antenna for the Australian specimens is also inserted near the middle of the prostomium, unlike in *P. limbata*, *P. varica*, and *P. spinachia* where it is inserted posteriorly. We were unable to obtain DNA sequence data from the samples which prevented us from comparing their relationships with other *Pseudomystides* species.

Protodrilidae Hatschek, 1888***Protodrilus* Hatschek, 1881*****Protodrilus* cf. *puniceus* Sato-Okoshi, Okoshi, & Fujiwara, 2015**

Fig. 24

Material examined. NHMUK ANEA 2022.432, IN2017_V03_100; 9 June 2017; off Byron Bay, NSW, Australia, beam trawl, start: 28.05°S 154.08°E, 999 m, end: 28.10°S 154.08°E, 1013 m. DNA vouchers: NHMUK ANEA 2022.432 (COI, 16S, 18S), WF_PRO_1 (16S), same locality.

Description. Body shape slender and filiform with head slightly larger than body (Fig. 24). Paired antennae inserted terminally; no eye spots visible. Pygidium with paired lateral lobes and a median cluster of cilia.

Distribution. IN2017_V03, Station 100. Pilot whale carcass, off Byron Bay, New South Wales, Australia in 999–1013 m.

Remarks. In the phylogenetic tree (Fig. 25) this species is placed well within the genus *Protodrilus* with *Protodrilus puniceus* Sato-Okoshi, Okoshi, & Fujiwara, 2015 described from whalefall off the coast of Japan as sister taxon. In 18S the uncorrected “p” distance is 0.02 between the two sister taxa, while the distances to other taxa are 0.08 and above. However, only sequences from the 18S gene were available from *P. puniceus*, preventing us from confirming or rejecting the identity of the new species based on molecular data.

Siboglinidae Caullery, 1914***Osedax* Rouse, Goffredi, & Vrijenhoek, 2004*****Osedax waadjum* sp. nov.**

urn:lsid:zoobank.org:act:382AE053-EDCF-4086-A819-2344D8CC40A8

Fig. 26

“*Osedax* sp. nov.” Gunton *et al.*, 2021: 129–130, fig. 27B, C

Holotype: AM W.53706, IN2017_V03_100; 9 June 2017; off Byron Bay, NSW, Australia, beam trawl, start: 28.05°S 154.08°E, 999 m, end: 28.10°S 154.08°E, 1013 m.

Paratypes: NHMUK ANEA 2022.400, NHMUK ANEA 2022.401, NHMUK ANEA 2022.402, NHMUK ANEA 2022.403, NMV F253031, NMV F253032, same locality as holotype. DNA vouchers: NHMUK ANEA 2022.400 (COI, 16S), AM W.53706 (COI, 16S, 18S), NHMUK ANEA 2022.401 (COI, 16S), NHMUK ANEA 2022.403 (16S), NHMUK ANEA 2022.402 (COI), NMV F253031 (16S), NMV F253032 (COI).

Description. Female tube long (25 mm, specimen NHMUK ANEA 2022.403), anteriorly thin, semi-transparent and appearing rounded and closed at the tip (Fig. 26A), posterior tube tough and creased. Females with crown of four palps fused for much of their length (6.8 mm in specimen NHMUK ANEA 2022.403), contracted within tubes and without obvious pinnules but slightly wrinkled and with distinct blood vessels in live specimens (Fig. 26B). Trunk (Fig. 26C) short



Figure 24. *Protodrilus cf. puniceus*. (A) anterior end, scale bar is 100 μm ; (B) anterior end, scale bar is 200 μm ; (C) whole animal, scale bar is 200 μm .

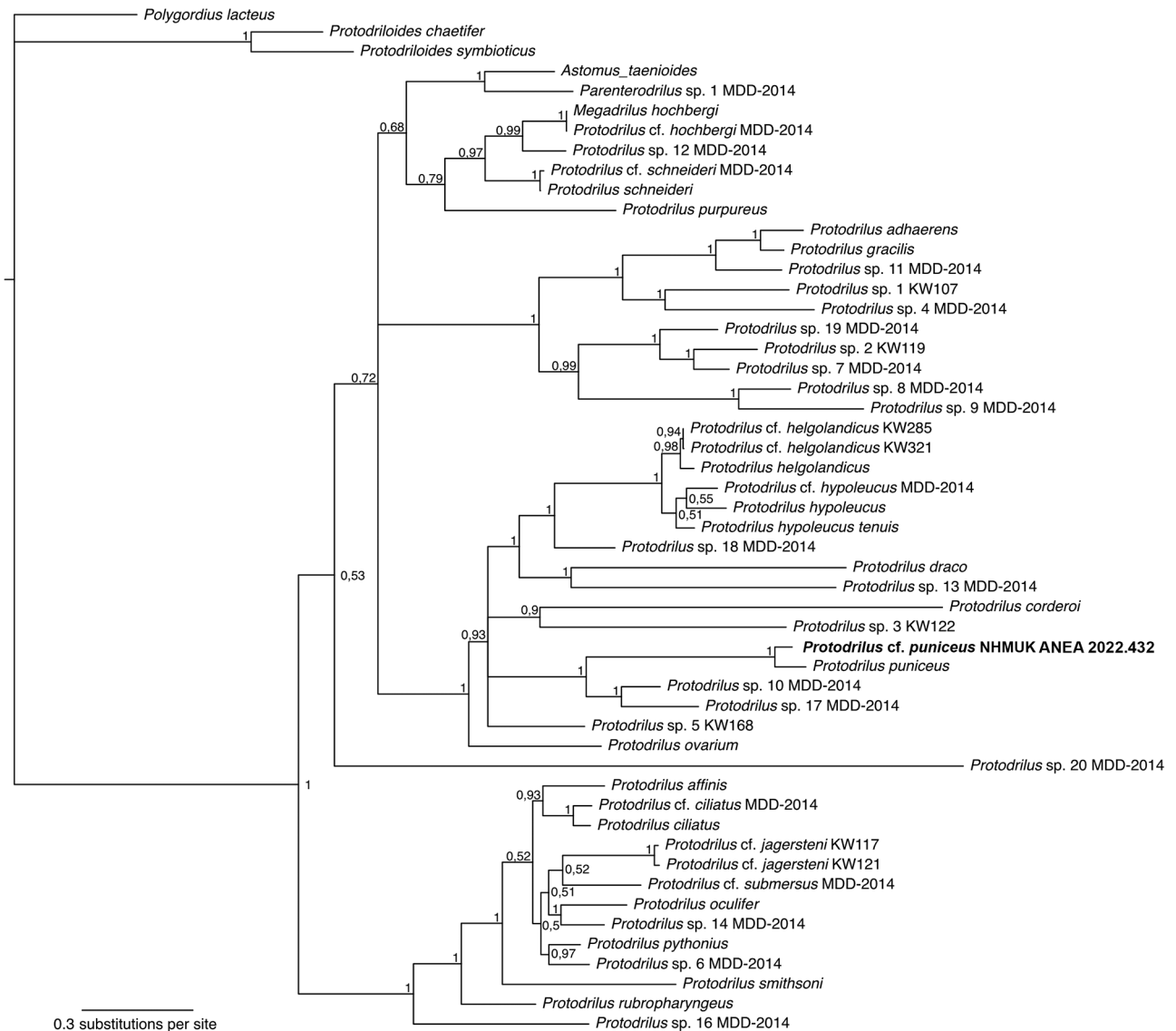


Figure 25. Phylogeny of the *Protodrilus* genus based on Bayesian analysis of a combined dataset of the genes COI, 16S and 18S. Numbers adjacent to nodes indicate posterior probabilities, and taxa for which sequences have been contributed by the present study are indicated in bold.

in relation to the length of the palps (0.6 mm in specimen NHMUK ANEA 2022.402). Oviduct extends from base of palps (Fig. 26D), opposite side of trunk bears a folded, wrinkled lobe (Fig. 26E). Ovisac not observed. Males 385 μ m in length (Fig. 26F), bearing hooked chaetae anteriorly, and observed at various positions within female tubes.

Distribution. IN2017_V03, Station 100. Pilot whale carcass, off Byron Bay, New South Wales, Australia in 999–1013 m.

Etymology. In the Arakwal Bundjalung language *Waadjum Darrigan Jubal* means “Whale Bone Grub”. In consultation with the Bundjalung of Byron Bay Aboriginal Corporation board of directors representing the Arakwal Bundjalung communities, we propose the scientific name “*Osedax waadjum*”.

Remarks. Genetic data confirms that these specimens comprise a new species that falls within the same clade as other nude palp *Osedax* species with good support (Fig. 27). The position of *Osedax waadjum* sp. nov. appears

basal in relation to all other nude palp species, with the exception of *Osedax deceptionensis* Taboada, Cristobo, Avila, Wiklund, & Glover, 2013. Uncorrected COI genetic distances between *O. waadjum* sp. nov. and other *Osedax* species are a minimum of 14% (Table S17), while within species they are less than or equal to 0.4%. *Osedax waadjum* sp. nov. is described mainly on the basis of genetic data as many of the specimens were damaged during removal from the whale bones. The closed-top tube morphology of this species resembles that of *Osedax lonnyi* Rouse, Goffredi, Johnson, & Vrijenhoek, 2018 and *Osedax jabba* Rouse, Goffredi, Johnson, & Vrijenhoek, 2018. Other nude palp *Osedax* species occupying a similar depth include *Osedax antarcticus* Glover, Wiklund, & Dahlgren, 2013, *Osedax docricketts* Rouse, Goffredi, Johnson, & Vrijenhoek, 2018, *Osedax knutei* Rouse, Goffredi, Johnson, & Vrijenhoek, 2018, and *Osedax westernflyer* Rouse, Goffredi, Johnson, & Vrijenhoek, 2018, described from the Southern Ocean or Eastern Pacific. *Osedax docricketts* and *O. westernflyer* also occur in Sagami Bay off Japan.

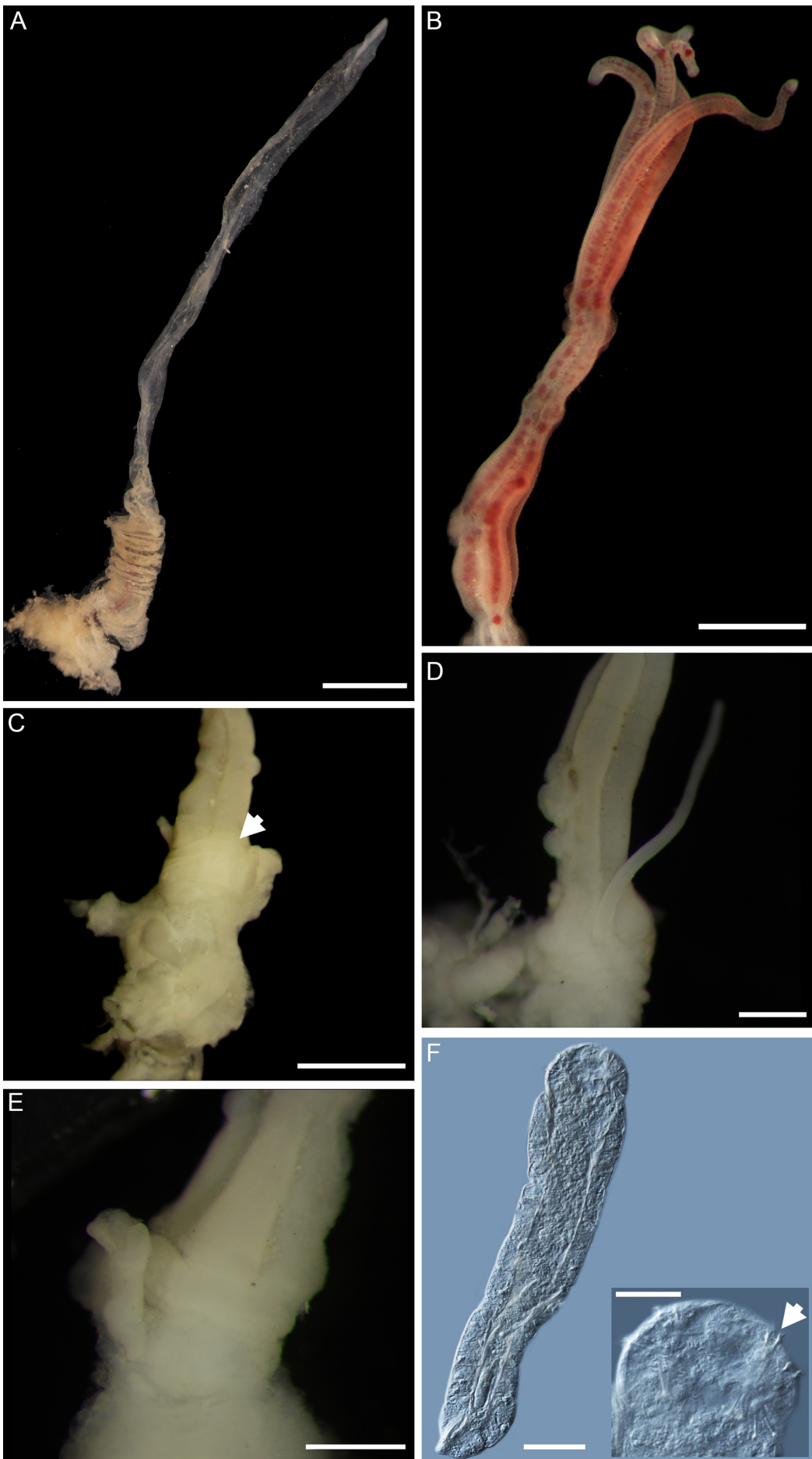


Figure 26. See caption on facing page.

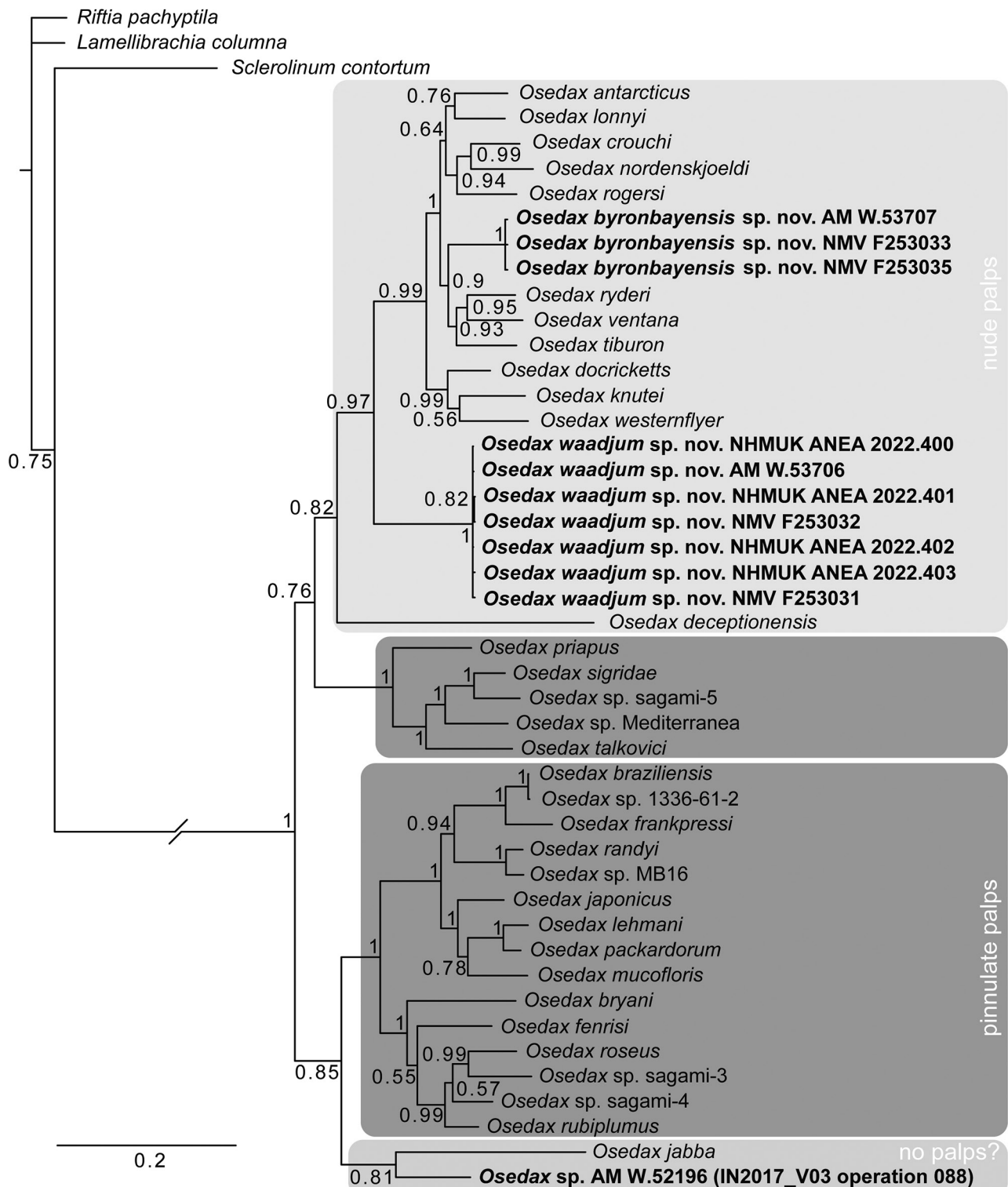


Figure 27. Phylogeny of the siboglinid genus *Osedax* based on Bayesian analysis of a combined dataset of the genes COI, 16S and 18S. Numbers adjacent to nodes indicate posterior probabilities, and taxa for which sequences have been contributed by the present study are indicated in bold. Clades containing individuals with nude, pinnulate or no palps are also highlighted.

Figure 26 (facing page). *Osedax waadjum* sp. nov. (A) Living female specimen inside tube (NHMUK ANEA 2022.403), scale is 3 mm; (B) anterior of living specimen outside of tube (NHMUK ANEA 2022.403), scale is 1 mm; (C) posterior of preserved specimen showing boundary between palps and trunk (arrowed), NHMUK ANEA 2022.402, scale is 1 mm; (D) posterior of preserved holotype specimen, AM W.53706, showing short oviduct emerging from top of trunk, scale is 500 μ m; (E) posterior of specimen AM W.53706 showing alternative side of trunk where a small crinkled lobe is present, scale is 500 μ m; (F) male specimen from tube of NHMUK ANEA 2022.401, with inset showing detail of hooked chaetae (arrowed). Scale is 50 μ m in main image and 25 μ m in inset.



Figure 28. *Osedax byronbayensis* sp. nov. holotype AM W.53707. (A) Ethanol-preserved holotype showing majority of tube, scale bar is 1 mm; (B) detail of palp inside tube (arrowed), scale bar is 500 µm.

Osedax byronbayensis sp. nov.

urn:lsid:zoobank.org:act:D8AA2600-5820-4531-A012-4B3D1F4C0664

Fig. 28

Holotype: AM W.53707, IN2017_V03_100; 9 June 2017; off Byron Bay, NSW, Australia, beam trawl, start: 28.05°S 154.08°E, 999 m, end: 28.10°S 154.08°E, 1013 m.

Paratypes: NMV F253033, NMV F253035, same locality as holotype. DNA vouchers: AM W.53707 (COI, 16S, 18S), NMV F253033 (COI), NMV F253035 (COI).

Description. Holotype incomplete, represented by majority of tube containing a fragment of tissue. Tube approximately 18 mm long, tapering anteriorly, and ending in a closed point (Fig. 28A). Tube material is easily torn. No males observed on tube. Tissue present within tube is possibly a single palp approximately 4 mm long and sinuous, surface appears smooth (Fig. 28B). Specimen not observed alive.

Distribution. IN2017_V03, Station 100. Pilot whale carcass, off Byron Bay, New South Wales, Australia in 999–1013 m.

Etymology. This species is named after the town of Byron Bay, Australia, off which this whale fall was discovered.

Remarks. *Osedax byronbayensis* sp. nov. is known only from three incomplete specimens, therefore a complete morphological description was not possible. Molecular data demonstrates the three specimens to belong to the same species with high support (Fig. 27); uncorrected COI *p*-distances between the three specimens are 0.4–0.6%. They are positioned in a clade with other nude palp *Osedax* species and demonstrate a minimum uncorrected COI *p*-distance of 12.7% to other *Osedax* species (to *Osedax ryderi* Rouse, Goffredi, Johnson, & Vrijenhoek, 2018; Table S17). As with *Osedax* species *Osedax crouchi* Amon, Wiklund, Dahlgren, Copley, Smith, Jamieson, & Glover, 2014, *Osedax nordenskjoldi* Amon, Wiklund, Dahlgren, Copley, Smith, Jamieson, & Glover, 2014, *Osedax rogersi* Amon, Wiklund, Dahlgren, Copley, Smith, Jamieson, & Glover, 2014, and *Osedax ventana* Rouse, Goffredi, Johnson, & Vrijenhoek, 2018, *O. byronbayensis* sp. nov. is described mainly on the basis of molecular data.

Sphaerodoridae Malmgren, 1867

Sphaerodoropsis Hartman & Fauchald, 1971

Sphaerodoropsis sp.

Fig. 29

Sphaerodoridae gen. spp. Gunton *et al.*, 2021: 138

Material examined. SPH_01, AM W.52205, IN2017_V03_100; 9 June 2017; off Byron Bay, NSW, Australia, beam trawl, start: 28.05°S 154.08°E, 999 m, end: 28.10°S 154.08°E, 1013 m. DNA vouchers: SPH_01 (COI, 18S, 16S), AM W.52205 (COI).

Description. Based on AM W.52205. Body ellipsoid (Fig. 29A). Dorsum four longitudinal rows of large tubercles. Macrotubercles smooth no terminal papillae. Parapodia with digitiform acicular lobe, ventral cirrus shorter (Fig. 29B–C). Approximately 13 chaetae per parapodia. Chaetae compound with blades, present in all chaetigers (Fig. 29D). Shaft wider at distal end, blades similar length along fascicles.

Distribution. IN2017_V03, Station 100. Pilot whale carcass, off Byron Bay, New South Wales, Australia in 999–1013 m.

Remarks. Similar to *Sphaerodoropsis exmouthensis* Hartmann-Schröder, 1981 re-described by Capa & Bakken (2015); type locality shallow water from Tantabiddi Creek, Exmouth, Western Australia. Our specimens have more chaetae per fascicle than *S. exmouthensis*. The species is genetically distinct from all other Sphaerodoridae (Table S18) and forms an unresolved clade with *Sphaerodoropsis* cf. *martinae* Desbruyères, 1980 and (*Ephesiella abyssorum* (Hansen, 1879)—*Sphaerodorum flavum* Ørsted, 1843—*Sphaerodoropsis* cf. *longianalpapilla* Böggemann, 2009—*Sphaerodoropsis aurantica* Capa & Rouse, 2015) (pp 0.91) (Fig. 30). Due to the poor morphological condition of our specimens and a poorly resolved phylogenetic tree, the species is not formally described here.

Phascolosomatidae

Stephen & Edmonds, 1972

Phascolosoma Leuckart, 1828

Phascolosoma undes. sp.

Fig. 31

Sipuncula fam. gen. spp. Gunton *et al.*, 2021: 156

Material examined. NHMUK ANEA 2022.405, AM W.52201, AM W.52202, AM W.52203, IN2017_V03_100; 9 June 2017; off Byron Bay, NSW, Australia, beam trawl, start: 28.05°S 154.08°E, 999 m, end: 28.10°S 154.08°E, 1013 m. DNA vouchers: NHMUK ANEA 2022.405 (COI, 16S, 18S), AM W.52201 (18S), AM W.52202 (18S), AM W.52203 (16S, 18S).

Description. Specimens AM W.52201, AM W.52202 and AM W.52203 all in poor condition, only two small anterior fragments (max. 4 mm length) and one posterior fragment remaining (Fig. 31A–B), thus morphological description is

very difficult. Small papillae on outside of body. No tentacles, introvert hooks, mouth or nephridiopores observed.

Distribution. IN2017_V03, Station 100. Pilot whale carcass, off Byron Bay, New South Wales, Australia in 999–1013 m.

Remarks. Bayesian analysis of combined dataset of COI, 16S and 18S sequence data reveals that our species is a sister group to *Phascolosoma* (*Phascolosoma*) *turnerae* Rice, 1985 although support is low (pp 0.5) (Fig. 32); average COI pairwise genetic distance between the two species is 26.7% (Table S19). In our analysis *Phascolosoma* sp. and all other *Phascolosoma* species, except *Phascolosoma capitatum* Gerould, 1913, are recovered as a poorly supported clade (pp. 0.5). This result partly agrees with Bayesian analysis on four genes (18S, 28S, H3 and COI) in Schulze, Cutler, & Giribet (2007), where all species of *Phascolosoma* except *P. capitatum* and *P. turnerae* formed a monophyletic group. Interestingly *P. turnerae* is also a deep-water species described from 366–1184 m associated with submerged wood (Rice, 1985), whereas all other species of *Phascolosoma* except for *P. capitatum* are shallow-water species. Due to the poor morphological condition of the specimens the species is not formally described here.

Discussion

In documenting the annelid community from the first discovery of a natural whale fall in deep Australian waters, this study provides vital information on the nature of whale-fall ecosystems in this part of the world, as well as their connections to other organic falls in the western Pacific and beyond. Given the dominance of polychaetes on this whale fall, it was likely in the enrichment/opportunistic stage of its decomposition (Smith *et al.*, 2015).

Composition and diversity of the whale-fall annelid community

Visually dominant taxa associated with this whale fall included a small mussel genetically near-identical to the species *Terua arcuatilis* described from whale falls off New Zealand (Dell, 1995), as well as the annelids *Eumida* cf. *longicirrata*, *Ophryotrocha* undes. spp., *Orbiniella* undes. spp., *Osedax* undes. spp., *Pleijelius* sp. and *Protodrilus* cf. *punicus*, while less abundant taxa include *Boudemos* sp., *Neanthes* undes. spp., *Nereis* sp., *Paramphinome* cf. *australis*, *Paramytha* cf. *ossicola*, *Phascolosoma* sp., *?Pseudomystides* sp., *Sphaerodoropsis* sp., *Microphthalmus* sp., and *Vrijenhoekia* undes. sp. (descriptions of *Pleijelius* sp. and *Boudemos* sp. to follow (C. Watson, personal communication). Compared with the nearest documented whale falls off Japan (Fujiwara *et al.*, 2007) as well as to a South Atlantic whale fall (Sumida *et al.*, 2016), polychaete species richness seems to be similar but the composition of taxa somewhat different. However, given the different sampling techniques between studies (some also sampled sediments around whale falls), it is difficult to directly relate this whale-fall community to others.

While *Terua arcuatilis* may be a regular colonizer of whale falls in this part of the world, to the best of our knowledge this is the first whale fall to include a dominant *Orbiniella* species, although orbiniids were also reported from sperm whale falls off Japan (Fujiwara *et al.*, 2007). In addition,

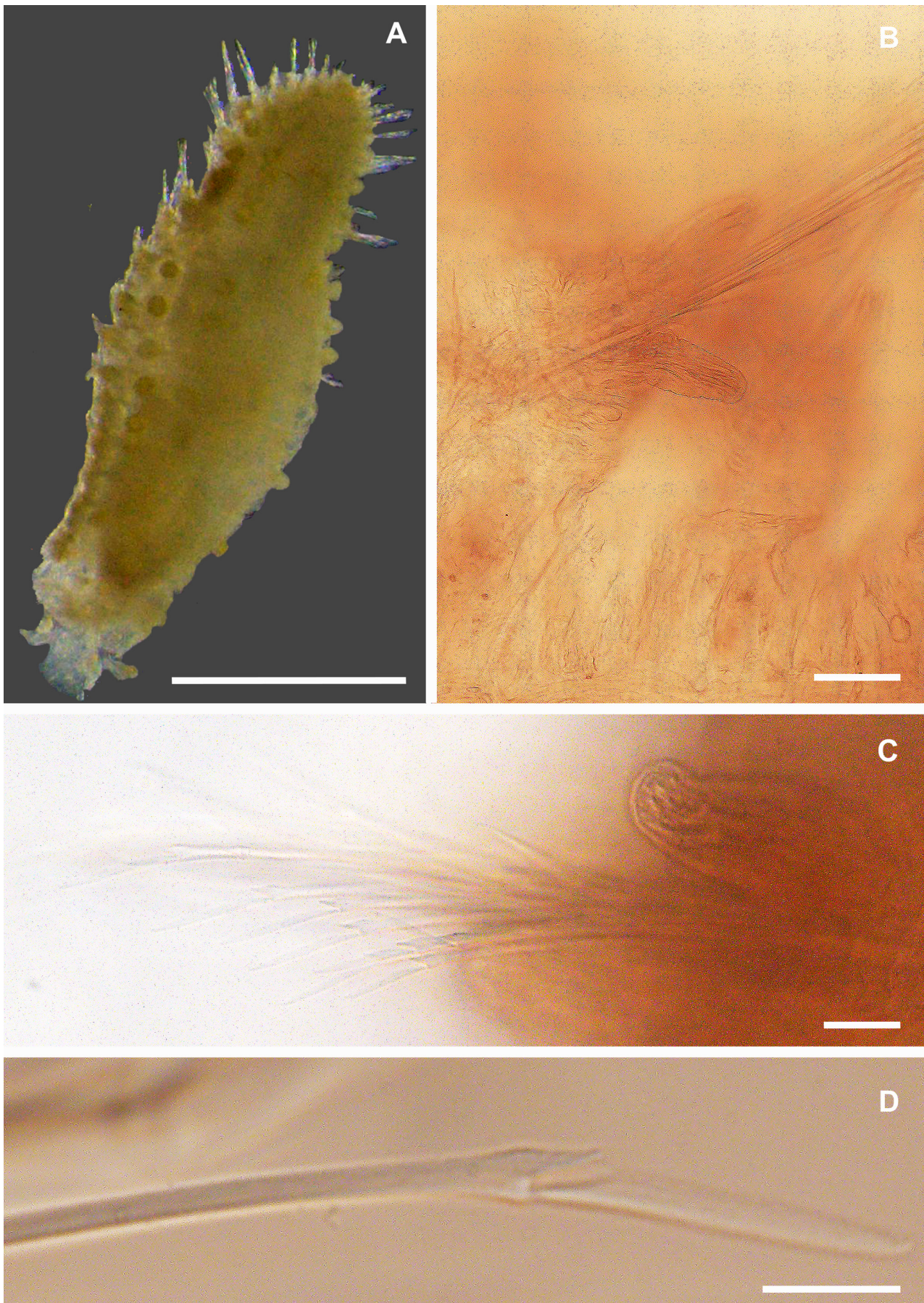


Figure 29. *Sphaerodoropsis* sp. (A) AM W.52205 Whole specimen scale bar 1 mm; (B) parapodia with digiform acicular lobe, scale bar is 50 μ m; (C) parapodia with digiform acicular lobe and compound chaetae, scale bar is 20 μ m; (D) compound chaetae with blades, scale bar is 20 μ m.

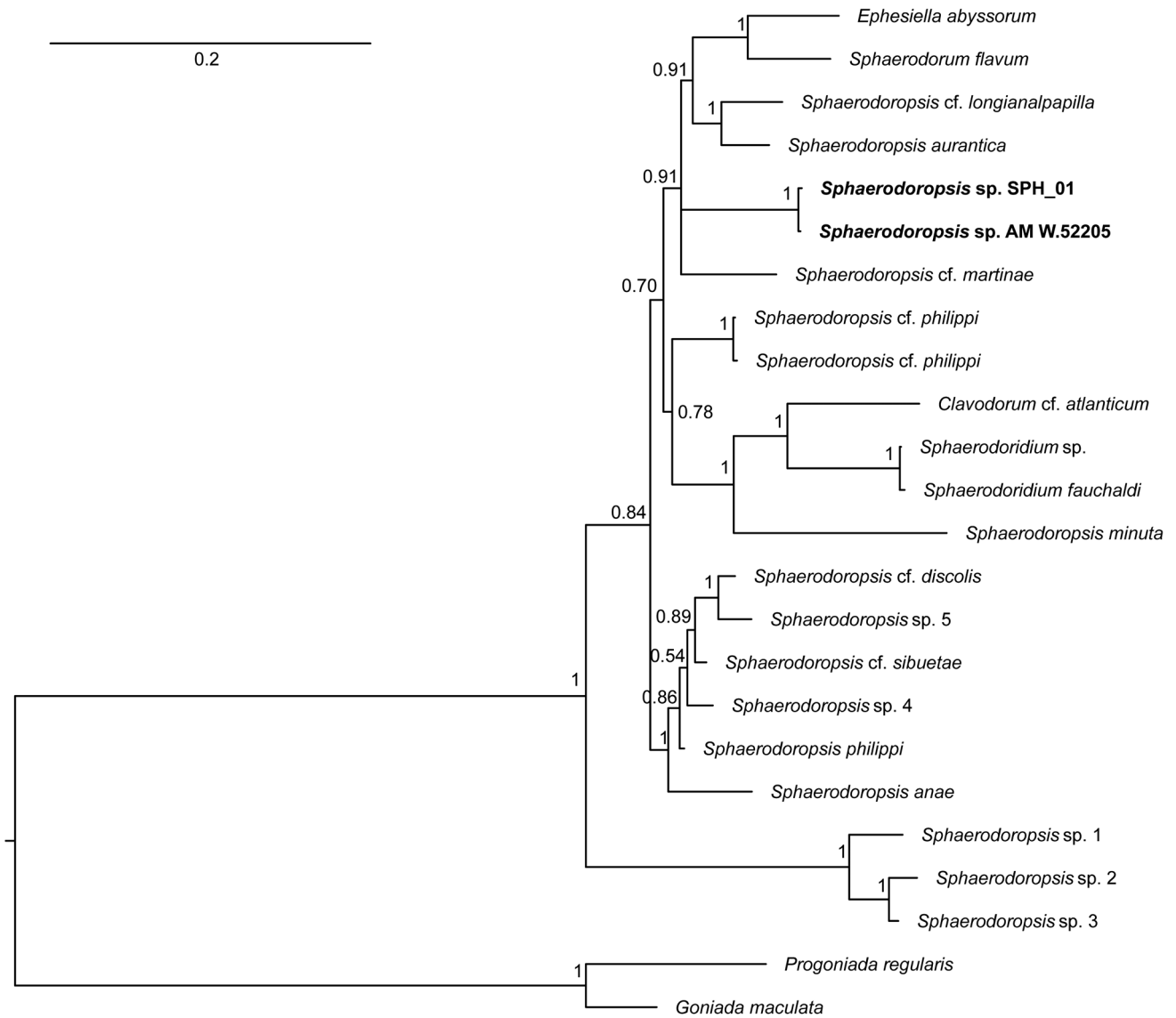


Figure 30. Phylogeny of the Sphaerodoridae family based on Bayesian analysis of the COI, 16S and 18S gene fragments. Numbers adjacent to nodes indicate posterior probabilities, and taxa for which sequences have been contributed by the present study are indicated in bold.

the annelid family Sphaerodoridae has not been recorded on whale bones to date; only one species *Sphaerephesia kitazatoi* (Shimabukuro *et al.*, 2017) has been observed in sediments around a whale-fall carcass from the south-west Atlantic Ocean at the base of the São Paulo Ridge (4204 m depth). The genus *Pseudomystides* (Phyllodocidae) has also not been recorded on whale bones (Böggemann, 2009). The majority of other annelids reported from this whale fall belong to genera that have been previously observed on whale falls and/or other chemosynthetic habitats. High abundances of protodrilids occurred on whale falls in western Pacific off Japan (Fujiwara *et al.*, 2007), off California (Braby *et al.*, 2007), as well as recently having been observed on Mid-Atlantic Ridge (near the Azores) (Silva *et al.*, 2021). Protodrilids are interstitial annelids with a worldwide distribution (Westheide, 1990), and might thus be expected to appear at whale falls globally. The dorvilleid genus *Ophryotrocha* is known for its preference for sites of organic enrichment and is also a frequent whale-fall colonizer globally (Wiklund, Glover, & Dahlgren, 2009). The genus *Osedax*, described from Australian waters for the

first time, also appears to be diverse in this part of the world with two species detected from this whale fall alone (Fig. 27), a further species known to occur off South Australia (G. Rouse, personal communication), and two additional species recently reported off New Zealand (Berman, 2022). The hesionid genus *Pleijelius* has been documented from both whale- and wood falls in the Atlantic (Sumida *et al.*, 2016; Silva *et al.*, 2021; Salazar-Vallejo & Orensanz, 2006; Saeedi *et al.*, 2019) and thus seems to also favour sites of organic enrichment. The phyllodocid *Eumida longicirrata* has also been reported from mud volcanoes in the Gulf of Cadiz (Ravara *et al.*, 2017), but this genus is not generally exclusive to chemosynthetic environments (De Oliveira *et al.*, 2015).

Less abundant polychaetes associated with the IN2017_V03 whale fall that are also already documented from whale falls include *Paramytha* cf. *ossicola*, *Microphthalmus* sp., *Vrijenhoekia timoharai* sp. nov., *Neanthes adriangloveri* sp. nov., *Neanthes visicete* sp. nov., Phascolosomatidae and Amphinomidae. Of these taxa, the genera *Microphthalmus* and *Vrijenhoekia* (along with *Pleijelius* sp.) were also

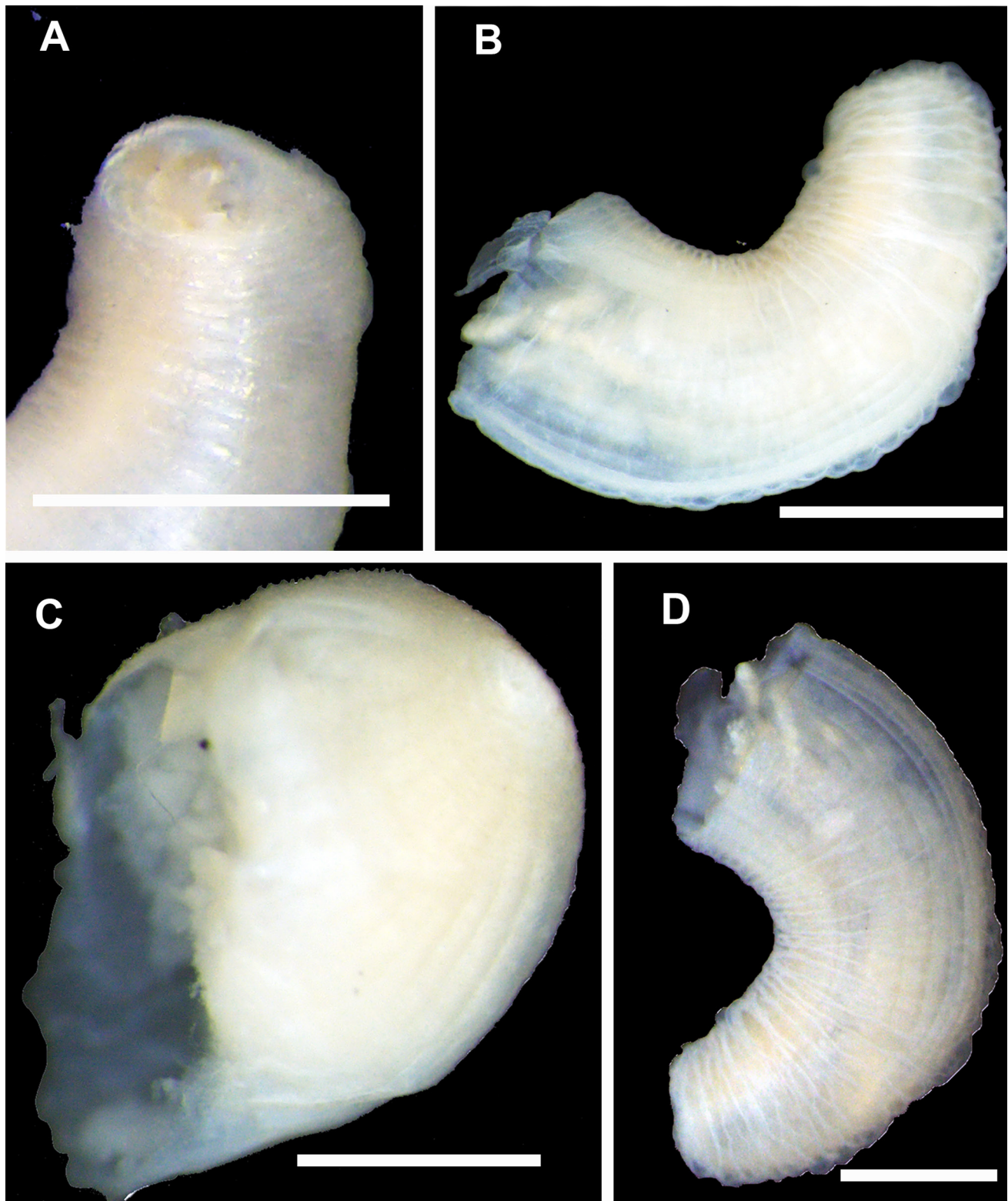


Figure 31. *Phascolosoma* sp. fragments. (A) AM W.52203 anterior fragment, scale bar is 1 mm; (B) AM W.52201 anterior fragment, scale bar is 1 mm; (C) AM W.52202 fragment, scale bar is 1 mm; (D) AM W.52203 anterior fragment, scale bar is 1 mm.

discovered to co-occur on a south-west Atlantic whale fall (Sumida *et al.*, 2016), *Vrijenhoekia* is also known from a Mid-Atlantic Ridge (Azores) whale fall as well as from the north-east Pacific (Summers, Pleijel, & Rouse, 2015; Pleijel *et al.*, 2008), and *Microphthalmus* also from the Pacific (Dahlgren *et al.*, 2004). The ampharetid genus *Paramytha*

is known from sunken cow bones in the north-east Atlantic and the Arctic vent site Loki's Castle (Queirós *et al.*, 2017; Kongsrud *et al.*, 2017), at which *Paramytha ossicola* was reported at high abundances of 2173 specimens (up to 3.37 individuals cm⁻²) on cow bones in the Setúbal Canyon (NE Atlantic) (Queirós *et al.*, 2017). However, its absence

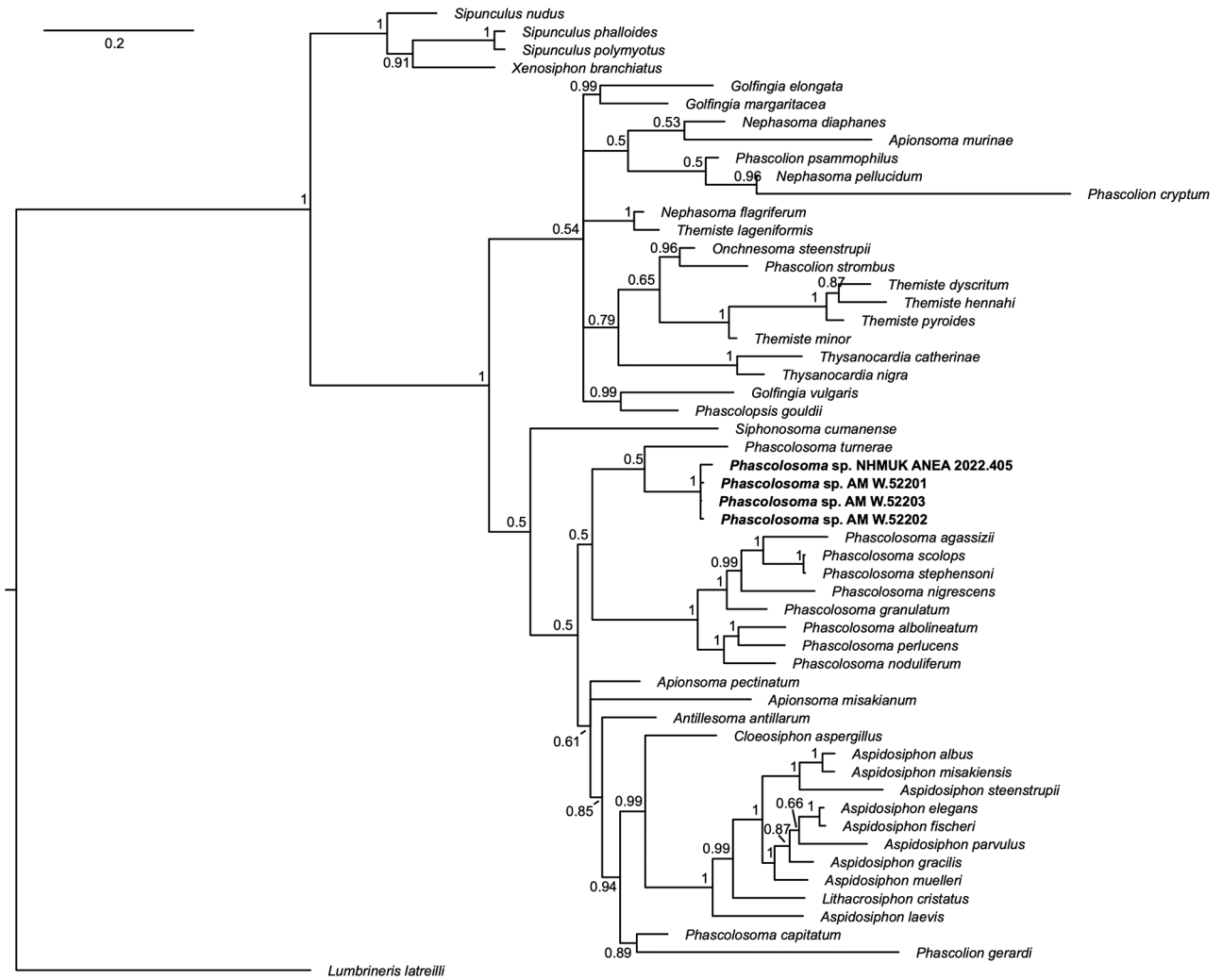


Figure 32. Phylogeny of Sipuncula based on Bayesian analysis of the COI, 16S and 18S gene fragments. Numbers adjacent to nodes indicate posterior probabilities, and taxa for which sequences have been contributed by the present study are indicated in bold.

was noted at the Mid-Atlantic Ridge (Azores) whale fall documented by Silva *et al.* (2021), and the finding of only three specimens in our material may be a result of the timing of sampling relative to decomposition as *Paramytha* is likely a deposit or detritus feeder best adapted to the enrichment-opportunistic successional stage. Nereidid species including the genus *Neanthes* also commonly occur on whale falls and are often associated with the late enrichment-opportunist and sulfophilic stages of deep-sea whale-fall successions (Shimabukuro *et al.*, 2017). Two unidentified Sipuncula species were reported in this study from an unusual whale-fall community in Monterey Bay (Goffredi *et al.*, 2004), while unidentified Amphinomidae have been observed on whale falls from the above region (Braby *et al.*, 2007).

Biogeographic and evolutionary observations

As well as revealing for the first time the composition of a whale-fall annelid community in the Australian region, this whale-fall discovery fills an important gap in the distribution of one of the most iconic whale-fall taxa, the bone-eating siboglinid genus *Osedax*. The occurrence and distribution of this genus is poorly known in the southern hemisphere as only six out of a current total of 27 described species

are known from this part of the world (five *Osedax* species from the Southern Ocean (Amon *et al.*, 2014; Glover *et al.*, 2013) and a single species reported off Brazil (Fujiwara *et al.*, 2019)). The phylogenetic position of *O. waadjum* sp. nov. is also interesting (Fig. 27), as this species appears to have a basal position with respect to the majority of other nude-palp species. Interestingly, the above is also mirrored by a new *Osedax* species from New Zealand (Berman, 2022). Notably, an *Osedax* sp. tissue fragment from IN2017_V03 operation 088, Central Eastern Marine Park, 4400 m depth, is closely related to the unusual palpless species *O. jabba* along with which it forms a clade basal to all pinnulate palp species (Fig. 27). In addition to unexplored diversity, it is likely that the southern hemisphere may reveal much about the evolution of this iconic genus.

The occurrences of *Paramytha* cf. *ossicola* and *Pleijelius* sp. on the IN2017_V03 whale fall represent the first records of these genera in the Pacific Ocean (Gunton *et al.*, 2021), and suggest a potentially global distribution for these likely chemosynthetic habitat-specialist genera. *Vrijenhoekia* and *Microphthalmus* sp. are recorded from the western Pacific for the first time, while the close genetic similarity between the *Protodrilus* cf. *puniceus* from this study and *P. puniceus* from off Japan (Fig. 21) may suggest potential connectivity along

the western Pacific for certain taxa, but more genetic data is needed to resolve this. Additionally, the close relationship between *Nereis* sp. and *Neanthes shinkai* (Fig. 16) may indicate the existence of nereidid lineage that specializes on whale falls, as well as indicating the inadequate generic concepts. The record of an eyeless *Eumida* species reported herein is also the shallowest documented so far (others are known from >3000 m depth).

Whale falls can act as species dispersal “stepping stones” (Smith *et al.*, 2015) and given that a number of whale species regularly traverse Australian waters bridging the Southern Ocean (such as humpback, fin and southern right whales (Aulich *et al.*, 2019; Carroll *et al.*, 2011; Groß *et al.*, 2020), New Zealand and the South Pacific region, natural whale falls in this region are also likely to be plentiful. Indeed, capturing a whale fall opportunistically during the IN2017_V03 voyage attests to this, and suggests connectivity in whale-fall taxa between these regions may be high. Further exploration of the deep ocean around Australia likely has much to reveal about these fascinating ecosystems, as well as about southern hemisphere deep-sea chemosynthetic environments in general.

ACKNOWLEDGEMENTS. The authors wish to thank the CSIRO Marine National Facility (MNF) for its support in the form of sea time on RV *Investigator*, support personnel, scientific equipment and data management. All data and samples acquired on the voyage are made publicly available in accordance with MNF Policy. We also thank all the scientific staff and crew who participated in voyage IN2017_V03. Project funding was provided by the Marine Biodiversity Hub, supported through the Australian Government’s National Environmental Science Program (NESP). MG is also grateful for support from a UK Natural Environment Research Council grant (NERC; number NE/R000670/1) and an Ifremer Postdoctoral Fellowship. LG is thankful for support from the Chadwick Biodiversity Fellowship from the Australian Museum. CG was funded by a grant RG18–21 from Australian Biological Resources Study (ABRS). Many thanks to William Zhang and Maria Wiklund for help editing images and making plates. We are also very grateful to Emma Sherlock for accessioning material at the NHM. Melanie Mackenzie for accessioning material at MV, and Stephen Keable for accessioning material at the AM. Images of preserved whale bones were taken by Platon Vafiadis, Museums Victoria.

Supplementary data

Supplementary Tables S1–S19 are published separately as a dataset at *figshare*:

<https://doi.org/10.6084/m9.figshare.22637491>

References

- Amon, D. J., H. Wiklund, T. G. Dahlgren, J. T. Copley, C. R. Smith, A. J. Jamieson, and A. G. Glover. 2014. Molecular taxonomy of *Osedax* (Annelida: Siboglinidae) in the Southern Ocean. *Zoologica Scripta* 43: 405–417. <https://doi.org/10.1111/zsc.12057>
- Aulich, M. G., R. D. McCauley, B. J. Saunders, and M. J. G. Parsons. 2019. Fin whale (*Balaenoptera physalus*) migration in Australian waters using passive acoustic monitoring. *Scientific Reports* 9(1): 8840. <https://doi.org/10.1038/s41598-019-45321-w>
- Bakken, T. 2002. A new species of *Neanthes* (Polychaeta: Nereididae) from southern Australia. *Memoirs of Museum Victoria* 59(2): 327–331. <https://doi.org/10.24199/j.mmv.2002.59.4>
- Bakken, T. 2006. Redescription of two new species of *Neanthes* (Polychaeta: Nereididae) possessing a large notopodial prechaetal lobe. *Scientia Marina* 70S3: 27–33. <https://doi.org/10.3989/scimar.2006.70s327>
- Bakken, T., C. J. Glasby, C. S. G. Santos, and R. S. Wilson. 2022. 7.13.3.3 Nereididae Blainville, 1818. In *Pleistoannelida, Errantia II*, 259–307. De Gruyter. <https://doi.org/10.1515/9783110647167-010>
- Bakken, T., and R. S. Wilson. 2005. Phylogeny of nereidids (Polychaeta, Nereididae) with paragnaths. *Zoologica Scripta* 34(5): 507–547. <https://doi.org/10.1111/j.1463-6409.2005.00200.x>
- Beesley, P. L., G. J. B. Ross, and C. J. Glasby. 2000. *Polychaetes & Allies: The Southern Synthesis*. Melbourne: CSIRO Publishing.
- Bergström, E. 1914. Zur systematik der polychaetenfamilie der Phyllocociden. *Zoologiska Bidrag Från Uppsala* 3: 37–224.
- Berman, G. 2022. Four new species of *Osedax* bone-worms from New Zealand and the Gulf of Mexico and range expansions for Pacific *Osedax* species. MSc Thesis, University of California San Diego. <https://escholarship.org/uc/item/3rt361jf>
- Blake, J. A. 2000. A new genus and species of polychaete worm (Family Orbiniidae) from methane seeps in the Gulf of Mexico, with a review of the systematics and phylogenetic relationships of the genera of Orbiniidae. *Cahiers de Biologie Marine* 41: 435–449.
- Blake, J. A. 2017. Polychaeta Orbiniidae from Antarctica, the Southern Ocean, the abyssal Pacific Ocean, and off South America. *Zootaxa* 4218(1): 1–145. <https://doi.org/10.11646/zootaxa.4218.1.1>
- Blake, J. A. 2021. New species and records of Orbiniidae (Annelida, Polychaeta) from continental shelf and slope depths of the Western North Atlantic Ocean. *Zootaxa* 4930(1): 1–123. <https://doi.org/10.11646/zootaxa.4930.1.1>
- Böttgermann, M. 2009. Polychaetes (Annelida) of the abyssal SE Atlantic. *Organisms Diversity & Evolution* 9: 251–428. <https://doi.org/10.1016/j.ode.2009.10.001>
- Braby, C. E., G. W. Rouse, S. B. Johnson, W. J. Jones, and R. C. Vrijenhoek. 2007. Bathymetric and temporal variation among *Osedax* boneworms and associated megafauna on whale-falls in Monterey Bay, California. *Deep-Sea Research I* 54: 1773–1791. <https://doi.org/10.1016/j.dsr.2007.05.014>
- Capa, M., and T. Bakken. 2015. Revision of the Australian Sphaerodoridae (Annelida) including the description of four new species. *Zootaxa* 4000(2): 227–267. <https://doi.org/10.11646/zootaxa.4000.2.3>
- Capa, M., and G. W. Rouse. 2015. Sphaerodoridae (Annelida) from Lizard Island, Great Barrier Reef, Australia, including the description of two new species and reproductive notes. *Zootaxa* 4019(1): 168–183. <https://doi.org/10.11646/zootaxa.4019.1.9>
- Carroll, E., N. Patenaude, A. Alexander, D. Steel, R. Harcourt, S. Childerhouse, S. Smith, J. Bannister, R. Constantine, and C. S. Baker. 2011. Population structure and individual movement of southern right whales around New Zealand and Australia. *Marine Ecology Progress Series* 432 (June): 257–268. <https://doi.org/10.3354/meps09145>
- Dahlgren, T. G., A. G. Glover, A. Baco, and C. R. Smith. 2004. Fauna of whale falls: systematics and ecology of a new polychaete (Annelida: Chrysopetalidae) from the deep Pacific Ocean. *Deep Sea Research Part I: Oceanographic Research Papers* 51(12): 1873–1887. <https://doi.org/10.1016/j.dsr.2004.07.017>

- Dahlgren, T. G., H. Wiklund, B. Källström, T. Lundälv, C. R. Smith, and A. G. Glover. 2006. A shallow-water whale-fall experiment in the north Atlantic. *Cahiers de Biologie Marine* 47(4): 385–389.
- Darriba, D., G. L. Taboada, R. Doallo, and D. Posada. 2012. JModelTest 2: more models, new heuristics and parallel computing. *Nature Methods* 9(8): 772.
<https://doi.org/10.1038/nmeth.2109>
- Day, J. H. 1963. Polychaete fauna of South Africa: Part 7. Species from depths between 1,000 and 3,330 meters west of Cape Town. *Annals of the South African Museum* 46(14): 353–371.
- De-Oliveira, V. M., D. Eibye-Jacobsen, and P. D.-C. Lana. 2015. Description of three new species of *Eumida* Malmgren, 1865 (Phyllodocidae, Annelida) from Southern and Southeastern Brazil. *Zootaxa* 3957(4): 425–440.
<https://doi.org/10.11646/zootaxa.3957.4.4>
- Dell, R. K. 1987. Mollusca of the family Mytilidae (Bivalvia) associated with organic remains from deep water off New Zealand, with revisions of the genera *Adipicola* Dautzenborg, 1927 and *Idasola* Iredale, 1915. *National Museum of New Zealand Records* 3: 17–36.
- Dell, R. K. 1995. New species and records of deep-water mollusca from off New Zealand. *Tuhinga* 2: 1–26.
- Desbruyères, D. 1980. Sphaerodoridae (Annelides Polychètes) profonds du Nord-Est Atlantique. *Bulletin Du Muséum d'Histoire Naturelle, Paris. Section A: Zoologie, Biologie et Écologie Animales. (Series 4)* 2(1): 109–128.
<https://doi.org/10.5962/p.283867>
- Drennan, R., H. Wiklund, M. Rabone, M. N. Georgieva, T. G. Dahlgren, and A. G. Glover. 2021. *Neanthes goodayi* sp. nov. (Annelida, Nereididae), a remarkable new annelid species living inside deep-sea polymetallic nodules. *European Journal of Taxonomy* 760: 160–185.
<https://doi.org/10.5852/ejt.2021.760.1447>
- Ehlers, E. 1868. Die Borstenwürmer (Annelida Chaetopoda) nach systematischen und anatomischen Untersuchungen dargestellt. *Wilhelm Engelmann, Leipzig* 2: 269–748.
- Ehlers, E. 1904. Neuseeländische Anneliden. Abhandlungen der Königlichen Gesellschaft der Wissenschaften zu Göttingen Mathematisch-Physikalische Klasse. *Neue Folge* 3(1): 1–80.
- Eibye-Jacobsen, D. 1991. A revision of *Eumida* Malmgren, 1865 (Polychaeta: Phyllodocidae). *Steenstrupia* 17(3): 81–140.
- Eklöf, J., F. Pleijel, and P. Sundberg. 2007. Phylogeny of benthic Phyllodocidae (Polychaeta) based on morphological and molecular data. *Molecular Phylogenetics and Evolution* 45(1): 261–271.
<https://doi.org/10.1016/j.ympev.2007.04.015>
- Fauvel, P. 1932. Annelida Polychaeta of the Indian Museum, Calcutta. *Memoirs of the Indian Museum* 12(1): 1–262.
- Fujiwara, Y., N. Jimi, P. Y. G. Sumida, M. Kawato, and H. Kitazato. 2019. New species of bone-eating worm *Osedax* from the abyssal South Atlantic Ocean (Annelida, Siboglinidae). *ZooKeys* 814: 53–69.
<https://doi.org/10.3897/zookeys.814.28869>
- Fujiwara, Y., M. Kawato, T. Yamamoto, T. Yamanaka, W. Sato-Okoshi, C. Noda, S. Tsuchida, *et al.*, 2007. Three-year investigations into sperm whale-fall ecosystems in Japan. *Marine Ecology* 28(1): 219–232.
<https://doi.org/10.1111/j.1439-0485.2007.00150.x>
- Gerould, J. H. 1913. The sipunculids of the eastern coast of North America. *Proceedings of the United States National Museum* 44: 373–437.
<https://doi.org/10.5479/si.00963801.44-1959.373>
- Gibbs, P. E. 1987. A new species of *Phascalosoma* (Sipuncula) associated with a decaying whale's skull trawled at 880 m depth in the southwest Pacific. *New Zealand Journal of Zoology* 14: 135–137.
<https://doi.org/10.1080/03014223.1987.10422691>
- Glover, A. G., H. Wiklund, S. Taboada, C. Avila, J. Cristobo, C. R. Smith, K. M. Kemp, A. J. Jamieson, and T. G. Dahlgren. 2013. Bone-eating worms from the Antarctic: the contrasting fate of whale and wood remains on the Southern Ocean seafloor. *Proceedings of the Royal Society B: Biological Sciences* 280: 20131390.
<https://doi.org/10.1098/rspb.2013.1390>
- Goffredi, S. K., C. K. Paull, K. Fulton-Bennett, L. A. Hurtado, and R. C. Vrijenhoek. 2004. Unusual benthic fauna associated with a whale fall in Monterey Canyon, California. *Deep Sea Research Part I: Oceanographic Research Papers* 51(10): 1295–1306.
<https://doi.org/10.1016/j.dsr.2004.05.009>
- Groß, J., P. Virtue, P. D. Nichols, P. Eisenmann, C. A. Waugh, and S. Bengtson Nash. 2020. Interannual variability in the lipid and fatty acid profiles of east Australia-migrating humpback whales (*Megaptera novaeangliae*) across a 10-year timeline. *Scientific Reports* 10(1): 18274.
<https://doi.org/10.1038/s41598-020-75370-5>
- Guindon, S., and O. Gascuel. 2003. A simple, fast and accurate method to estimate large phylogenies by maximum likelihood. *Systematic Biology* 52: 696–704.
<https://doi.org/10.1080/10635150390235520>
- Gunton, L. M., E. K. Kupriyanova, T. Alvestad, L. Avery, J. A. Blake, O. Biriukova, M. Böttgermann, *et al.* 2021. Annelids of the eastern Australian abyss collected by the 2017 RV “Investigator” voyage. *ZooKeys* 1020: 1–198.
<https://doi.org/10.3897/zookeys.1020.57921>
- Hansen, G. A. 1879. Annelider fra den norske Nordhavsexpedition i 1876. *Nyt Magazin for Naturvidenskaberne, Christiania* 24(1): 1–17.
- Hartman, O. 1967. Polychaetous annelids collected by the USNS Eltanin and Staten Island cruises, chiefly from Antarctic Seas. 2: 1–387. *Allan Hancock Monographs in Marine Biology* 2: 1–387.
- Hartmann-Schröder, G. 1958. Einige Polychaeten aus dem Küstengrundwasser der Bimini-Inseln (Bahamas). *Kieler Meeresforschungen* 14(2): 233–240.
- Hartmann-Schröder, G. 1975. Polychaeten der Iberischen Tiefsee, gesammelt auf der 3. Reise der Meteor im Jahre 1966. *Mitteilungen Aus Dem Hamburgischen Zoologischen Museum Und Institut* 72: 47–73.
- Hartmann-Schröder, G. 1981. Zur Kenntnis des Eulitorals der australischen Küsten unter besonderer Berücksichtigung der Polychaeten und Ostracoden. Teil 6. Die Polychaeten der tropisch-subtropischen Westküste Australiens (zwischen Exmouth im Norden und Cervantes im Süden). *Mitteilungen Aus Dem Hamburgischen Zoologischen Museum Und Institut* 78: 19–96.
- Hartmann-Schröder, G. 1983. Zur Kenntnis einiger Foraminiferengehäuse bewohnender Polychaeten aus dem Nordostatlantik. *Mitteilungen Aus Dem Hamburgischen Zoologischen Museum Und Institut* 80: 169–176.
- Hsueh, P.-W. 2019. *Neanthes* (Annelida: Nereididae) from Taiwanese waters, with description of seven new species and one new species record. *Zootaxa* 4554(1): 173–198.
<https://doi.org/10.11646/zootaxa.4554.1.5>
- Kearse, M., R. Moir, A. Wilson, S. Stones-Havas, M. Cheung, S. Sturrock, S. Buxton, *et al.*, 2012. Geneious Basic: an integrated and extendable desktop software platform for the organization and analysis of sequence data. *Bioinformatics* 28(12): 1647–1649.
<https://doi.org/10.1093/bioinformatics/bts199>
- Kirkegaard, J. B. 1995. Bathyal and abyssal polychaetes (errant species). *Galathea Reports* 17: 7–56.
- Knox, G. A. 1960. Biological results of the Chatham Islands 1954 Expedition. Part 3. Polychaeta errantia. *New Zealand Department of Scientific and Industrial Research Bulletin* 139(3): 77–143.

- Kongsrud, J. A., M. H. Eilertsen, T. Alvstad, K. Kongshavn, and H. T. Rapp. 2017. New species of Ampharetidae (Annelida: Polychaeta) from the Arctic Loki Castle vent field. *Deep Sea Research Part II: Topical Studies in Oceanography* 137 (March): 232–245.
<https://doi.org/10.1016/j.dsr2.2016.08.015>
- Kudenov, J. D. 1993. Amphinomidae and Euphosinidae (Annelida: Polychaeta) principally from Antarctica, the Southern Ocean, and Subantarctic regions. *Biology of Antarctic Series 22, Antarctic Research Series* 58: 93–150.
<https://doi.org/10.1029/AR058p0093>
- León-González, J. Á. de, and S. I. Salazar-Vallejo. 2003. Four new nereidid species (Annelida, Polychaeta) collected during the MUSORSTOM cruises in the Indo-Pacific Ocean. *Zoosystema* 25(3): 365–375.
- Malaquin, A., and A. Dehorne. 1907. Les annelides polychètes de la Baie d'Amboine. *Revue Suisse de Zoologie* 15: 335–400.
<https://doi.org/10.5962/bhl.part.82525>
- Malmgren, A. J. 1865. Nordiska Hafs-Annulater [part one of three]. *Öfversigt Af Königlich Vetenskapsakademiens Förhandlingar; Stockholm* 22(1): 51–110.
- Marshall, B. A. 1987. Osteopeltidae (Mollusca: Gastropoda): a new family of limpets associated with whale bone in the deep sea. *Journal of Molluscan Studies* 53: 121–27.
<https://doi.org/10.1093/mollus/53.2.121>
- Marshall, B. A. 1994. Deep-sea gastropods from the New Zealand region associated with recent whale bones and an Eocene turtle. *Nautilus* 108: 1–8.
- McIntosh, W. C. 1868. Report on the annelids dredged off the Shetland Islands by Mr. Gwyn Jeffreys in 1867. *Annals and Magazine of Natural History (Series 4)* 2(10): 249–252.
<https://doi.org/10.1080/00222936808695797>
- McIntosh, W. C. 1885. Report on the Annelida Polychaeta collected by H.M.S. Challenger during the years 1873–1876. Report on the Scientific Results of the Voyage of H.M.S. Challenger during the years 1873–76. *Zoology* 12 (part 34).
- Monro, C. C. A. 1930. Polychaete worms. *Discovery Reports* 2: 1–222.
- Moore, J. P. 1903. Descriptions of two new species of Polychaeta from Wood's Hole, Massachusetts. *Proceedings of the Academy of Natural Sciences of Philadelphia*. 55: 720–726.
- O'Hara, T. D., A. Williams, S. T. Ahyong, P. Alderslade, T. Alvstad, D. Bray, I. Burghardt, et al., 2020. The lower bathyal and abyssal seafloor fauna of eastern Australia. *Marine Biodiversity Records* 13(1): 11.
<https://doi.org/10.1186/s41200-020-00194-1>
- Örsted, A. S. 1843. Annulorum danicorum conspectus. *Auctore A.S. Örsted. Fasc. I. Maricolae*.
<https://doi.org/10.5962/bhl.title.11849>
- Parapar, J., J. Moreira, and G. V. Helgason. 2015. First record of genus *Orbiniella* Day, 1954 (Polychaeta: Orbiniidae) in North Atlantic Ocean with the description of a new species. *Zootaxa* 4006(2): 330–346.
<https://doi.org/10.11646/zootaxa.4006.2.5>
- Petersen, M. E., and F. Pleijel. 1993. *Pseudomystides spinachia* Petersen & Pleijel, new species. *Marine Invertebrates of Scandinavia* 8: 118–124.
- Pleijel, F., G. W. Rouse, C. Ruta, H. Wiklund, and A. Nygren. 2008. *Vrijenhoekia balaenophila*, a new hesionid polychaete from a whale fall off California. *Zoological Journal of the Linnean Society* 152(4): 625–634.
<https://doi.org/10.1111/j.1096-3642.2007.00360.x>
- Queirós, J. P., A. Ravara, M. H. Eilertsen, J. A. Kongsrud, and A. Hilário. 2017. *Paramytha ossicola* sp. nov. (Polychaeta, Ampharetidae) from mammal bones: Reproductive biology and population structure. *Deep Sea Research Part II: Topical Studies in Oceanography* 137: 349–358.
<https://doi.org/10.1016/j.dsr2.2016.08.017>
- Ravara, A., D. Ramos, M. A. L. Teixeira, F. O. Costa, and M. R. Cunha. 2017. Taxonomy, distribution and ecology of the order Phyllococida (Annelida, Polychaeta) in deep-sea habitats around the Iberian margin. *Deep Sea Research Part II: Topical Studies in Oceanography* 137: 207–231.
<https://doi.org/10.1016/j.dsr2.2016.08.008>
- Ravara, A., H. Wiklund, and M. R. Cunha. 2021. Four new species and further records of Dorvilleidae (Annelida, Polychaeta) from deep-sea organic substrata, NE Atlantic. *European Journal of Taxonomy* 736: 44–81.
<https://doi.org/10.5852/ejt.2021.736.1251>
- Read, G., and K. Fauchald. 2023. World Polychaeta Database. *Orbiniella branchiata* Hartman, 1967. *World Register of Marine Species*.
<https://www.marinespecies.org/aphia.php?p=taxdetails&id=329837>
- Reish, D. J., F. E. Anderson, K. M. Horn, and J. Hardege. 2014. Molecular phylogenetics of the *Neanthes acuminata* (Annelida: Nereididae) species complex. *Memoirs of Museum Victoria* 71: 271–278.
<https://doi.org/10.24199/j.mmv.2014.71.20>
- Rice, M. E. 1985. Description of a wood-dwelling sipunculan, *Phascalosoma turnerae*, new species. *Proceedings of the Biological Society of Washington* 98: 54–60.
- Ronquist, F., M. Teslenko, P. van der Mark, D. L. Ayres, A. Darling, S. Höhna, B. Larget, L. Liu, M. A. Suchard, and J. P. Huelsenbeck. 2012. MrBayes 3.2: efficient Bayesian phylogenetic inference and model choice across a large model space. *Systematic Biology* 61(3): 539–542.
<https://doi.org/10.1093/sysbio/sys029>
- Rouse, G. W., S. K. Goffredi, S. B. Johnson, and R. C. Vrijenhoek. 2018. An inordinate fondness for *Osedax* (Siboglinidae: Annelida): fourteen new species of bone worms from California. *Zootaxa* 4377(4): 451–489.
<https://doi.org/10.11646/zootaxa.4377.4.1>
- Saeedi, H., A. F. Bernardino, M. Shimabukuro, G. Falchetto, and P. Y. G. Sumida. 2019. Macrofaunal community structure and biodiversity patterns based on a wood-fall experiment in the deep South-west Atlantic. *Deep Sea Research Part I: Oceanographic Research Papers* 145: 73–82.
<https://doi.org/10.1016/j.dsr.2019.01.008>
- Saint-Joseph, A. 1888. Les annélides polychètes des côtes de Dinard. Seconde partie. *Annales Des Sciences Naturelles, Zoologie et Paléontologie, Paris, Série 7* 5(2): 141–338.
- Salazar-Vallejo, S. I., and J. M. Orensanz. 2006. *Pleijelius longae* n. gen., n. sp., a remarkable deep water polychaete from the Northwestern Atlantic (Polychaeta: Hesionidae). *Scientia Marina* 70: 157–166.
<https://doi.org/10.3989/scimar.2006.70s3157>
- San Martín, G., P. Álvarez-Campos, Y. Kondo, J. Núñez, M. A. Fernández-Álamo, F. Pleijel, F. E. Goetz, A. Nygren, and K. Osborn. 2021. New symbiotic association in marine annelids: ectoparasites of comb jellies. *Zoological Journal of the Linnean Society* 191(3): 672–694.
<https://doi.org/10.1093/zoolinnean/zlaa034>
- Santos, C. S., F. Pleijel, P. Lana, and G. W. Rouse. 2006. Phylogenetic relationships within Nereididae (Annelida: Phyllococida). *Invertebrate Systematics* 19(6): 557–576.
<https://doi.org/10.1071/IS05001>
- Sato-Okoshi, W., K. Okoshi, and Y. Fujiwara. 2015. A new species of *Protodrilus* (Annelida, Protodrilidae), covering bone surfaces bright red, in whale-fall ecosystems in the Northwest Pacific. *Biological Bulletin* 229(2): 209–219.
<https://doi.org/10.1086/BBLv229n2p209>
- Schulze, A., E. B. Cutler, and G. Giribet. 2007. Phylogeny of sipunculan worms: a combined analysis of four gene regions and morphology. *Molecular Phylogenetics and Evolution* 42(1): 171–192.
<https://doi.org/10.1016/j.ympev.2006.06.012>

- Shimabukuro, M., O. Carrerette, J. M. Alfaro-Lucas, A. E. Rizzo, K. M. Halanych, and P. Y. G. Sumida. 2019. Diversity, distribution and phylogeny of Hesionidae (Annelida) colonizing whale falls: new species of *Sirsoe* and connections between ocean basins. *Frontiers in Marine Science* 6: 478.
<https://doi.org/10.3389/fmars.2019.00478>
- Shimabukuro, M., A. E. Rizzo, J. M. Alfaro-Lucas, Y. Fujiwara, and P. Y. G. Sumida. 2017. *Sphaerodoropsis kitazatoi*, a new species and the first record of Sphaerodoridae (Annelida: Phyllococida) in SW Atlantic abyssal sediments around a whale carcass. *Deep Sea Research Part II: Topical Studies in Oceanography* 146: 18–26.
<https://doi.org/10.1016/j.dsr2.2017.04.003>
- Shimabukuro, M., C. S. G. Santos, J. M. Alfaro-Lucas, Y. Fujiwara, and P. Y. G. Sumida. 2017. A new eyeless species of *Neanthes* (Annelida: Nereididae) associated with a whale-fall community from the deep Southwest Atlantic Ocean. *Deep Sea Research Part II: Topical Studies in Oceanography* 146: 27–34.
<https://doi.org/10.1016/j.dsr2.2017.10.013>
- Silva, A. P., A. Colaço, A. Ravara, J. Jakobsen, K. Jakobsen, and D. Cuvelier. 2021. The first whale fall on the Mid-Atlantic Ridge: Monitoring a year of succession. *Deep Sea Research Part I: Oceanographic Research Papers* 178: 103662.
<https://doi.org/10.1016/j.dsr.2021.103662>
- Smith, C. R., and A. R. Baco. 2003. Ecology of whale falls at the deep-sea floor. *Oceanography and Marine Biology: an Annual Review* 41: 311–354.
- Smith, C. R., A. G. Glover, T. Treude, N. D. Higgs, and D. J. Amon. 2015. Whale-fall ecosystems: recent insights into ecology, paleoecology, and evolution. *Annual Review of Marine Science* 7(1): 571–596.
<https://doi.org/10.1146/annurev-marine-010213-135144>
- Smith, C. R., H. Kukert, R. A. Wheatcroft, P. A. Jumars, and J. W. Deming. 1989. Vent fauna on whale remains. *Nature* 341(6237): 27–28.
<https://doi.org/10.1038/341027a0>
- Solis-Weiss, V., and K. Fauchald. 1989. Orbiniidae (Annelida: Polychaeta) from mangrove root-mats in Belize, with a revision of Protoariciin genera. *Proceedings of the Biological Society of Washington* 102(3): 772–792.
- Sumida, P. Y. G., J. M. Alfaro-Lucas, M. Shimabukuro, H. Kitazato, J. A. A. Perez, A. Soares-Gomes, T. Toyofuku, A. O. S. Lima, K. Ara, and Y. Fujiwara. 2016. Deep-sea whale fall fauna from the Atlantic resembles that of the Pacific Ocean. *Scientific Reports* 6(1): 22139.
<https://doi.org/10.1038/srep22139>
- Summers, M., F. Pleijel, and G. W. Rouse. 2015. Whale falls, multiple colonisations of the deep, and the phylogeny of Hesionidae (Annelida). *Invertebrate Systematics* 29(2): 105–123.
<https://doi.org/10.1071/IS14055>
- Swofford, D. L. 2002. *PAUP*. Phylogenetic Analysis Using Parsimony (*and Other Methods)*. Version 4. Sunderland, MA: Sinauer Associates.
- Teixeira, M. A. L., P. E. Vieira, F. Pleijel, B. R. Sampieri, A. Ravara, F. O. Costa, and A. Nygren. 2020. Molecular and morphometric analyses identify new lineages within a large *Eumida* (Annelida) species complex. *Zoologica Scripta* 49(2): 222–235.
<https://doi.org/10.1111/zsc.12397>
- Théel, H. J. 1879. Les annélides polychètes des mers de la Nouvelle-Zemble. *Kungliga Svenska Vetenskapsakademiens Handlingar* 16: 1–75.
- Uschakov, P. V. 1958. Two new *Phyllidoidea* from the Kurile-Kamchatka Trench. *Trudy Instituta Okeanologii Akademii Nauk SSSR* 27: 204–207.
- Uschakov, P. V. 1972. Fauna of the USSR. Polychaetes. Vol. I. Polychaetes of the suborder Phyllocociformia of the Polar Basin and the North-Western part of the Pacific (Family Phyllococidae, Alciopidae, Tomopteridae, Typhloscolecidae and Lacydoniidae). *Akademiya Nauk SSSR* 102: 1–272.
- Villalobos-Guerrero, T. F., and I. Idris. 2021. Reproductive morphology and redescrptions of some *Neanthes* Kinberg, 1865 (Annelida: Nereididae) species from the southeastern Asian seas, with comparative synoptic tables of accepted species. *The European Zoological Journal* 88(1): 556–594.
<https://doi.org/10.1080/24750263.2021.1899318>
- Villalobos-Guerrero, T. F., J. Kara, C. Simon, and I. Idris. 2022. Systematic review of *Neanthes* Kinberg, 1865 (Annelida: Errantia: Nereididae) from southern Africa, including a preliminary molecular phylogeny of the genus. *Marine Biodiversity* 52(2): 21.
<https://doi.org/10.1007/s12526-021-01244-2>
- Wada, H., T. Naganuma, K. Fujioka, H. Ditazato, K. Kawamura, and Y. Akazawa. 1994. The discovery of the Torishima whale bone animal community and its meaning: the results of revisit dives by the “Shinkai 6500.” *JAMSTEC Deep-Sea Research* 10: 38–47.
- Westheide, W. 1990. *Polychaetes: Interstitial Families*. Oegstgeest, Netherlands: Universal Book Services/W. Backhuys.
- Westheide, W. 2013. *Microphthalmus mahensis* sp.n. (Annelida, Phyllococida) together with an annotated key of the genus. *Helgoland Marine Research* 67(3): 413–422.
<https://doi.org/10.1007/s10152-012-0332-1>
- Wiklund, H., I. V. Altamira, A. G. Glover, C. R. Smith, A. R. Baco, and T. Dahlgren. 2012. Systematics and biodiversity of *Ophryotrocha* (Annelida, Dorvilleidae) with descriptions of six new species from deep-sea whale-fall and wood-fall habitats in the north-east Pacific. *Systematics and Biodiversity* 10(2): 243–259.
<https://doi.org/10.1080/14772000.2012.693970>
- Wiklund, H., A. G. Glover, and T. G. Dahlgren. 2009. Three new species of *Ophryotrocha* (Annelida: Dorvilleidae) from a whale-fall in the North-East Atlantic. *Zootaxa* 2228(1): 43–56.
<https://doi.org/10.11646/zootaxa.2228.1.3>
- Wilson, R. S. 1984. *Neanthes* (Polychaeta: Nereididae) from Victoria with descriptions of two new species. *Proceedings of the Royal Society of Victoria* 96(4): 209–226.